

Identification of Underlying Dynamic System from Noisy Data with Splines

Yujie Zhao, Xiaoming Huo, and Yajun Mei ^{*}

School of Industrial and Systems Engineering, Georgia Institute of Technology

March 1, 2025

Abstract

In this paper, we propose a two-stage method called *Spline Assisted Partial Differential Equation involved Model Identification (SAPDEMI)* to efficiently identify the underlying partial differential equation (PDE) models from the noisy data. In the first stage – *functional estimation stage* – we employ the cubic spline to estimate the unobservable derivatives, which serve as candidates included the underlying PDE models. The contribution of this stage is that, it is computational efficient because it only requires the computational complexity of the linear polynomial of the sample size, which achieves the lowest possible order of complexity. In the second stage – *model identification stage* – we apply Least Absolute Shrinkage and Selection Operator (Lasso) to identify the underlying PDE models. The contribution of this stage is that, we focus on the model selections, while the existing literature mostly focuses on parameter estimations. Moreover, we develop statistical properties of our method for correct identification, where the main tool we use is the primal-dual witness (PDW) method. Finally, we validate our theory through various numerical examples.

Keywords: partial differential equation, model identification, cubic spline, Lasso

^{*}The authors gratefully acknowledge *NSF grant DMS-2015405 and the Transdisciplinary Research Institute for Advancing Data Science (TRIAD) (a part of the TRIPODS program at NSF and locates at Georgia Tech, enabled by the NSF grant CCF-1740776), NSF grant DMS-2015363.*

1 Introduction

In practice, one is often encountered with noisy data coming from an unknown partial differential equation (PDE):

$$\begin{aligned} \mathcal{D} = \{(x_i, t_n, u_i^n) : & x_i \in (0, X_{\max}) \subseteq \mathbb{R}, \forall i = 0, \dots, M-1, \\ & t_n \in (0, T_{\max}) \subseteq \mathbb{R}, \forall n = 0, \dots, N-1\} \in \Omega. \end{aligned} \quad (1)$$

Here $t_n \in \mathbb{R}$ is the temporal variable with $t_n \in (0, T_{\max})$ for $n = 0, 1, \dots, N-1$, and we call N the *temporal resolution*. And $x_i \in \mathbb{R}$ is the spatial variable with $x_i \in (0, X_{\max})$ for $i = 0, 1, \dots, M-1$, and we call M the *spatial resolution*. We use T_{\max}, X_{\max} to denote the upper bound of the temporal variable and spatial variable, respectively.

In the above dataset \mathcal{D} , the variable u_i^n is a representation of ground truth $u(x_i, t_n)$ contaminated by noise following normal distribution with zero mean and stand deviation σ :

$$u_i^n = u(x_i, t_n) + \epsilon_i^n \quad \epsilon_i^n \stackrel{i.i.d.}{\sim} N(0, \sigma^2), \quad (2)$$

where $u(x, t)$ is the underlying PDE model from where \mathcal{D} is generated.

For this type of noisy dataset \mathcal{D} , we are typically interested in identifying its underlying PDE model:

$$\begin{aligned} \frac{\partial}{\partial t} u(x, t) = & \beta_{00}^* + \sum_{k=0}^{q_{\max}} \sum_{i=1}^{p_{\max}} \beta_{k^i}^* \left[\frac{\partial^k}{\partial^k x} u(x, t) \right]^i + \\ & \sum_{\substack{i+j \leq p_{\max} \\ i, j > 0}} \sum_{\substack{0 < k < l \\ l \leq q_{\max}}} \beta_{k^i, l^j}^* \left[\frac{\partial^k}{\partial^k x} u(x, t) \right]^i \left[\frac{\partial^l}{\partial^l x} u(x, t) \right]^j, \end{aligned} \quad (3)$$

where the left-hand side of the above equation is the partial derivative with respect to the temporal variable t , while the right side hand is the p_{\max} th order polynomial of the derivatives with respect to the spatial variable x up to the q_{\max} th order. For notation simplifications, we denote the ground truth coefficient vector $\beta^* = (\beta_{00}^*, \beta_{01}^*, \beta_{11}^*, \dots, \beta_{q_{\max} p_{\max}}^*)$

as $\boldsymbol{\beta}^* = (\beta_1^*, \beta_2^*, \beta_3^*, \dots, \beta_K^*)^\top$ where $K = 1 + (p_{\max} + 1)q_{\max} + \frac{1}{2}q_{\max}(q_{\max} + 1)(p_{\max} - 1)!$. It should be noted that, in practice, the majority of the entries in $\boldsymbol{\beta}^*$ are zero. For instance, in the transport equation $\frac{\partial}{\partial t}u(x, t) = a\frac{\partial}{\partial x}u(x, t)$ with any $a \neq 0$, we only have $\beta_3^* \neq 0$ and $\beta_i^* = 0$ for any $i \neq 3$ (see Olver, 2014, Section 2.2). So we know the coefficient $\boldsymbol{\beta}^*$ in (3) is sparse.

To identify the above model, one needs to overcome two technical issues. First, derivatives are unobservable from \mathcal{D} and have to be estimated from noisy observations of the values of the function. Second, there could be lots of data-driven PDE models that suit the noisy data very well. Among all these models, a simple model would be desirable. However, it is not clear how can we identify the simple model.

In this paper, we propose a two-stage method – *Spline Assisted Partial Differential Equation involved Model Identification (SAPDEMI)* – to efficiently identify the underlying PDE models from the noisy data \mathcal{D} . The first stage is called *functional estimation stage*, where we estimate all the derivatives from the noisy data \mathcal{D} , including $\frac{\partial}{\partial t}u(x, t)$, $\frac{\partial}{\partial x}u(x, t)$ and so on. In this stage, the main tool we use is the cubic spline, where we first use the cubic spline to fit the noisy data, and then we approximate the derivatives of the true dynamic models as the derivatives of the cubic splines. The second stage is called *model identification stage*, where we identify the underlying PDE models from the noisy data \mathcal{D} . In this stage, we apply the Least Absolute Shrinkage and Selection Operator (Lasso) (see Tibshirani, 1996) to identify the derivatives (or their combinations) that are included in the underlying models. To ensure the correctness of the identification, we develop sufficient conditions for correct identification and the asymptotic properties of the identified models, where the main tool we use is the primal-dual witness (PDW) method (see Hastie et al., 2015, Chapter 11).

The structure of the rest of this section is described as follows. In Section 1.1, we survey the existing methods to solve the above PDE identification problem. In Section 1.2, we articulate our contributions of this paper.

1.1 Literature Review

The pioneering representative work to identify the underlying dynamic models from the noisy data is Liang and Wu (2008). This method is also a two-stage method, where in the functional estimation stage, Liang and Wu (2008) use the local polynomial regression to estimate the value of the function and its derivatives. Then, in the model identification stage, Liang and Wu (2008) use the least squares model. Following this pioneering work, other researchers conduct various extensions.

The first type of extension is to modify the function estimation stage of Liang and Wu (2008), and we classify the existing extensions into two categories: (1) the numerical differentiation, and (2) the basis expansion.

In the numerical differentiation category (see Wu et al., 2012; Brunton et al., 2016; Tran and Ward, 2017), the derivative $\frac{\partial}{\partial x}u(x, t)$ is naively approximated as

$$\frac{\partial}{\partial x}u(x, t) \approx \frac{u(x + \Delta x, t) - u(x - \Delta x, t)}{2\Delta x},$$

where $(x + \Delta x, t), (x - \Delta x, t)$ are the two closest points of (x, t) in the x -domain. The essence of numerical differentiation is to approximate the first-order derivative as the slope of a nearby secant line. Although the implementation of numerical differentiation is very easy, it could be highly biased because its accuracy is highly dependent on the value of Δx . On the one hand, if Δx is too small, the subtraction will yield a large rounding error (see Ueberhuber, 2012; Butt, 2008). In fact, all the finite-difference formulae are ill-conditioned

(see Fornberg, 1981) and due to cancellation will produce a value of zero if Δx is small enough (see Squire and Trapp, 1998). On the other hand, if Δx is too large, though the calculation of the slope of the secant line will be more accurately calculated, the estimation of the slope of the tangent by using the secant line could be poor. However, in our case, the size of Δx is decided by the noisy data \mathcal{D} , which could be very small or very large. So if we naively use numerical differentiation to estimate the derivatives from the noisy data \mathcal{D} , it could be highly possible that we will get biased estimations.

In the basis expansion category, researchers first approximate the unknown dynamic curves by basis expansion and then approximate the derivatives of underlying dynamic curves as the derivatives of the approximation curves. As for the choice of basis in the basis expansion, there are multiple choices in the existing literature. The most popular basis is the polynomial basis, which is already used by Liang and Wu (2008). Other examples of polynomial basis can be found in Bär et al. (1999); Schaeffer (2017); Rudy et al. (2017); Parlitz and Merkwirth (2000); Voss et al. (1999). One popular choice of basis is spline basis (see Ramsay et al., 2007; Ramsay, 1996; Wu et al., 2012; Xun et al., 2013; Wang et al., 2019). The major limitation of the above method is that it evolves with high computational complexity. For instance, the local polynomial basis requires computational complexity of order $\max\{O(M^2N), O(MN^2)\}$ in the functional estimation stage. However, our proposed SAPDEMI method only requires computational complexity of order $O(MN)$. This is the lowest possible bound in theory in the functional estimation stage because it is the complexity of reading in the data set \mathcal{D} .

The second type of extension is to modify the model identification stage of Liang and Wu (2008). The existing methods fall in the framework of the (penalized) least squares method, and we mainly divide them into three categories: (1) the least squares method,

(2) the ℓ_2 -penalized least squares method, and (3) the ℓ_1 -penalized least squares method.

In the least squares method category, Miao et al. (2009) use the least squares method to estimate the parameters in unknown ordinary differential equation (ODE) models. Bär et al. (1999) and Wu et al. (2012) use the least squares to estimate the parameters in unknown PDE models. The major limitation of this method is that it can lead to overfitting models.

In the ℓ_2 -penalized least squares method category, Xun et al. (2013); Azzimonti et al. (2015) and Wang et al. (2019) penalize the smoothness of the unknown PDE models, which shares similar ideas with the reproducing kernel Hilbert space (RKHS). And essentially speaking, this method falls in the framework of the ℓ_2 -penalized least squares method. Although this method can avoid overfitting by introducing the ℓ_2 -penalty, it has limited power to do “model selection” instead of “parameter estimation”. Specifically, they assume that the form of the dynamic models (either ODE or PDE) is known, and their goal is to estimate the coefficients in the given model. However, in real practice, the form of the dynamic model is potentially unknown. Under this scenario, instead of “parameter estimation”, we also need to do “model selection”.

In the ℓ_1 -penalized least squares method category, Schaeffer (2017) identifies the unknown dynamic models through the ℓ_1 -penalized least squares method, and later the author discusses the design of an efficient algorithm with proximal mapping method. But the authors do not discuss the asymptotic statistical property of the identified model. Recently, Kang et al. (2019) utilize the similar method as Schaeffer (2017) to identify the unknown dynamic models. Although Kang et al. (2019) demonstrated some empirical successes, the rigorous theoretical justification still remains vague. So this category is not fully explored in terms of the statistical property.

During the investigation of the literature of ODE/PDE identification, we also find some research work published outside the statistical journals. These researchers investigate the importance of the ODE/PDE identification problem, but they do not develop a statistical theory on their methods, which is what we do in this paper. For instance, Mangan et al. (2017) assume that the derivatives are already known in the functional estimation stage and then they utilize the Akaike information criterion (AIC) to realize the model selection in the model identification stage. But the theoretical property of the selected model is not analyzed. Another example is Rudy et al. (2017), wherein the model identification stage, the authors first use the ℓ_2 -penalized least squares method to estimate the parameter β , and then manually shrinkage the small coefficients to zero by applying the hard-threshold method to realize the model selection. Other similar papers include Brunton et al. (2016); Tran and Ward (2017); Mangan et al. (2016); Schaeffer et al. (2013). The methods in the above papers may work in special cases, but their statistical properties are not established, and the rigorous proofs remain an open question in these papers.

1.2 Our Contribution

In this section, we discuss the contributions of our proposed SAPDEMI method.

First, our proposed SAPDEMI method is computationally efficient in the functional estimation stage. Specifically, we only require computationally complexity of order $O(MN)$, which is the lowest possible order in this stage. And the popularly used local polynomial regression requires computational complexity of order $\max\{O(M^2N), O(MN^2)\}$, which is more computationally expensive than our proposed SAPDEMI method.

Second, our proposed SAPDEMI method realizes “model selection”, instead of to “parameter estimations” in the model identification stage. The existing methods, for instance

Bär et al. (1999); Miao et al. (2009); Wu et al. (2012); Xun et al. (2013); Azzimonti et al. (2015); Wang et al. (2019), can only realize “parameter estimation”, where they always assume that the form of the underlying PDE models is known. However, our proposed SAPDEMI method can identify the underlying PDE models without knowing the form of the underlying PDE models.

Finally, we develop sufficient conditions for correct identification, and we also establish the statistical properties of our identified models, which has not been seen in the literature.

The remaining of the paper is organized as follows. In Section 2, we develop the technical details of our proposed SAPDEMI method. In Section 3, we present our main theory, including the sufficient conditions for correct identification, and the statistical properties of our identified models. In Section 4, we conduct numerical experiments to validate the main theory in Section 3. In Section 5, we summarize this paper and discuss the future research.

2 Proposed Method: SAPDEMI

In this section, we develop an efficient statistical method called SAPDEMI to identify the underlying PDE model from noisy data \mathcal{D} . Our proposed SAPDEMI method is a two-stage method to identify the unknown PDE models. The first stage is called *functional estimation stage*, where we estimate the function values and their derivatives from the noisy data \mathcal{D} in (1). These functional values and their derivatives serve as the input values in the second stage. The second stage is called *model identification stage*, where we identify the underlying PDE model.

For the notations throughout the paper, scalars are denoted by lowercase letters (e.g.,

β). Vectors are denoted by lowercase bold face letters (e.g., β), and its i th entry is denoted as β_i . Matrices are denoted by uppercase boldface letter (e.g., \mathbf{B}), and its (i, j) th entry is denoted as B_{ij} . For the vector $\beta \in \mathbb{R}^p$, its k th norm is defined as $\|\beta\|_k := (\sum_{i=1}^p |\beta_i|^k)^{1/k}$. For the matrix $\mathbf{B} \in \mathbb{R}^{m \times n}$, its Frobenius norm is defined as $\|\mathbf{B}\|_F = \sqrt{\sum_{i=1}^m \sum_{j=1}^n |B_{ij}|^2}$, and its p, q th norm is defined as $\|\mathbf{B}\|_{p,q} = \max_{\mathbf{x} \neq \mathbf{0}} \frac{\|\mathbf{B}\mathbf{x}\|_q}{\|\mathbf{x}\|_p}$. We write $f(n) = O(g(n))$, if there exists a positive real number G and a real number n_0 such that $|f(n)| \leq Gg(n)$ for all $n > n_0$.

The structure of this section is described as follows. In Section 2.1, we introduce the function estimation stage. In Section 2.2, we describe the model identification stage.

2.1 Functional Estimation Stage

In this section, we discuss the functional estimation stage of our proposed SAPDEMI method, i.e., estimating the functional values and their derivatives from the noisy data \mathcal{D} in (1). These derivatives include the derivatives with respect to the spatial variable x and the derivatives with respect to the temporal variable t . In this section, we will take the derivatives with respect to spatial variable x as an example, and the derivatives with respect to the temporal variable t can be derived similarly.

The main tool we use is the cubic spline. Suppose there is a cubic spline $s(x)$ over the knots $\{(x_i, u_i^n)\}_{i=0,1,\dots,M-1}$ satisfying the following properties (see McKinley and Levine, 1998):

1. $s(x) \in C^2[x_0, x_{M-1}]$, where $C^2[x_0, x_{M-1}]$ denotes the sets of function whose 0th, first and second derivatives are continuous in the domain $[x_0, x_{M-1}]$ with the assumption that $x_0 < x_1 < \dots < x_{M-1}$;

2. For any $i = 1, \dots, M-1$, $s(x)$ is a polynomial of degree 3 on the subinterval $[x_{i-1}, x_i]$;
3. For the two end-point x_0, x_{M-1} , we have $s''(x_0) = s''(x_{M-1}) = 0$, where $s''(x)$ is the second derivative of $s(x)$.

By fitting data $\{(x_i, u_i^n)\}_{i=0,1,\dots,M-1}$ (with a general fixed $n \in \{0, 1, \dots, N-1\}$) into the above cubic spline $s(x)$, one can solve $s(x)$ as the minimizer of the following optimization problem:

$$J_\alpha(s) = \alpha \sum_{i=0}^{M-1} w_i [u_i^n - s(x_i)]^2 + (1 - \alpha) \int_{x_0}^{x_{M-1}} s''(x)^2 dx, \quad (4)$$

where the first term $\alpha \sum_{i=0}^{M-1} w_i [u_i^n - s(x_i)]^2$ is the weighted sum of squared residuals, and we take the weight $w_0 = w_1 = \dots = w_{M-1} = 1$ in our paper. In the second term $(1 - \alpha) \int_{x_0}^{x_{M-1}} s''(x)^2 dx$, $s''(x)$ is the second derivative of $s(x)$, and this term is the penalty of smoothness. In the above optimization problem, the parameter $\alpha \in (0, 1]$ trades off the goodness of fit and the smoothness of the cubic spline. By minimizing the above optimization problem with respect to $s(x)$, we can get the estimate of $s(x)$, its first derivative $s'(x)$ and its second derivative $s''(x)$. If the cubic spline approximates the underlying PDE curves very well, then we could declare that the derivatives of the underlying dynamic system can be approximated by the derivatives of the cubic spline $s(x)$, i.e., we have $\widehat{u(x, t_n)} \approx \widehat{s(x)}$, $\frac{\partial}{\partial x} \widehat{u(x, t_n)} \approx \widehat{s'(x)}$, $\frac{\partial^2}{\partial x^2} \widehat{u(x, t_n)} \approx \widehat{s''(x)}$ (see Ahlberg et al., 1967; Rubin and Graves Jr, 1975; Rashidinia and Mohammadi, 2008).

For the above optimization problem, there is a closed-form solution, which is summarized as follows. First of all, the value of cubic spline $s(x)$ at the point $\{x_0, x_1, \dots, x_{M-1}\}$, i.e., $\widehat{\mathbf{s}} = \left(\widehat{s(x_0)}, \widehat{s(x_1)}, \dots, \widehat{s(x_{M-1})} \right)^\top$, can be solved as

$$\widehat{\mathbf{s}} = [\alpha \mathbf{W} + (1 - \alpha) \mathbf{A}^\top \mathbf{M} \mathbf{A}]^{-1} \alpha \mathbf{W} \mathbf{u}^n, \quad (5)$$

which can be used to approximate the 0th order derivative of the underlying PDE models, i.e., $\widehat{\mathbf{s}} \approx \widehat{\mathbf{f}} = \left(\widehat{u(x_0, t_n)}, \widehat{u(x_1, t_n)}, \dots, \widehat{u(x_{M-1}, t_n)} \right)^\top$. Here the matrix $\mathbf{W} = \text{diag}(w_0, w_1, \dots, w_{M-1}) \in \mathbb{R}^{M \times M}$, the vector $\mathbf{u}^n = (u_0^n, \dots, u_{M-1}^n)^\top \in \mathbb{R}^M$, and the matrix $\mathbf{A} \in \mathbb{R}^{(M-2) \times M}$, $\mathbf{M} \in \mathbb{R}^{(M-2) \times (M-2)}$ are defined as

$$\mathbf{A} = \begin{pmatrix} \frac{1}{h_0} & -\frac{1}{h_0} - \frac{1}{h_1} & \frac{1}{h_1} & 0 & \dots & 0 & 0 & 0 \\ 0 & \frac{1}{h_1} & -\frac{1}{h_1} - \frac{1}{h_2} & \frac{1}{h_2} & \dots & 0 & 0 & 0 \\ \vdots & \vdots & \vdots & \vdots & \ddots & \vdots & \vdots & \vdots \\ 0 & 0 & 0 & 0 & \dots & \frac{1}{h_{M-3}} & -\frac{1}{h_{M-3}} - \frac{1}{h_{M-2}} & \frac{1}{h_{M-2}} \end{pmatrix}, \quad (6)$$

$$\mathbf{M} = \begin{pmatrix} \frac{h_0+h_1}{3} & \frac{h_1}{6} & 0 & \dots & 0 & 0 \\ \frac{h_1}{6} & \frac{h_1+h_2}{3} & \frac{h_2}{6} & \dots & 0 & 0 \\ 0 & \frac{h_2}{6} & \frac{h_2+h_3}{3} & \dots & 0 & 0 \\ \vdots & \vdots & \vdots & \ddots & \vdots & \vdots \\ 0 & 0 & 0 & \dots & \frac{h_{M-4}+h_{M-3}}{3} & \frac{h_{M-3}}{6} \\ 0 & 0 & 0 & \dots & \frac{h_{M-3}}{6} & \frac{h_{M-3}+h_{M-2}}{3} \end{pmatrix}. \quad (7)$$

with $h_i = x_{i+1} - x_i$ for $i = 0, 1, \dots, M-2$. For the mathematical details on how to derive (5) from (4), please refer to Appendix A. Similarly, we can derive the first order derivatives and second order derivatives, which can also be found in Appendix A.

The advantage of the cubic spline in the functional estimation stage is that, its computational complexity is only a linear polynomial of the sample size. See the following proposition.

Proposition 2.1. Given data \mathcal{D} in (1), if we use the cubic spline in the functional estimation stage, i.e., estimate $\mathbf{X} \in \mathbb{R}^{MN \times K}$ via the cubic spline in (18) with $\alpha \in (0, 1]$ and $\nabla_t \mathbf{u} \in \mathbb{R}^{MN}$ from the cubic spline with $\bar{\alpha} \in (0, 1]$ similar in (4), then the computation

complexity in this stage is of order

$$\max\{O(p_{\max}MN), O(K^3)\},$$

where p_{\max} is the highest polynomial order in (3), M is the spatial resolution, N is the temporal resolution and K is the number of columns of \mathbf{X} .

The proof of the above proposition can be found in Appendix F.1.

As suggested by Proposition 2.1, when $p_{\max}, K \ll M, N$ (which is often the case in practice), it only requires $O(MN)$ numerical operations of the functional estimation stage. This is the lowest possible order of complexity in this stage because MN is exactly the number of the sample size and reading the data is an order $O(MN)$ task. So it can be concluded that it is very efficient to use cubic spline because its computational complexity achieves the lowest possible order of complexity.

For comparison, we discuss the computational complexity of the local polynomial regression, which is widely used in existing literature (see Liang and Wu, 2008; Bär et al., 1999; Schaeffer, 2017; Rudy et al., 2017; Parlitz and Merkwirth, 2000; Voss et al., 1999).

Proposition 2.2. Given data \mathcal{D} in (1), if we use the local polynomial regression in the functional estimation stage, i.e., estimate $\mathbf{X} \in \mathbb{R}^{MN \times K}, \nabla_t \mathbf{u} \in \mathbb{R}^{MN}$ via the local polynomial regression described as in Appendix F.2, then the computation complexity of this stage is of order

$$\max\{O(q_{\max}^2 M^2 N), O(MN^2), O(q_{\max}^3 MN), O(p_{\max} MN), O(K^3)\},$$

where p_{\max} is the highest polynomial order in (3), q_{\max} is the highest order of derivatives in (3), M is the spatial resolution, N is the temporal resolution, and K is the number of columns of \mathbf{X} .

If we set $q_{\max} = 2$ to match the derivative order of the local polynomial regression to the cubic spline, then the computation complexity is of order

$$\max\{O(M^2N), O(MN^2), O(p_{\max}MN), O(K^3)\}.$$

As suggested by Proposition 2.2, the computational complexity of local polynomial regression is much higher than that in the cubic spline. But the advantage of local polynomial regression is that it can derive any order of derivatives, i.e., $q_{\max} \geq 0$ in (3), while for the cubic spline, $q_{\max} = 2$. In applications, this should be sufficient because most of the PDE models are governed by derivatives up to the second derivative, for instance, heat equation, wave equation, Laplace's equation, Helmholtz equation, Poisson's equation, and so on. In our paper, we mainly use cubic spline as an illustration example due to its simplification and computational efficiency. Readers can extend our proposed SAPDEMI method to the higher-order spline with $q_{\max} > 2$ if they are interested in higher-order derivatives. We summarize the pros and cons of the cubic spline and the local polynomial regression in Table 1.

2.2 Model Identification Stage

In this section, we discuss the model identification stage of our proposed SAPDEMI method, where we want to identify the PDE model in (3).

The model in (3) can be regarded as a linear regression model whose response variable is the derivative with respect to temporal variable t , i.e., $\frac{\partial u(x,t)}{\partial t}$, and the covariates involve with the derivative with respect to spatial variable x , including $\frac{\partial}{\partial x}u(x_i, t_n), \frac{\partial^2}{\partial x^2}u(x_i, t_n), \dots, \left(\frac{\partial^2}{\partial x^2}u(x_i, t_n)\right)^{p_{\max}}$. Because we have MN observations in the dataset \mathcal{D} in (1), the response

Table 1: Pros and cons of the cubic spline and the local polynomial regression in the functional estimation stage

method	cubic spline	local polynomial regression
pros	only requires computational complexity $O(MN)$ in the functional estimation stage	can solve derivatives up to any order
cons	can only solve derivatives up to second order. If higher-order derivatives are required, extensions from cubic spline to higher-order splines are needed.	requires computational complexity $\max\{(M^2N), O(MN^2)\}$ in the functional estimation stage

¹ In this table, we assume that $p_{\max}, q_{\max}, K \ll M, N$ for simplification, where p_{\max} is the highest polynomial order in (3), q_{\max} is the highest order of derivatives desirable in (3), and K is the number of columns of \mathbf{X} in (9).

vector is of length MN :

$$\nabla_t \mathbf{u} = (\widehat{\frac{\partial u(x_0, t_0)}{\partial t}}, \widehat{\frac{\partial u(x_1, t_0)}{\partial t}}, \dots, \widehat{\frac{\partial u(x_{M-1}, t_0)}{\partial t}}, \widehat{\frac{\partial u(x_0, t_1)}{\partial t}}, \dots, \widehat{\frac{\partial u(x_{M-1}, t_{N-1})}{\partial t}})^\top \in \mathbb{R}^{MN}, \quad (8)$$

and design matrix is of dimension $MN \times K$:

$$\mathbf{X} = (\widehat{\mathbf{x}}_0^0, \widehat{\mathbf{x}}_1^0, \dots, \widehat{\mathbf{x}}_{M-1}^0, \widehat{\mathbf{x}}_1^1, \dots, \widehat{\mathbf{x}}_{M-1}^{N-1})^\top \in \mathbb{R}^{MN \times K}, \quad (9)$$

where the $nN + i + 1$ st row of the above matrix \mathbf{X} is

$$\widehat{\mathbf{x}}_i^n = \left(1, \widehat{u(x_i, t_n)}, \widehat{\frac{\partial}{\partial x} u(x_i, t_n)}, \widehat{\frac{\partial^2}{\partial x^2} u(x_i, t_n)}, \left(\widehat{u(x_i, t_n)}\right)^2, \widehat{u(x_i, t_n)} \frac{\partial}{\partial x} \widehat{u(x_i, t_n)}, \widehat{u(x_i, t_0)} \frac{\partial^2}{\partial x^2} \widehat{u(x_i, t_n)}, \dots, \left(\widehat{\frac{\partial^2}{\partial x^2} u(x_i, t_n)}\right)^{p_{\max}} \right)^\top \in \mathbb{R}^K.$$

The K components of $\widehat{\mathbf{x}}_i^n$ are candidate terms in the PDE model. And all the derivatives listed in (8), (9) are estimated from the functional estimation stage in Section 2.1.

After figuring out the response vector $\nabla_t \mathbf{u}$ and the design matrix \mathbf{X} , we use Lasso to identify the non-zero coefficients in (3):

$$\widehat{\boldsymbol{\beta}} = \arg \min_{\boldsymbol{\beta}} \frac{1}{2MN} \|\nabla_t \mathbf{u} - \mathbf{X} \boldsymbol{\beta}\|_2^2 + \lambda \|\boldsymbol{\beta}\|_1 \quad (10)$$

where $\lambda > 0$ is a turning parameter that controls the trade off of the sparsity of $\boldsymbol{\beta}$ and the goodness of fit. Given the ℓ_1 penalty in (10), $\widehat{\boldsymbol{\beta}}$ will be sparse, i.e., only a few of its entries will likely be non-zero. Accordingly, we can identify the underlying PDE model as

$$\frac{\partial}{\partial t} u(x, t) = \mathbf{x}^\top \widehat{\boldsymbol{\beta}}. \quad (11)$$

where

$$\mathbf{x} = \left(1, u(x, t), \frac{\partial}{\partial x} u(x, t), \frac{\partial^2}{\partial x^2} u(x, t), (u(x, t))^2, u(x_i, t) \frac{\partial}{\partial x} u(x, t), u(x, t) \frac{\partial^2}{\partial x^2} u(x, t), \dots, \left(\frac{\partial^2}{\partial x^2} u(x, t) \right)^{p_{\max}} \right)^\top \in \mathbb{R}^K.$$

It remains to discuss the numerical method to solve the optimization problem in (10). It is noted that there is no closed-form solution for (10) due to the ℓ_1 penalty. The existing algorithms to solve (10) is to iteratively update the estimator until convergence. One of the widely used algorithm to solve (10) is the coordinate descent, because it is well established in R within a package named *glmnet* (see Friedman et al., 2010) and Matlab within a function called *lasso*(\cdot). The main idea of the coordinate descent is to update the estimator in a coordinate-wise fashion, which is the main difference between the coordinate descent and regular gradient descent. And the convergence rate of the coordinate descent to solve (10) is $O(1/k)$, where k is the number of iteration executed (see Beck and Tetruashvili, 2013; Tseng, 2001). The detailed implementation of the coordinate descent to (10) is presented in Appendix B.

2.3 Overview of Our Proposed SAPDEMI method

In this section, we summarized our proposed SAPDEMI method into pseudo-code showing in Algorithm 1.

Algorithm 1: Pseudo code of our proposed SAPDEMI method

Input:

1. Data from the unknown PDE model as in (1);
2. Penalty parameter used in the Lasso identify model: $\lambda > 0$;
3. Smoothing parameter used in the cubic spline: $\alpha, \bar{\alpha} \in (0, 1]$.

Output: The identified/recovered PDE model.

1 Functional estimation stage:

2 Estimate $\mathbf{X}, \nabla_t \mathbf{u}$ by cubic spline with $\alpha, \bar{\alpha} \in (0, 1]$.

3 Model identification stage:

4 The unknown PDE system is recovered as: $\frac{\partial}{\partial t} u(x, t) = \mathbf{x}^\top \hat{\boldsymbol{\beta}}$, where
 $\hat{\boldsymbol{\beta}} = \arg \min_{\boldsymbol{\beta}} \frac{1}{2MN} \|\nabla_t \mathbf{u} - \mathbf{X} \boldsymbol{\beta}\|_2^2 + \lambda \|\boldsymbol{\beta}\|_1$ and $\mathbf{x} =$

$$\left(1, \ u(x, t), \ \frac{\partial u(x, t)}{\partial x}, \ \frac{\partial^2 u(x, t)}{\partial x^2}, \ (u(x, t))^2, \ u(x, t) \frac{\partial u(x, t)}{\partial x}, \ \dots, \ \left(\frac{\partial^2 u(x, t)}{\partial x^2} \right)^{p_{\max}} \right)^\top.$$

3 Recovery Theory

In this section, we present our main theorems. These two main theorems serve to evaluate the statistical prosperity of our identified PDE model. The evaluation is done from two aspects.

First, we check if our identified PDE model contains derivatives included in the underlying PDE models. This is the so-called *support set recovery*. Mathematically speaking,

it is to check if $\text{supp}(\widehat{\boldsymbol{\beta}}) \subseteq \text{supp}(\boldsymbol{\beta}^*)$, where $\widehat{\boldsymbol{\beta}}$ is the minimizer of (10), $\boldsymbol{\beta}^*$ is the ground truth, and $\text{supp}(\cdot)$ is an operator that collects the sets of indices of the non-zero entries of the input variable, i.e., $\text{supp}(\boldsymbol{\beta}) = \{i : \beta_i \neq 0, \forall i, 1 \leq i \leq K\}$ for a general vector $\boldsymbol{\beta} \in \mathbb{R}^K$. However, the support recovery depends on the choice of the penalty parameter λ . If we choose λ too large, then accordingly $\widehat{\boldsymbol{\beta}}$ would be a vector of all zero entries, which leads to $\text{supp}(\widehat{\boldsymbol{\beta}}) = \emptyset$ (empty set). On the other hand, if we choose λ too small, then $\widehat{\boldsymbol{\beta}}$ is not sparse enough, which makes it fail to identify the PDE models. The proper way to select λ hopefully leads to correct recovery of the support set recovery, i.e., we have $\text{supp}(\widehat{\boldsymbol{\beta}}) \subseteq \text{supp}(\boldsymbol{\beta}^*)$. We will discuss the selection of λ to realize the above objective in Theorem 3.1.

Second, we are interested in the estimation error bound of our estimator, i.e., $\|\widehat{\boldsymbol{\beta}}_{\mathcal{S}} - \boldsymbol{\beta}_{\mathcal{S}}^*\|_{\infty}$, where $\mathcal{S} = \text{supp}(\boldsymbol{\beta}^*)$, vector $\widehat{\boldsymbol{\beta}}_{\mathcal{S}}$ is the subvector of $\widehat{\boldsymbol{\beta}}$ only containing elements whose indices are in \mathcal{S} , and vector $\boldsymbol{\beta}_{\mathcal{S}}^*$ is the subvector of $\boldsymbol{\beta}^*$ only contains elements whose indices are in \mathcal{S} . The upper bound of the above estimation error will be discussed in Theorem 3.2.

The structure of this section is described as follows. In Section 3.1, we present the conditions for our main theorems. In Section 3.2, we state our two main theorems.

3.1 Our Conditions for the Theorems

In this section, we introduce some key conditions used in our paper. We begin with three frequently used conditions in ℓ_1 -regularized regression models. They were typically used to provide sufficient conditions for exact sparse recovery (see Hastie et al., 2015, Chapter 11). Besides, we also introduce some conditions from cubic splines, which serve for bounding the estimation error of the cubic splines (see Silverman, 1984, (2.5)-(2.8)). For the verification of these conditions, please refer to Section E for more details.

Condition 3.1 (Invertibility Condition). Suppose for the design matrix \mathbf{X} defined in (9) which is constructed by candidates of derivatives, we have that matrix $\mathbf{X}_S^\top \mathbf{X}_S$ is invertible almost surely, where \mathbf{X}_S is the columns of \mathbf{X} whose indices are in \mathcal{S} . Here $\mathcal{S} = \text{supp}(\boldsymbol{\beta}^*)$ where $\boldsymbol{\beta}^*$ is the ground truth and $\text{supp}(\boldsymbol{\beta}^*) = \{i : \beta_i^* \neq 0, \forall i, 1 \leq i \leq K\}$.

Condition 3.2 (Mutual Incoherence Condition). For some *incoherence parameter* $\mu \in (0, 1]$ and $P_\mu \in [0, 1]$, we have $\mathbb{P}(\|\mathbf{X}_{S^c}^\top \mathbf{X}_S (\mathbf{X}_S^\top \mathbf{X}_S)^{-1}\|_\infty \leq 1 - \mu) \geq P_\mu$, where the matrix \mathbf{X}_S is the columns of \mathbf{X} whose indices are in \mathcal{S} and matrix \mathbf{X}_{S^c} is the complement of \mathbf{X}_S .

Condition 3.3 (Minimal Eigenvalue Condition). There exists some constant $C_{\min} > 0$ such that $\Lambda_{\min}(\frac{1}{NM} \mathbf{X}_S^\top \mathbf{X}_S) \geq C_{\min}$, almost surely. Here $\Lambda_{\min}(\mathbf{A})$ denotes the minimal eigenvalue of a square matrix $\mathbf{A} \in \mathbb{R}^{n \times n}$. This condition can be considered as a strengthened version of Condition 3.1.

Condition 3.4 (Knots c.d.f. Convergence Condition). Suppose for the sequence of the empirical distribution function over the design points $x_0 < x_1 < \dots < x_{M-1}$ with different sample size M is denoted as $F_M(x)$, i.e., $F_M(x) = \frac{1}{M} \sum_{i=0}^{M-1} \mathbb{1}\{x_i \leq x\}$, there exists an absolutely continuous distribution function F on $[x_0, x_{M-1}]$ such that $F_M \rightarrow F$ uniformly as $M \rightarrow +\infty$. Here $\mathbb{1}\{A\}$ is the indicator of event A . Suppose for the sequence of the empirical distribution function over the design points $t_0 < t_1 < \dots < t_{N-1}$ with different sample size N is denoted as $G_N(x)$, there exists an absolutely continuous distribution function G on $[t_0, t_{N-1}]$ such that $G_N \rightarrow G$ uniformly as $N \rightarrow +\infty$.

Condition 3.5 (Knots p.d.f. Convergence Condition). Suppose the first derivative of the function F, G (defined in Condition 3.4) is denoted as f, g , respectively, then we have

$$0 < \inf_{[x_0, x_{M-1}]} f \leq \sup_{[x_0, x_{M-1}]} f < +\infty \text{ and } 0 < \inf_{[t_0, t_{N-1}]} g \leq \sup_{[t_0, t_{N-1}]} g < +\infty,$$

and f, g also have bounded first derivatives on $[x_0, x_{M-1}], [t_0, t_{N-1}]$, respectively.

Condition 3.6 (Gentle Decrease of Smoothing Parameter in Splines Condition). Suppose that $\zeta(M) = \sup_{[x_0, x_{M-1}]} |F_M - F|$, $\bar{\zeta}(N) = \sup_{[t_0, t_{N-1}]} |G_N - G|$, where F_M, G_M, F, G are defined in Condition 3.4. The smoothing parameter $\alpha, \bar{\alpha}$ in (4), which are used to estimate the derivatives with respective to x, t , respectively, depend on M, N in such a way that $\alpha \rightarrow 0$ and $\alpha^{-1/4}\zeta(M) \rightarrow 0$ as $M \rightarrow +\infty$. and $\bar{\alpha} \rightarrow 0$ and $\bar{\alpha}^{-1/4}\bar{\zeta}(N) \rightarrow 0$ as $N \rightarrow +\infty$.

3.2 Main Theory

In this section, we present our main theory, where Theorem 3.1 develops the lower bound of λ to realize the correct recovery of the support set, and Theorem 3.2 develops the upper bound of the estimation error.

First, we develop the theory on the lower bound of λ to realize the correct recovery of the support set, i.e., $\mathcal{S}(\hat{\beta}) \subseteq \mathcal{S}(\beta^*)$, where $\mathcal{S}(\hat{\beta}) = \{i : \hat{\beta}_i \neq 0, \forall i, 1 \leq i \leq K\}$ and $\mathcal{S}(\beta^*) = \{i : \beta_i^* \neq 0, \forall i, 1 \leq i \leq K\}$. And $\hat{\beta}$ is the optimum of (10), β^* is the ground truth of the underlying PDE models.

Theorem 3.1. Provided with the data in (1) and suppose the conditions in Lemma C.1 and Corollary C.1 hold and Condition 3.1 - 3.6 also hold, if we take $M = O(N)$, then there exists a constant $\mathcal{C}_{(\sigma, \|u\|_{L^\infty(\Omega)})} > 0$, which is independent of spatial resolution M and temporal resolution N , such that if we set the cubic spline smoothing parameter with the spatial variable x in (4) as $\alpha = O\left((1 + M^{-4/7})^{-1}\right)$, set the cubic spline smoothing parameter with the temporal variable t as $\bar{\alpha} = O\left((1 + N^{-4/7})^{-1}\right)$, and set the turning parameter

$$\lambda \geq \mathcal{C}(\sigma, \|u\|_{L^\infty(\Omega)}) \frac{\sqrt{K} \log(N)}{\mu N^{3/7-r}}, \quad (12)$$

to identify the PDE model in (10) for some $r \in (0, \frac{3}{7})$ with sufficient large N , then with

probability greater than $P_\mu - \underbrace{O(Ne^{-Nr})}_{P'}$, we can have $\mathcal{S}(\hat{\beta}) \subseteq \mathcal{S}(\beta^*)$. Here K is the number of columns of the design matrix \mathbf{X} in (10), and μ, P_μ are defined in Condition 3.2.

The proof of the above theorem can be found in Appendix F.5. To ease the understanding of the proofs of main theorems, readers can refer to some lemmas in Appendix C.

The above theorem states the lower bound of λ to realize the correct recovery of the support set recovery. And this lower bound in (12) is affected by several factors. First, it is affected by the temporal resolution N : as N increases, there is more flexibility in tuning this penalty parameter λ . Second, the lower bound in (12) is affected by the incoherence parameter μ : if μ is small, then the lower bound increases. This is because small μ means that the group of feature variable candidates are similar to each other. It should be noted that μ is decided by the dataset \mathcal{D} itself (see Condition 3.2). Third, this lower bound in (12) is affected by the number of columns of the matrix \mathbf{X} . If the number of columns in \mathbf{X} is very large, then it requires larger λ to identify the significant feature variables among lots of feature variable candidates.

We also point out that, the large probability $P_\mu - P'$ converges to P_μ as $N \rightarrow +\infty$. This limiting probability P_μ is determined by the data \mathcal{D} (see Condition (3.2)). So we know that when N is very large, our proposed SAPDEMI method can realize $\mathcal{S}(\hat{\beta}) \subseteq \mathcal{S}(\beta^*)$.

Now, we develop the theorem to obtain the estimation error bound.

Theorem 3.2. Suppose the conditions in Theorem 3.1 hold, then with probability greater than $1 - O(Ne^{-Nr}) \rightarrow 1$, there exist a $\dot{N} > 0$, such that when $N > \dot{N}$, we have

$$\|\hat{\beta}_S - \beta_S^*\|_\infty \leq \sqrt{K} C_{\min} \left(\sqrt{K} \mathcal{C}_{(\sigma, \|u\|_{L^\infty(\Omega)})} \frac{\log(N)}{N^{3/7-r}} + \lambda \right),$$

where K is the number of columns of the matrix \mathbf{X} , \mathcal{S} is the support set of $\boldsymbol{\beta}^*$, i.e., $\mathcal{S} := \{i : \beta_i^* \neq 0, \forall i = 1, \dots, K\}$ and vector $\widehat{\boldsymbol{\beta}}_{\mathcal{S}}, \boldsymbol{\beta}_{\mathcal{S}}^*$ are the subvector of $\widehat{\boldsymbol{\beta}}, \boldsymbol{\beta}^*$ only contains elements whose indices are in \mathcal{S} . Viewing from this theorem, we can see that when $N \rightarrow +\infty$, the error bound will converge to 0.

The proof of the above theorem can be found in Appendix F.6.

From the above theorem, we can see that, the estimation error bound for the ℓ_∞ -norm of the coefficient error in (13) consists of two components. The first component is affected by the temporal resolution N , and the number of feature variable candidates K . As $N \rightarrow +\infty$, this first component convergence to 0 without explicit dependence on the choice of feature variable selected from (10). The second component is $\sqrt{K}C_{\min}\lambda$. When N increases to $+\infty$, this second component will also converge to 0. This is because, as stated in Theorem 3.1, we find that when $N \rightarrow +\infty$, the lower bound of λ – which realizes correct support recovery – converges to 0. So the accuracy of the coefficient estimation will improve if we increase the temporal resolution N .

By combining statements in Theorem 3.1 and Theorem 3.2 together, we find that when the minimum absolute value of the nonzero entries of $\boldsymbol{\beta}^*$ is large enough, then with the adequate choice of lambda, the exact recovery can be guaranteed. Mathematically speaking, when $\min_{i \in \mathcal{S}} |(\boldsymbol{\beta}_{\mathcal{S}}^*)_i| > \sqrt{K}C_{\min} \left(\sqrt{K}\mathcal{C}_{(\sigma, \|u\|_{L^\infty(\Omega)})} \frac{\log(N)}{N^{3/7-r}} + \lambda \right)$, the vector $\widehat{\boldsymbol{\beta}}$ will have a correct signed-support, where $(\boldsymbol{\beta}_{\mathcal{S}}^*)_i$ refers to the i th element in vector $\boldsymbol{\beta}_{\mathcal{S}}^*$. This helps for the selection of the penalty parameters λ . Besides, the solution paths plot also helps with the selection of the penalty parameters λ , and we will discuss it in Section 4 under concrete examples.

4 Numerical Examples

In this section, we conduct numerical examples to verify the computational efficiency and the statistical accuracy of our proposed SAPDEMI method. The computational efficiency refers to the computational complexity of the functional estimation stage is of a linear polynomial of the sample size MN ; The statistical accuracy measures our proposed SAPDEMI can correctly identify the underlying PDE models with high probability. Besides, we also check the whether Condition 3.1 - Condition 3.6 hold in Appendix E.

The numerical examples include (1) the transport equation, (2) the inviscid Burgers' equation and (3) the viscous Burgers' equation. We select these three PDE models as representatives because all these PDE models play fundamental roles in modeling physical phenomenon and demonstrate characteristic behaviors shared by a more complex system, such as dissipation and shock-formation (see Haberman, 1983). Besides, the difficulty to identify the above PDE models increase from the first example — the transport equation – to the last example – the viscous Burgers' equation..

For the computational efficiency, the results of these three examples are the nearly same, because the computational complexity only depends on the dimension of the noisy data, i.e., the dimension of $\mathbf{X}, \nabla_t \mathbf{u}$, and it is independent of which type of PDE model it comes from. So we only present a detailed discussion of the computational efficiency in the first example – the transport equation.

4.1 Example 1: Transport Equation

The PDE problem we used in this subsection is the transport equation (see Olver, 2014, Section 2.2):

$$\begin{cases} \frac{\partial}{\partial t}u(x, t) = a \frac{\partial}{\partial x}u(x, t) & \forall 0 \leq x \leq X_{\max}, 0 \leq t \leq T_{\max}; \\ u(x, 0) = f(x); \end{cases} \quad (13)$$

where we set $f(x) = 2 \sin(4x)$, $a = -2$, $X_{\max} = 1$, $T_{\max} = 0.1$. From the above settings, we know there is a closed-form solution, which is $u(x, t) = 2 \sin(4x - 8t)$.

The dynamic pattern of the above transport equation is visualized in Figure 1. In this figure, (a),(b),(c) are the ground truth, noisy observation under $\sigma = 0.05$ and $\sigma = 0.1$, respectively. From this figure, we can see that the larger the noise, the more un-smoothed the shape of the transport equation would be, which potentially leads to more difficulties in the PDE model identification.

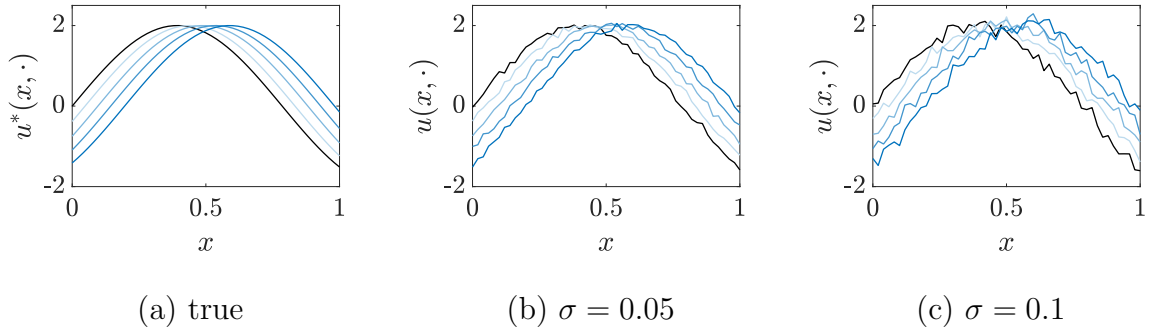


Figure 1: The curves of the transport equation ($M = N = 100$)

First of all, let us take a look at the computational complexity of the functional estimation stage. To show the efficiency of the cubic spline, which is used in our SAPDEMI method, we select the local polynomial regression as a benchmark, whose detailed descriptions can be found in Appendix F.2. We visualize the number of numerical operations in

the functional estimation stage of the above two methods in Figure 2, where the x-axis is the logarithm of M or N , and the y-axis is the logarithm of the number of numerical operations. The numbers to plot this figure is summarized in Table 2 in Appendix D. In Figure 2, two scenarios are discussed: (1) M is fixed as 20 and N varies from 200 to 2000; (2) N is fixed as 20 and M varies from 200 to 2000. As we can see from Figure 2 that, as M or N increases, the number of numerical operations in the functional estimation stage becomes larger. And cubic spline needs fewer numerical operations, compared with local polynomial regression. Furthermore, if we conduct a simple linear regression of the four lines in Figure 2, we find that in (a), the slope of the cubic spline (blue solid line) is 0.9998, and as N goes to infinity, the slope will get closer to 1. This validates that the computational complexity of cubic spline is of order $O(N)$ when M is fixed (given $K, p_{\max} \ll N$). Besides, in (b) the slope of the cubic spline (blue solid line) is 1.274, and as M goes to infinity, the slope will get closer to 1. This validates that the computational complexity of cubic spline is of order $O(M)$ when N is fixed (given $K, p_{\max} \ll M$). Therefore, we numerically verify that when $K \ll M, N$ and $p_{\max} \ll M, N$, the computational complexity of cubic spline is of order $O(MN)$ (given $K, p_{\max} \ll N$). Similarly, for local polynomial (see Proposition 2.2), we know that when M is fixed (Figure 2(a)), the slope of the local polynomial regression (pink dashed line) is 1.822, which validates that the computational complexity of the local polynomial is of order $O(N^2)$ when M is fixed. And as N goes to infinity, the slope gets closer to 2. Besides, when N is fixed (Figure 2(b)), the slope of the local polynomial regression (pink dashed line) is 1.960, which validate that the computational complexity of local polynomial regression when N is fixed is of order $O(M^2)$. And as M goes to infinity, the slope will get closer to 2. This validates that the computational complexity of the local polynomial regression method is $\max\{O(M^2N), O(MN^2)\}$ when $K, p_{\max} \ll N$.

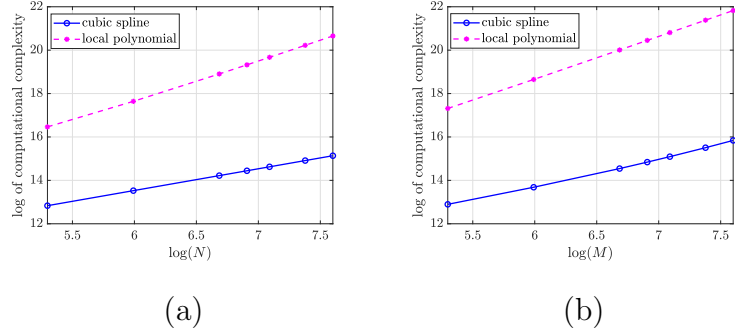


Figure 2: (a) Computational complexity of cubic spline (blue solid line) & local polynomial regression (red dash line) with fixed $M=20$, (b) computational complexity of cubic spline (blue solid line) & local polynomial regression (red dashed line) with fixed $N=20$

Second, we numerically verify that with high probability, our proposed SAPDEMI can correctly identify the underlying PDE models. From the formula of the transport equation in equation (13), we know that the correct feature variable is only $\frac{\partial}{\partial x}u(x, t)$, which should be identified. While other feature variables, for examples, $u(x, t)$, $\frac{\partial^2}{\partial x^2}u(x, t)$ etc., should not be identified. We discuss the identification accuracy our proposed SAPDEMI under different sample size ($M = N = 100, M = N = 150, M = N = 200$) and different magnitude of noise level ($\sigma = \{0.01, 0.05, 0.1, 0.25, 0.5, 0.75, 0.8, 0.9, 1\}$). We find that, for this transport equation, the accuracy stays at 100% under the different magnitude of σ and sample size M, N . To explain the high accuracy, we plot the solution paths in Figure 3 under different magnitude of σ , i.e., $\sigma = 0.01, 0.1, 1$. The x-axis of Figure 3 is λ , which increases from a very small number to a large number. The y-axis of Figure 3 is the coefficients corresponding to all candidates of feature variables. The red lines present the coefficient corresponding to $\frac{\partial}{\partial x}u(x, t)$, which is the correct feature variable. While the black dashed lines present the coefficient corresponding to other incorrect feature variables, which shouldn't be selected.

It can be seen from Figure 3 that, though large noise increases the difficulty to realize correct identification, we can increase λ to overcome this difficulty, and thus realize correct PDE identification. This solution paths plot can help with the selection of the penalty parameters λ . For (a),(b) in Figure 3, we find there is only one solution path that keeps non-zero as λ increase, then this covariate should be identified. For Figure 3(c), there are several solution paths that keep non-zero, then the selection of λ depends on (1) how many covariates desirable in the model, (2) the change-points of λ . The change-points refer to the value of λ where the support set changes. For instance, in Figure 3(c), the change-points are $\lambda^1 = 0.2, \lambda^2 = 0.4, \lambda^3 = 1$. Since the distance between λ^1, λ^2 is very close, we would much prefer to select λ^3 for correct support recovery.

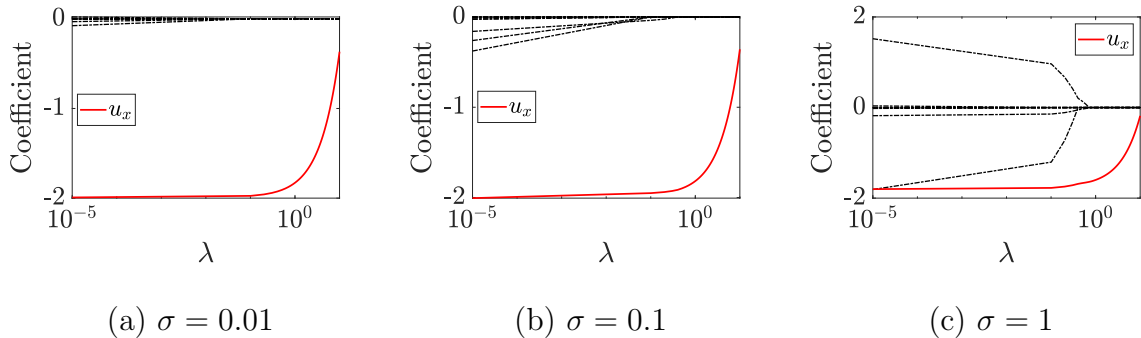


Figure 3: The solution paths of the identification in the transport equation under different magnitude of noise levels, i.e., $\sigma = 0.01, 0.1, 1$. The red lines present the coefficient corresponding to $\frac{\partial}{\partial x}u(x, t)$, which is the correct feature variable. While the black dashed lines present the coefficient corresponding to other incorrect feature variables, which shouldn't be selected. Here we set $M = N = 100$, and u_x is the simplification of $\frac{\partial}{\partial x}u(x, t)$.

4.2 Example 2: Inviscid Burgers' Equation

In this section, we take a little more challenging example – the inviscid Burgers' equation (see Olver, 2014, Section 8.4), whose definition is shown as follows:

$$\begin{cases} \frac{\partial}{\partial t}u(x, t) = -\frac{1}{2}u(x, t)\frac{\partial}{\partial x}u(x, t) \\ u(x, 0) = f(x) \quad 0 \leq x \leq X_{\max} \\ u(0, t) = u(1, t) = 0 \quad 0 \leq t \leq T_{\max} \end{cases}, \quad (14)$$

where we set $f(x) = \sin(2\pi x)$, $X_{\max} = 1$, $T_{\max} = 0.1$. Figure 4(a),(b),(c) show the shape of its ground truth, noisy observation under $\sigma = 0.05$, $\sigma = 0.1$, respectively.

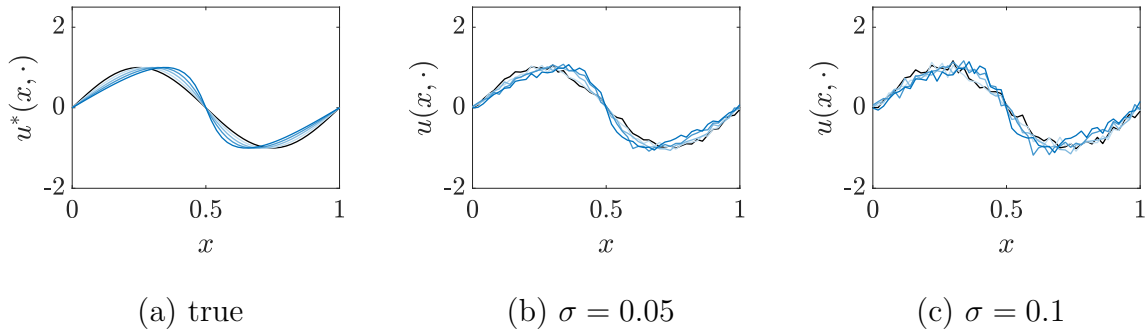


Figure 4: The curves of the inviscid Burgers' equation ($M = 50, N = 50$)

For this inviscid Burgers' equation, we declare that with high probability, our proposed SAPDEMI can correctly identify it. The simulation results are summarized in Figure 8(a) and . From this figure, we find the accuracy stays above 99% when σ ranges from 0.01 to 1. Also, as suggested by Figure 8(a), the accuracy decrease as σ increase, which makes sense because large noise makes it more difficult to realize correct identification. The effect of noise to PDE identification can be found in the solution paths plot in Figure 5, where we can see that the length of λ -interval for correct identification decreases as σ increases.

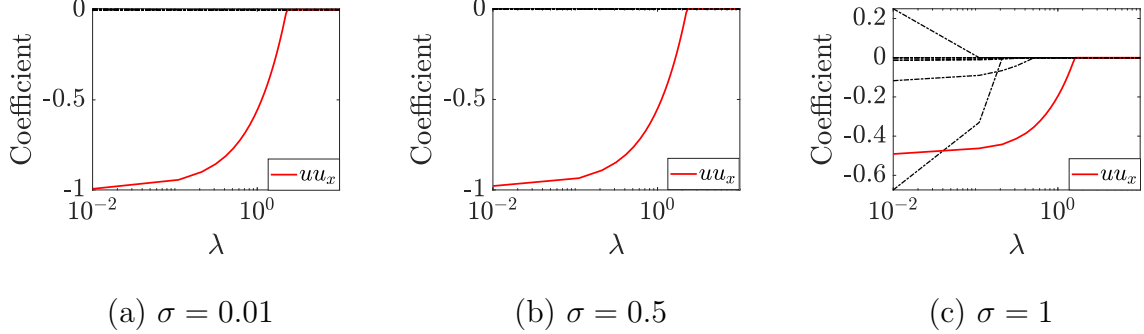


Figure 5: The solution paths of the identification in the inviscid Burger's equation under different magnitude of noise levels, i.e., $\sigma = 0.01, 0.5, 1$. The red lines present the coefficient corresponding to $u(x, t) \frac{\partial}{\partial x} u(x, t)$. While the black dashed lines present the coefficient corresponding to other feature variables. Here we set $M = N = 100$ and the label u, u_x are the simplification of to $u(x, t), \frac{\partial}{\partial x} u(x, t)$, respectively.

4.3 Example 3: Viscous Burgers' Equation

In this section, we take a more challenging example, i.e., viscous Burgers' equation (see Olver, 2014, Section 8.4):

$$\begin{cases} \frac{\partial}{\partial t} u(x, t) = -\frac{1}{2} u(x, t) \frac{\partial}{\partial x} u(x, t) + \nu \frac{\partial^2}{\partial x^2} u(x, t) \\ u(x, 0) = f(x) \\ u(0, t) = u(1, t) = 0 \end{cases} \quad 0 \leq x \leq X_{\max}, \quad 0 \leq t \leq T_{\max}, \quad (15)$$

where we set $f(x) = \sin^2(4\pi x) + \sin^3(2\pi x)$, $X_{\max} = 1$, $T_{\max} = 0.1$, $\nu = 0.1$. Figure 6 shows the shape of the viscous Burgers' equation, where (a),(b),(c) are the ground truth, noisy observation under $\sigma = 0.05$ and $\sigma = 0.1$, respectively.

Based on the simulation results in Figure 8(b) and Table 3, we conclude that with high probability, our proposed SAPDEMI can correctly identify the underlying viscous Burgers' equation, with the reasons given as follows. When $M = N = 200$, the accuracy stays at

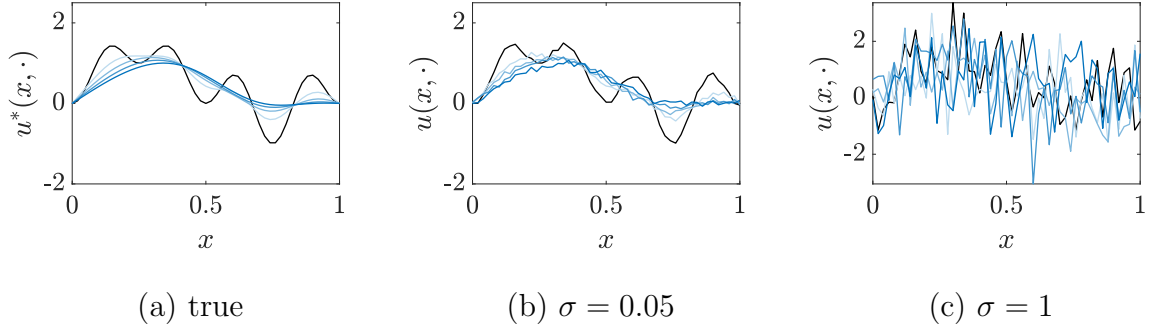


Figure 6: The curves of the viscous Burgers' equation ($M = 50, N = 50$)

100% for all levels of $\sigma \in [0.01, 1]$. When $M = N = 150$, the accuracy stays above 90% for all levels of $\sigma \in [0.01, 1]$. When $M = N = 100$, the accuracy are above 70% when $\sigma \in [0.01, 0.5]$, and reduces to around 50% when $\sigma = 1$, which makes sense because as reselected by Figure 7, when σ increase from 0.01 to 1, the length of λ -interval for correct identification decreases, which make it more difficult to realize correct identification. So if we encounter a heavily noised dataset \mathcal{D} , a larger sample size is preferred.

5 Conclusion

In this paper, we propose a two-stage method called SAPDEMI to efficiently identify the underlying PDE models from the noisy data in \mathcal{D} . In the first stage – functional estimation stage – we employ the cubic spline to estimate the unobservable derivatives, which serve as input variables for the second stage. In the second stage – model identification stage – we apply the Lasso to identify the underlying PDE model. The contributions of our proposed SAPDEMI method are: (1) it is computationally efficient because it only requires the computational complexity of order $O(MN)$, which achieves the lowest possible order

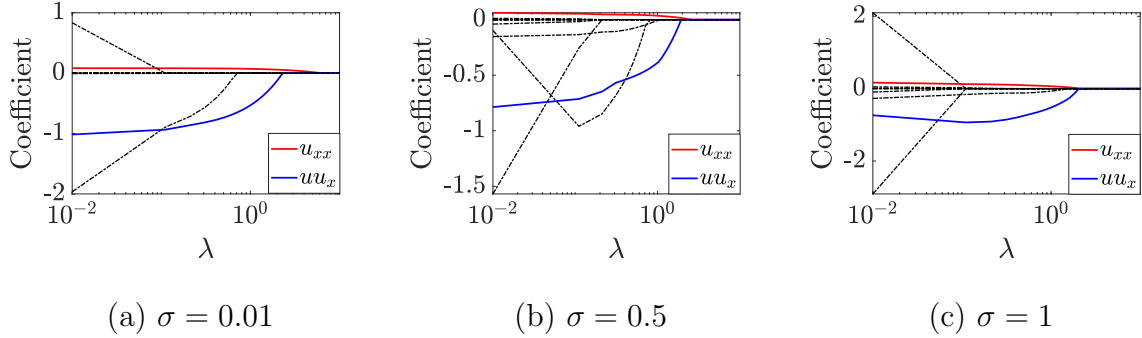
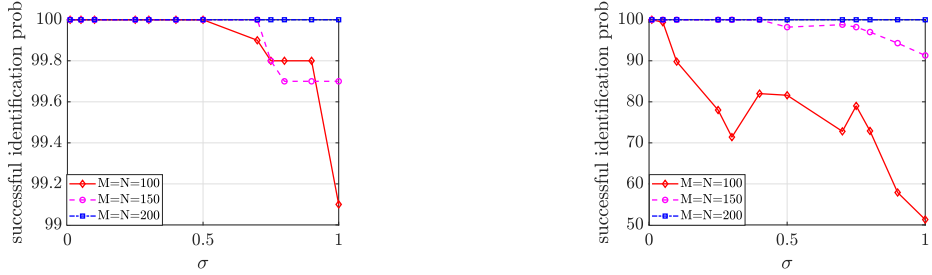


Figure 7: The solution paths of the identification in the viscous Burger's equation under different magnitude of noise levels, i.e., $\sigma = 0.01, 0.5, 1$. The red and blue lines present the coefficient corresponding to $\frac{\partial^2}{\partial x^2}u(x, t)$ and $u(x, t)\frac{\partial}{\partial x}u(x, t)$, respectively, while the black dashed lines present the coefficient corresponding to other feature variables. Here $M = N = 100$ and the label u_{xx}, uu_x are the simplification of $u(x, t)\frac{\partial}{\partial x}u(x, t), \frac{\partial^2}{\partial x^2}u(x, t)$, respectively.

of complexity; (2) we focus on the model selections, while the existing literature mostly focuses on parameter estimations; (3) we develop asymptotic properties of our method for correct identification, which is not reported by the existing literature.

After developing this SAPDEMI method, we realize there are lots of promising future research directions. First, in our paper, we take $x \in \mathbb{R}$ as an illustration example, and it would be interesting to investigate the case when the spatial variable $\mathbf{x} \in \mathbb{R}^d$ ($d \geq 2$) due to its wide existence in practice. Second, future research could consider the interaction between the spatial variable and the temporal variable. For instance, we can explore the time-varying coefficient $\beta(t) = (\beta_1(t), \dots, \beta_K(t))^\top$ in (3). Besides, we can also consider the case when the ϵ_i^n in (2) has spatial-temporal patterns. In our paper, because we aim at showing the methodology to solve the PDE identification problem, we do not discuss the



(a) example 2: inviscid Burgers equation (b) example 3: viscous Burgers equation

Figure 8: The successful identification probability curves under different magnitude of σ and sample size M, N . The successful identification probability of the example 1 – transport equation – stays in 100% for $\sigma \in [0.01, 1]$ and $M, N \in \{100, 150, 200\}$, and we neglect the figure for this 100% accuracy. Seeing from these figures, we can find that example 3 – viscous Burgers equation – is the hardest, and example 1 – transport equation – is the easiest. (The numbers to plot this figure can be found in Table 3 in Appendix D.)

above future research directions in detail and hopefully, our paper provides a good starting point for further research.

References

Ahlberg, J., J. Walsh, R. Bellman, and E. N. Nilson (1967). *The theory of splines and their applications*. Academic press.

Azzimonti, L., L. M. Sangalli, P. Secchi, M. Domanin, and F. Nobile (2015). Blood flow velocity field estimation via spatial regression with PDE penalization. *Journal of the American Statistical Association* 110(511), 1057–1071.

Bär, M., R. Hegger, and H. Kantz (1999). Fitting partial differential equations to space-time dynamics. *Physical Review E* 59(1), 337.

Beck, A. and L. Tetruashvili (2013). On the convergence of block coordinate descent type methods. *SIAM journal on Optimization* 23(4), 2037–2060.

Brunton, S. L., J. L. Proctor, and J. N. Kutz (2016). Discovering governing equations from data by sparse identification of nonlinear dynamical systems. *Proceedings of the national academy of sciences* 113(15), 3932–3937.

Butt, R. (2008). *Introduction to numerical analysis using MATLAB*. Laxmi Publications, Ltd.

Craven, P. and G. Wahba (1978). Smoothing noisy data with spline functions. *Numerische mathematik* 31(4), 377–403.

Fan, J., T. Gasser, I. Gijbels, M. Brockmann, and J. Engel (1997). Local polynomial regression: optimal kernels and asymptotic minimax efficiency. *Annals of the Institute of Statistical Mathematics* 49(1), 79–99.

Fornberg, B. (1981). Numerical differentiation of analytic functions. *ACM Transactions on Mathematical Software (TOMS)* 7(4), 512–526.

Friedman, J., T. Hastie, and R. Tibshirani (2010). Regularization paths for generalized linear models via coordinate descent. *Journal of statistical software* 33(1), 1.

Haberman, R. (1983). *Elementary applied partial differential equations*, Volume 987. Prentice Hall Englewood Cliffs, NJ.

Hastie, T., R. Tibshirani, and M. Wainwright (2015). *Statistical learning with sparsity: the lasso and generalizations*. CRC press.

Kang, S. H., W. Liao, and Y. Liu (2019). Ident: Identifying differential equations with numerical time evolution. *arXiv preprint arXiv:1904.03538*.

Liang, H. and H. Wu (2008). Parameter estimation for differential equation models using a framework of measurement error in regression models. *Journal of the American Statistical Association* 103(484), 1570–1583.

Mack, Y.-p. and B. W. Silverman (1982). Weak and strong uniform consistency of kernel regression estimates. *Zeitschrift für Wahrscheinlichkeitstheorie und verwandte Gebiete* 61(3), 405–415.

Mangan, N. M., S. L. Brunton, J. L. Proctor, and J. N. Kutz (2016). Inferring biological networks by sparse identification of nonlinear dynamics. *IEEE Transactions on Molecular, Biological and Multi-Scale Communications* 2(1), 52–63.

Mangan, N. M., J. N. Kutz, S. L. Brunton, and J. L. Proctor (2017). Model selection for dynamical systems via sparse regression and information criteria. *Proceedings of the Royal Society A: Mathematical, Physical and Engineering Sciences* 473(2204), 20170009.

McKinley, S. and M. Levine (1998). Cubic spline interpolation. *College of the Redwoods* 45(1), 1049–1060.

Messer, K. et al. (1991). A comparison of a spline estimate to its equivalent kernel estimate. *The Annals of Statistics* 19(2), 817–829.

Miao, H., C. Dykes, L. M. Demeter, and H. Wu (2009). Differential equation modeling of HIV viral fitness experiments: model identification, model selection, and multimodel inference. *Biometrics* 65(1), 292–300.

Olver, P. J. (2014). *Introduction to partial differential equations*. Springer.

Parlitz, U. and C. Merkwirth (2000). Prediction of spatiotemporal time series based on reconstructed local states. *Physical review letters* 84(9), 1890.

Ramsay, J. O. (1996). Principal differential analysis: Data reduction by differential operators. *Journal of the Royal Statistical Society: Series B (Methodological)* 58(3), 495–508.

Ramsay, J. O., G. Hooker, D. Campbell, and J. Cao (2007). Parameter estimation for differential equations: a generalized smoothing approach. *Journal of the Royal Statistical Society: Series B (Statistical Methodology)* 69(5), 741–796.

Rashidinia, J. and R. Mohammadi (2008). Non-polynomial cubic spline methods for the solution of parabolic equations. *International Journal of Computer Mathematics* 85(5), 843–850.

Rice, J. and M. Rosenblatt (1983). Smoothing splines: regression, derivatives and deconvolution. *The annals of Statistics*, 141–156.

Rosenblatt, M. (1952). Remarks on a multivariate transformation. *The annals of mathematical statistics* 23(3), 470–472.

Rubin, S. G. and R. A. Graves Jr (1975). A cubic spline approximation for problems in fluid mechanics. *NASA STI/Recon Technical Report N* 75, 33345.

Rudy, S. H., S. L. Brunton, J. L. Proctor, and J. N. Kutz (2017). Data-driven discovery of partial differential equations. *Science Advances* 3(4), e1602614.

Schaeffer, H. (2017). Learning partial differential equations via data discovery and sparse optimization. *Proceedings of the Royal Society A: Mathematical, Physical and Engineering Sciences* 473(2197), 20160446.

Schaeffer, H., R. Caflisch, C. D. Hauck, and S. Osher (2013). Sparse dynamics for partial differential equations. *Proceedings of the National Academy of Sciences* 110(17), 6634–6639.

Silverman, B. W. (1978). Weak and strong uniform consistency of the kernel estimate of a density and its derivatives. *The Annals of Statistics*, 177–184.

Silverman, B. W. (1984). Spline smoothing: the equivalent variable kernel method. *The Annals of Statistics*, 898–916.

Squire, W. and G. Trapp (1998). Using complex variables to estimate derivatives of real functions. *SIAM review* 40(1), 110–112.

Tibshirani, R. (1996). Regression shrinkage and selection via the lasso. *Journal of the Royal Statistical Society: Series B (Methodological)* 58(1), 267–288.

Tran, G. and R. Ward (2017). Exact recovery of chaotic systems from highly corrupted data. *Multiscale Modeling & Simulation* 15(3), 1108–1129.

Tseng, P. (2001). Convergence of a block coordinate descent method for nondifferentiable minimization. *Journal of optimization theory and applications* 109(3), 475–494.

Tusnády, G. (1977). A remark on the approximation of the sample df in the multidimensional case. *Periodica Mathematica Hungarica* 8(1), 53–55.

Ueberhuber, C. W. (2012). *Numerical computation 1: methods, software, and analysis*. Springer Science & Business Media.

Voss, H. U., P. Kolodner, M. Abel, and J. Kurths (1999). Amplitude equations from spatiotemporal binary-fluid convection data. *Physical review letters* 83(17), 3422.

Wang, D., K. Liu, and X. Zhang (2019). Spatiotemporal thermal field modeling using partial differential equations with time-varying parameters. *IEEE Transactions on Automation Science and Engineering*.

Winkelbauer, A. (2012). Moments and absolute moments of the normal distribution. *arXiv preprint arXiv:1209.4340*.

Wu, H., H. Xue, and A. Kumar (2012). Numerical discretization-based estimation methods for ordinary differential equation models via penalized spline smoothing with applications in biomedical research. *Biometrics* 68(2), 344–352.

Xun, X., J. Cao, B. Mallick, A. Maity, and R. J. Carroll (2013). Parameter estimation of partial differential equation models. *Journal of the American Statistical Association* 108(503), 1009–1020.

A Derivation of the 0-th, First, Second Derivative of the Cubic Spline in (4).

In this section, we focus on solving the derivatives of $u(x, t_n)$ with respective to x , i.e., $\left\{u(x_i, t_n), \frac{\partial}{\partial x}u(x_i, t_n), \frac{\partial^2}{\partial x^2}u(x_i, t_n)\right\}_{i=0,1,\dots,M-1}$ for any $n = 0, 1, \dots, N - 1$. To realize this objective, we first fix t as t_n for a general $n \in \{0, 1, \dots, N - 1\}$. Then we use cubic spline to fit data $\{(x_i, u_n^i)\}_{i=0,1,\dots,M-1}$.

Suppose the cubic polynomial spline over the knots $\{(x_i, u_n^i)\}_{i=0,1,\dots,M-1}$ is $s(x)$. So under good approximation, we can regard $s(x), s'(x), s''(x)$ as the estimators of $u(x_i, t_n), \frac{\partial}{\partial x}u(x_i, t_n), \frac{\partial^2}{\partial x^2}u(x_i, t_n)$, where $s'(x), s''(x)$ is the first and second derivatives of $s(x)$, respectively.

Let first take a look at the zero-order derivatives of $s(x)$. By introducing matrix algebra, the objective function in equation (4) can be rewritten as

$$J_\alpha(s) = \alpha(\mathbf{u}_\cdot^n - \mathbf{f})^\top \mathbf{W}(\mathbf{u}_\cdot^n - \mathbf{f}) + (1 - \alpha)\mathbf{f}^\top \mathbf{A}^\top \mathbf{M}^{-1} \mathbf{A}\mathbf{f} \quad (16)$$

where vector

$$\mathbf{f} = \begin{pmatrix} s(x_0) \\ s(x_1) \\ \vdots \\ s(x_{M-1}) \end{pmatrix} \triangleq \begin{pmatrix} f_0 \\ f_1 \\ \vdots \\ f_{M-1} \end{pmatrix}, \mathbf{u}_\cdot^n = \begin{pmatrix} u_0^n \\ u_1^n \\ \vdots \\ u_{M-1}^n \end{pmatrix}$$

and matrix $\mathbf{W} = \text{diag}(w_0, w_1, \dots, w_{M-1})$ and matrix \mathbf{A} is defined in (6). By taking the derivative of (16) with respective to \mathbf{f} and set it as zero, we have

$$\widehat{\mathbf{f}} = [\alpha\mathbf{W} + (1 - \alpha)\mathbf{A}^\top \mathbf{M} \mathbf{A}]^{-1} \alpha \mathbf{W} \mathbf{u}_\cdot^n. \quad (17)$$

Then we solve the second-order derivative with respective to x . Let us first suppose that the cubic spline $s(x)$ in $[x_i, x_{i+1}]$ is denoted $s_i(x)$, and we denote $s_i''(x_i) = \sigma_i, s_i''(x_{i+1}) =$

σ_{i+1} . Then we have $\forall x \in [x_i, x_{i+1}]$ ($0 \leq i \leq M-2$),

$$s_i''(x) = \sigma_i \frac{x_{i+1} - x}{h_i} + \sigma_{i+1} \frac{x - x_i}{h_i},$$

where matrix \mathbf{M} is defined in (7). This is because $s_i''(x)$ with $x \in [x_i, x_{i+1}]$ is a linear function. By taking a double integral of the above equation, we have

$$s_i(x) = \frac{\sigma_i}{6h_i}(x_{i+1} - x)^3 + \frac{\sigma_{i+1}}{6h_i}(x - x_i)^3 + c_1(x - x_i) + c_2(x_{i+1} - x), \quad (18)$$

where c_1, c_2 is the unknown parameters to be estimated. Because $s_i(x)$ interpolates two endpoints (x_i, f_i) and (x_{i+1}, f_{i+1}) , if we plug x_i, x_{i+1} into the above $s_i(x)$, we have

$$\begin{cases} f_i &= s_i(x_i) = \frac{\sigma_i}{6}h_i^2 + c_2h_i \\ f_{i+1} &= s_i(x_{i+1}) = \frac{\sigma_{i+1}}{6}h_i^2 + c_1h_i, \end{cases}$$

where we can solve c_1, c_2 as

$$\begin{cases} c_1 &= (f_{i+1} - \frac{\sigma_{i+1}}{6}h_i^2)/h_i \\ c_2 &= (f_i - \frac{\sigma_i}{6}h_i^2)/h_i. \end{cases}$$

By plugging in the value of c_1, c_2 into equation (18), we have ($0 \leq i \leq M-2$)

$$s_i(x) = \frac{\sigma_i}{6h_i}(x_{i+1} - x)^3 + \frac{\sigma_{i+1}}{6h_i}(x - x_i)^3 + \left(\frac{f_{i+1}}{h_i} - \frac{\sigma_{i+1}h_i}{6} \right) (x - x_i) + \left(\frac{f_i}{h_i} - \frac{\sigma_i h_i}{6} \right) (x_{i+1} - x)$$

with its first derivative as

$$s_i'(x) = -\frac{\sigma_i}{2h_i}(x_{i+1} - x)^2 + \frac{\sigma_{i+1}}{2h_i}(x - x_i)^2 + \frac{f_{i+1} - f_i}{h_i} - \frac{h_i}{6}(\sigma_{i+1} - \sigma_i). \quad (19)$$

Because $s'_{i-1}(x_i) = s'_i(x_i)$, we have ($1 \leq i \leq M-2$)

$$\frac{1}{6}h_{i-1}\sigma_{i-1} + \frac{1}{3}(h_{i-1} + h_i)\sigma_i + \frac{1}{6}h_i\sigma_{i+1} = \frac{f_{i+1} - f_i}{h_i} - \frac{f_i - f_{i-1}}{h_{i-1}}. \quad (20)$$

Equation (20) gives $M-2$ equations. Recall $\sigma_0 = \sigma_{M-1} = 0$, so totally we get M equations, which is enough to solve M parameters, i.e., $\sigma_0, \sigma_1, \dots, \sigma_{M-1}$. We write out the above system of linear equations, where we hope to identify a fast numerical approach to solve it. The system of linear equations is:

$$\left\{ \begin{array}{lclclcl} & \frac{1}{3}(h_0 + h_1)\sigma_1 & + & \frac{1}{6}h_1\sigma_2 & = & \frac{u_2^n - u_1^n}{h_1} - \frac{f_1 - f_0}{h_0} \\ \frac{1}{6}h_1\sigma_1 & + & \frac{1}{3}(h_1 + h_2)\sigma_2 & + & \frac{1}{6}h_2\sigma_3 & = & \frac{f_3 - f_2}{h_1} - \frac{f_2 - f_1}{h_0} \\ & & & \vdots & & & \\ \frac{1}{6}h_{M-4}\sigma_{M-4} & + & \frac{1}{3}(h_{M-4} + h_{M-3})\sigma_{M-3} & + & \frac{1}{6}h_{M-3}\sigma_{M-2} & = & \frac{f_{M-2} - f_{M-3}}{h_{M-3}} - \frac{f_{M-3} - f_{M-4}}{h_{M-4}} \\ \frac{1}{6}h_{M-3}\sigma_{M-3} & + & \frac{1}{3}(h_{M-3} + h_{M-2})\sigma_{M-2} & & & = & \frac{f_{M-1} - f_{M-2}}{h_{M-2}} - \frac{f_{M-2} - f_{M-3}}{h_{M-3}} \end{array} \right. .$$

From the above system of equation, we can see that the second derivative of cubic spline $s(x)$ can be solved by the above system of linear equation, i.e.,

$$\widehat{\boldsymbol{\sigma}} = \mathbf{M}^{-1} \mathbf{A} \widehat{\mathbf{f}} \quad (21)$$

where vector $\widehat{\mathbf{f}}$ is defined in (17), matrix $\mathbf{A} \in \mathbb{R}^{(M-2) \times M}$ is defined in (6), and matrix $\mathbf{M} \in \mathbb{R}^{(M-2) \times (M-2)}$ is defined as (7).

Finally, we focus on solving the first derivative of cubic spline $s(x)$. Let $\theta_i = s'(x_i)$ for $i = 0, 1, \dots, M-1$, then we have

$$\begin{aligned} s_i(x) &= \theta_i \frac{(x_{i+1}-x)^2(x-x_i)}{h_i^2} - \theta_{i+1} \frac{(x-x_i)^2(x_{i+1}-x)}{h_i^2} + f_i \frac{(x_{i+1}-x)^2[2(x-x_i)+h_i]}{h_i^3} + \\ &\quad f_{i+1} \frac{(x-x_i)^2[2(x_{i+1}-x)+h_i]}{h_i^3} \\ s'_i(x) &= \theta_i \frac{(x_{i+1}-x)(2x_i+x_{i+1}-3x)}{h_i^2} - \theta_{i+1} \frac{(x-x_i)(2x_{i+1}+x_i-3x)}{h_i^2} + 6 \frac{u_{i+1}^n - u_i^n}{h_i^3} (x_{i+1} - x)(x - x_i) \\ s''_i(x) &= -2\theta_i \frac{2x_{i+1}+x_i-3x}{h_i^2} - 2\theta_{i+1} \frac{2x_i+x_{i+1}-3x}{h_i^2} + 6 \frac{u_{i+1}^n - u_i^n}{h_i^3} (x_{i+1} + x_i - 2x) \end{aligned}$$

By plugging x_i into $s''_i(x)$ and $s''_{i-1}(x)$, we have

$$\left\{ \begin{array}{lcl} s''_i(x) & = & -2\theta_i \frac{2x_{i+1}+x_i-3x}{h_i^2} - 2\theta_{i+1} \frac{2x_i+x_{i+1}-3x}{h_i^2} + 6 \frac{f_{i+1} - f_i}{h_i^3} (x_{i+1} + x_i - 2x) \\ s''_{i-1}(x) & = & -2\theta_{i-1} \frac{2x_i+x_{i-1}-3x}{h_{i-1}^2} - 2\theta_i \frac{2x_{i-1}+x_i-3x}{h_i^2} + 6 \frac{f_i - f_{i-1}}{h_{i-1}^3} (x_i + x_{i-1} - 2x) \end{array} \right.$$

which gives

$$\begin{cases} s_i''(x) &= \frac{-4}{h_i} \theta_i + \frac{-2}{h_i} \theta_{i+1} + 6 \frac{f_{i+1} - f_i}{h_i^2} \\ s_{i-1}''(x) &= \frac{2}{h_{i-1}} \theta_{i-1} + \frac{4}{h_{i-1}} \theta_i - 6 \frac{f_i - f_{i-1}}{h_{i-1}^2}. \end{cases}$$

Because $s_i''(x_i) = s_{i-1}''(x_i)$, we have ($\forall i = 1, 2, \dots, M-2$)

$$\begin{aligned} \frac{-4}{h_i} \theta_i + \frac{-2}{h_i} \theta_{i+1} + 6 \frac{f_{i+1} - f_i}{h_i^2} &= \frac{2}{h_{i-1}} \theta_{i-1} + \frac{4}{h_{i-1}} \theta_i - 6 \frac{f_i - f_{i-1}}{h_{i-1}^2} \\ \Leftrightarrow \frac{2}{h_{i-1}} \theta_{i-1} + \left(\frac{4}{h_{i-1}} + \frac{4}{h_i}\right) \theta_i + \frac{2}{h_i} \theta_{i+1} &= 6 \frac{f_{i+1} - f_i}{h_i^2} + 6 \frac{f_i - f_{i-1}}{h_{i-1}^2} \\ \Leftrightarrow \frac{1}{h_{i-1}} \theta_{i-1} + \left(\frac{2}{h_{i-1}} + \frac{2}{h_i}\right) \theta_i + \frac{1}{h_i} \theta_{i+1} &= 3 \frac{f_{i+1} - f_i}{h_i^2} + 3 \frac{f_i - f_{i-1}}{h_{i-1}^2}. \end{aligned}$$

By organizing the above system of equation into matrix algebra, we have

$$\begin{aligned} &\begin{pmatrix} \frac{1}{h_0} & \frac{2}{h_0} + \frac{2}{h_1} & \frac{1}{h_1} & 0 & \dots & 0 & 0 & 0 \\ 0 & \frac{1}{h_1} & \frac{2}{h_1} + \frac{2}{h_2} & 0 & \dots & 0 & 0 & 0 \\ \vdots & \vdots & \vdots & \vdots & \ddots & \vdots & \vdots & \vdots \\ 0 & 0 & 0 & 0 & \dots & \frac{1}{h_{M-3}} & \frac{2}{h_{M-3}} + \frac{2}{h_{M-2}} & \frac{1}{h_{M-2}} \end{pmatrix} \begin{pmatrix} \theta_0 \\ \theta_1 \\ \theta_2 \\ \vdots \\ \theta_{M-1} \end{pmatrix} \\ &= \begin{pmatrix} 3 \frac{f_2 - f_1}{h_1^2} + 3 \frac{f_1 - f_0}{h_0^2} \\ 3 \frac{f_3 - f_2}{h_2^2} + 3 \frac{f_2 - f_1}{h_1^2} \\ \vdots \\ 3 \frac{f_{M-1} - f_{M-2}}{h_{M-2}^2} + 3 \frac{f_{M-2} - f_{M-3}}{h_{M-3}^2} \end{pmatrix}. \end{aligned}$$

For the endpoint θ_0 , because $s_0''(x_0) = 0$, we have

$$s_0''(x) = -2\theta_0 \frac{2x_1 + x_0 - 3x}{h_0^2} - 2\theta_1 \frac{2x_0 + x_1 - 3x}{h_0^2} + 6 \frac{f_1 - f_0}{h_0^3} (x_1 + x_0 - 2x).$$

When we take the value of x as x_0 , we have

$$\begin{aligned}
s_0''(x_0) &= -2\theta_0 \frac{2x_1+x_0-3x_0}{h_0^2} - 2\theta_1 \frac{2x_0+x_1-3x_0}{h_0^2} + 6 \frac{f_1-f_0}{h_0^3} (x_1 + x_0 - 2x_0) \\
&= \frac{-4}{h_0} \theta_0 + \frac{-2}{h_0} \theta_1 + 6 \frac{f_1-f_0}{h_0^2} \\
&= 0
\end{aligned}$$

For the two endpoint θ_{M-1} , because $s''_{M-2}(x_{M-1}) = 0$, we have

$$\begin{aligned}
s''_{M-2}(x) &= -2\theta_{M-2} \frac{2x_{M-1}+x_{M-2}-3x}{h_{M-2}^2} - 2\theta_{M-1} \frac{2x_{M-2}+x_{M-1}-3x}{h_{M-2}^2} + \\
&\quad 6 \frac{f_{M-1}-f_{M-2}}{h_{M-2}^3} (x_{M-1} + x_{M-2} - 2x)
\end{aligned}$$

When we take the value of x as x_{M-1} , we have

$$\begin{aligned}
s''_{M-2}(x_{M-1}) &= -2\theta_{M-2} \frac{2x_{M-1}+x_{M-2}-3x_{M-1}}{h_{M-2}^2} - 2\theta_{M-1} \frac{2x_{M-2}+x_{M-1}-3x_{M-1}}{h_{M-2}^2} + \\
&\quad 6 \frac{f_{M-1}-f_{M-2}}{h_{M-2}^3} (x_{M-1} + x_{M-2} - 2x_{M-1}) \\
&= \frac{2}{h_{M-2}} \theta_{M-2} + \frac{4}{h_{M-2}} \theta_{M-1} - 6 \frac{f_{M-1}-f_{M-2}}{h_{M-2}^2} \\
&= 0.
\end{aligned}$$

So the first order derivative $\boldsymbol{\theta} = (\theta_0, \theta_1, \dots, \theta_{M-1})^\top$ can be solved by

$$\begin{aligned}
 & \left(\underbrace{\begin{pmatrix} \frac{2}{h_0} & \frac{1}{h_0} & 0 & 0 & \dots & 0 & 0 & 0 \\ \frac{1}{h_0} & \frac{2}{h_0} + \frac{2}{h_1} & \frac{1}{h_1} & 0 & \dots & 0 & 0 & 0 \\ 0 & \frac{1}{h_1} & \frac{2}{h_1} + \frac{2}{h_2} & 0 & \dots & 0 & 0 & 0 \\ \vdots & \vdots & \vdots & \vdots & \ddots & \vdots & \vdots & \vdots \\ 0 & 0 & 0 & 0 & \dots & \frac{1}{h_{M-3}} & \frac{2}{h_{M-3}} + \frac{2}{h_{M-2}} & \frac{1}{h_{M-2}} \\ 0 & 0 & 0 & 0 & \dots & 0 & \frac{1}{h_{M-2}} & \frac{2}{h_{M-2}} \end{pmatrix}}_{\mathbf{Q} \in \mathbb{R}^{M \times M}} \right) \underbrace{\begin{pmatrix} \theta_0 \\ \theta_1 \\ \theta_2 \\ \theta_3 \\ \theta_4 \\ \vdots \\ \theta_{M-1} \end{pmatrix}}_{\boldsymbol{\theta}} \\
 &= \underbrace{\begin{pmatrix} 3\frac{f_1-f_0}{h_0^2} \\ 3\frac{f_2-f_1}{h_1^2} + 3\frac{f_1-f_0}{h_0^2} \\ 3\frac{f_3-f_2}{h_2^2} + 3\frac{f_2-f_1}{h_1^2} \\ \vdots \\ 3\frac{f_{M-1}-f_{M-2}}{h_{M-2}^2} + 3\frac{f_{M-2}-f_{M-3}}{h_{M-3}^2} \\ 3\frac{f_{M-1}-f_{M-2}}{h_{M-2}^2} \end{pmatrix}}_{\mathbf{q}}
 \end{aligned}$$

In matrix algebra, the first order derivative $\boldsymbol{\theta} = (\theta_0, \theta_1, \dots, \theta_{M-1})^\top$ can be solved by

$$\hat{\boldsymbol{\theta}} = \mathbf{Q}^{-1} \hat{\mathbf{q}} = \mathbf{Q}^{-1} \mathbf{B} \hat{\mathbf{f}}, \quad (22)$$

where $\hat{\mathbf{f}}$ is defined in (17), and matrix $\mathbf{B} \in \mathbb{R}^{M \times M}$ is defined as

$$\mathbf{B} = \begin{pmatrix} \frac{-3}{h_0^2} & \frac{3}{h_0^2} & 0 & 0 & \dots & 0 & 0 & 0 \\ \frac{-3}{h_0^2} & \frac{3}{h_0^2} - \frac{3}{h_1^2} & \frac{3}{h_1^2} & 0 & \dots & 0 & 0 & 0 \\ 0 & \frac{-3}{h_1^2} & \frac{3}{h_1^2} - \frac{3}{h_2^2} & \frac{3}{h_2^2} & \dots & 0 & 0 & 0 \\ \vdots & \vdots & \vdots & \vdots & \ddots & \vdots & \vdots & \vdots \\ 0 & 0 & 0 & 0 & \frac{-3}{h_{M-3}^2} & \frac{3}{h_{M-3}^2} - \frac{3}{h_{M-2}^2} & \frac{3}{h_{M-2}^2} & \frac{3}{h_{M-2}^2} \\ 0 & 0 & 0 & 0 & 0 & \frac{-3}{h_{M-2}^2} & \frac{3}{h_{M-2}^2} & \frac{3}{h_{M-2}^2} \end{pmatrix}.$$

B Coordinate Gradient Descent to Solve (3).

In this section, we briefly review the implement of the coordinate descent algorithm in Friedman et al. (2010) to solve (10). The main idea of the coordinate descent is to update the estimator in a coordinate-wise fashion, which is the main difference between the coordinate descent and regular gradient descent. For instance, in the k -th iteration, the coordinate descent updates the iterative estimator $\boldsymbol{\beta}^{(k)}$ by using partial of the gradient information, instead of the whole gradient information. Mathematically speaking, in the k -th iteration, the coordinate descent optimizes $F(\boldsymbol{\beta}) = \frac{1}{2MN} \|\nabla_t \mathbf{u} - \mathbf{X}\boldsymbol{\beta}\|_2^2 + \lambda \|\boldsymbol{\beta}\|_1$ with respective to $\boldsymbol{\beta}$ by

$$\beta_j^{(k+1)} = \arg \min_{\beta_j} F((\beta_1^{(k)}, \beta_2^{(k)}, \dots, \beta_{j-1}^{(k)}, \beta_j, \beta_{j+1}^{(k)}, \dots, \beta_K^{(k)}))$$

for all $j = 1, 2, \dots, K$. To minimize the above optimization problem, we can derive the first derivative and set it as 0:

$$\frac{\partial}{\partial \beta_j} F(\boldsymbol{\beta}^{(k)}) = \frac{1}{MN} (\mathbf{e}_j^\top \mathbf{X}^\top \mathbf{X} \boldsymbol{\beta}^{(k)} - \nabla_t \mathbf{u}^\top \mathbf{X} \mathbf{e}_j) + \lambda \text{sign}(\beta_j) = 0,$$

where \mathbf{e}_j is a vector of length K whose entries are all zero except the j -th entry is 1. By solving the above equation, we can solve $\beta_j^{(k+1)}$ by

$$\beta_j^{(k+1)} = S \left(\nabla_t \mathbf{u}^\top \mathbf{X} \mathbf{e}_j - \sum_{l \neq j} (\mathbf{X}^\top \mathbf{X})_{jl} \beta_l^{(k)}, MN\lambda \right) \Big/ (\mathbf{X}^\top \mathbf{X})_{jj},$$

where $S(\cdot)$ is the soft-thresholding function defined as

$$S(x, \alpha) = \begin{cases} x - \alpha & \text{if } x \geq \alpha \\ x + \alpha & \text{if } x \leq -\alpha \\ 0 & \text{otherwise} \end{cases}.$$

The detailed procedure of this algorithm is summarized in Algorithm 2.

Algorithm 2: Algorithm for the coordinate descent to minimize $F(\boldsymbol{\beta})$

Input: response vector $\nabla_t \mathbf{u}$, design matrix \mathbf{X} , and number of iterations M

Output: coefficient estimation $\hat{\boldsymbol{\beta}}$

- 1 **Initialize** $\boldsymbol{\beta}^{(0)}$
- 2 **for** $\ell = 1, \dots, \mathcal{L}$ **do**
- 3 **for** $j = 1, \dots, K$ **do**
- 4 $\boldsymbol{\beta}_j^{(\ell)} = S \left(\nabla_t \mathbf{u}^\top \mathbf{X} \mathbf{e}_j - \sum_{l \neq j} (\mathbf{X}^\top \mathbf{X})_{jl} \beta_l^{(\ell-1)}, MN\lambda \right) \Big/ (\mathbf{X}^\top \mathbf{X})_{jj}$
- 5 $\hat{\boldsymbol{\beta}} = \boldsymbol{\beta}^{(\mathcal{L})}$

The soft-thresholding function $S(x, \alpha) = (x - \alpha) \mathbb{1}\{x \geq \alpha\} + (x + \alpha) \mathbb{1}\{x \leq -\alpha\} + 0 \times \mathbb{1}\{x \in (-\alpha, \alpha)\}$ where $\mathbb{1}\{x \in A\}$ is an indicator function, i.e., $\mathbb{1}\{x \in A\} = 1$ if $x \in A$, and otherwise $\mathbb{1}\{x \in A\} = 0$.

C Some Important Lemmas

In this section, we present some important preliminaries, which are important blocks for the proofs of the main theories. To begin with, we first give the upper bound of $\widehat{u(x, t_n)} - u(x, t_n)$ for $x \in \{x_0, x_1, \dots, x_{M-1}\}$, which is distance between the ground truth $u(x, t_n)$ and the estimated zero-order derivatives by cubic spline $\widehat{u(x, t_n)}$.

Lemma C.1. Assume that

1. for any fixed $n = 0, 1, \dots, N - 1$, we have the spatial variable x is sorted in nondecreasing order, i.e., $x_0 < x_1 \dots < x_{M-1}$;
2. for any fixed $n = 0, 1, \dots, N - 1$, we have the ground truth function $f^*(x) := u(x, t_n) \in C^4$, where C^4 refers to the set of functions that is forth-time differentiable;
3. for any fixed $n = 0, 1, \dots, N - 1$, we have $\frac{\partial^2}{\partial x^2} u(x_0, t_n) = \frac{\partial^2}{\partial x^2} u(x_{M-1}, t_n) = 0$, and $\frac{\partial^3}{\partial x^3} u(x_0, t_n) \neq 0, \frac{\partial^3}{\partial x^3} u(x_{M-1}, t_n) = 0$;
4. for any fixed $n = 0, 1, \dots, N - 1$, the value of third order derivative of function $f^*(x) := u(x, t_n)$ at point $x = 0$ is bounded, i.e., $\frac{d^3}{dx^3} f^*(0) < +\infty$;
5. for any U_i^n generated by the underlying PDE system $U_i^n = u(x_i, t_n) + w_i^n$ with $w_i^n \stackrel{i.i.d.}{\sim} N(0, \sigma^2)$, we have $\eta^2 := \max_{i=0, \dots, M-1, n=0, \dots, N-1} E(U_i^n)^2$ is bounded;
6. for function $K(x) = \frac{1}{2}e^{-|x|/\sqrt{2}} [\sin(|x|\sqrt{2}) + \pi/4]$, we assume that it is uniformly continuous with modulus of continuity w_K and of bounded variation $V(K)$ and we also assume that $\int |K(x)|dx, \int |x|^{1/2}|dK(x)|, \int |x \log |x||^{1/2}|dK(x)|$ are bounded and denote $K_{\max} := \max_{x \in \max_{x \in [0, x_{\max}] \cup [0, T_{\max}]}} K(x)$;
7. the smoothing parameter in (4) is set as $\alpha = (1 + M^{-4/7})^{-1}$;

8. the Condition 3.4 - Condition 3.5 hold.

Then there exist finite positive constant $\mathcal{C}_{(\sigma, \|u\|_{L^\infty(\Omega)})} > 0, C_{(\sigma, \|u\|_{L^\infty(\Omega)})} > 0, \tilde{C}_{(\sigma, \|u\|_{L^\infty(\Omega)})} > 0, Q_{(\sigma, \|u\|_{L^\infty(\Omega)})} > 0, \gamma_{(M)} > 0, \omega_{(M)} > 1$, such that for any ϵ satisfying

$$\epsilon > \mathcal{C}_{(\sigma, \|u\|_{L^\infty(\Omega)})} \max \left\{ 4K_{\max} M^{-3/7}, 4AM^{-3/7}, 4\sqrt{2} \frac{d^3}{dx^3} f^*(0) M^{-3/7}, \frac{16 \left[C_{(\sigma, \|u\|_{L^\infty(\Omega)})} \log(M) + \gamma_{(M)} \right] \log(M)}{M^{3/7}}, 16 \sqrt{\frac{\omega_{(M)}}{7}} \tilde{C}_{(\sigma, \|u\|_{L^\infty(\Omega)})} \frac{\sqrt{\log(M)}}{M^{3/7}} \right\},$$

there exist a $\dot{M} > 0$, such that when $M > \dot{M}$, we have

$$P \left[\sup_{x \in [0, X_{\max}]} \left| \widehat{\frac{\partial^k}{\partial x^k} u(x, t_n)} - \frac{\partial^k}{\partial x^k} u(x, t_n) \right| > \epsilon \right] < 2M e^{-\frac{(M^{3/7} - \|u\|_{L^\infty(\Omega)})^2}{2\sigma^2}} + Q_{(\sigma, \|u\|_{L^\infty(\Omega)})} e^{-L\gamma_{(M)}} + 4\sqrt{2} \eta^4 M^{-\omega_{(M)}/7}$$

for $k = 0, 1, 2$. Here $A = \sup_{\alpha} \int |u|^s f_M(\alpha, u) du \times \int_{x \in [0, X_{\max}]} |K(x)| dx$.

Proof. See Appendix F.3. \square

In the above lemma, we add $(\sigma, \|u\|_{L^\infty(\Omega)})$ as the subscript of constants $\mathcal{C}, C, \tilde{C}, Q$ to emphasize that these constant are independent of the temporal resolution N and spatial resolution M , and only depends on the noisy data \mathcal{D} in (1) itself. We add M as the subscript of constants γ, ω to emphasize that γ, ω are function of the spatial resolution M , and we will discuss the value of γ, ω in Lemma C.2.

The above lemma show the closeness between $\widehat{\frac{\partial^k}{\partial x^k} u(x, t_n)}$ and $\frac{\partial^k}{\partial x^k} u(x, t_n)$ for $k = 0, 1, 2$. This results can be easily extend of the closeness between $\widehat{\frac{\partial}{\partial t} u(x_i, t)}$ and $\frac{\partial}{\partial t} u(x_i, t)$, which is shown in the following corollary.

Corollary C.1. Assume that

1. for any fixed $i = 0, 1, \dots, M-1$, we have the spatial variable t is sorted in nondecreasing order, i.e., $t_0 < t_1 \dots < t_{N-1}$;
2. for any fixed $i = 0, 1, \dots, M-1$, we have the ground truth function $f^*(t) := u(x_i, t) \in C^4$, where C^4 refers to the set of functions that is forth-time differentiable;
3. for any fixed $i = 0, 1, \dots, M-1$, we have $\frac{\partial^2}{\partial t^2} u(x_i, t_0) = \frac{\partial^2}{\partial t^2} u(x_i, t_{N-1}) = 0$, and $\frac{\partial^3}{\partial t^3} u(x_i, t_0) \neq 0, \frac{\partial^3}{\partial t^3} u(x_i, t_{N-1}) = 0$;
4. for any fixed $i = 0, 1, \dots, M-1$, the value of third order derivative of function $\bar{f}^*(x) := u(x_i, t)$ at point $t = 0$ is bounded, i.e., $\frac{d^3}{dt^3} \bar{f}^*(0) < +\infty$;
5. for any U_i^n generated by the underlying PDE system $U_i^n = u(x_i, t_n) + w_i^n$ with $w_i^n \stackrel{i.i.d.}{\sim} N(0, \sigma^2)$, we have $\max_{i=0, \dots, M-1, n=0, \dots, N-1} E(U_i^n)^2$ is bounded;
6. for function $K(x) = \frac{1}{2}e^{-|x|/\sqrt{2}} [\sin(|x|\sqrt{2}) + \pi/4]$, we have $K(x)$ is uniformly continuous with modulus of continuity w_K and of bounded variation $V(K)$, and we also assume that $\int_{x \in [0, X_{\max}]} |K(x)| dx, \int |x|^{1/2} |dK(x)|, \int |x \log |x||^{1/2} |dK(x)|$ are bounded and denote $K_{\max} := \max_{x \in [0, X_{\max}] \cup [0, T_{\max}]} K(x)$;
7. the smoothing parameter in (4) is set as $\bar{\alpha} = O\left(\left(1 + N^{-4/7}\right)^{-1}\right)$;
8. the Condition 3.4 - Condition 3.5 hold.

then there exist finite positive constant $\mathcal{C}_{(\sigma, \|u\|_{L^\infty(\Omega)})} > 0, C_{(\sigma, \|u\|_{L^\infty(\Omega)})} > 0, \tilde{C}_{(\sigma, \|u\|_{L^\infty(\Omega)})} > 0, Q_{(\sigma, \|u\|_{L^\infty(\Omega)})} > 0, \gamma_{(N)} > 0, \omega_{(N)} > 1$, such that for any ϵ satisfying

$$\epsilon > \mathcal{C}_{(\sigma, \|u\|_{L^\infty(\Omega)})} \max \left\{ 4K_{\max} N^{-3/7}, 4\bar{A}N^{-3/7}, 4\sqrt{2} \frac{d^3}{dx^3} f^*(0) N^{-3/7}, \frac{16 \left[C_{(\sigma, \|u\|_{L^\infty(\Omega)})} \log(N) + \gamma_{(N)} \right] \log(N)}{N^{3/7}}, 16 \sqrt{\frac{\omega_{(N)}}{7}} \tilde{C}_{(\sigma, \|u\|_{L^\infty(\Omega)})} \frac{\sqrt{\log(N)}}{N^{3/7}} \right\},$$

there exist a $\dot{N} > 0$, such that when $N > \dot{N}$, we have

$$P \left[\sup_{t \in [0, T_{\max}]} \left| \frac{\partial}{\partial t} \widehat{u(x_i, t)} - \frac{\partial}{\partial t} u(x_i, t) \right| > \epsilon \right] < 2N e^{-\frac{(N^{3/7} - \|u\|_{L^\infty(\Omega)})^2}{2\sigma^2}} + Q_{(\sigma, \|u\|_{L^\infty(\Omega)})} e^{-L\gamma(N)} + 4\sqrt{2}\eta^4 N^{-\omega(N)/7}.$$

Here $\bar{A} = \sup_{\alpha} \int |u|^s \bar{f}_N(\alpha, u) du \times \int_{t \in [0, T_{\max}]} |K(x)| dx$.

After bounding the error of all the derivatives, we then aim to bound $\|\nabla_t \mathbf{u} - \mathbf{X}\beta^*\|_\infty$. It is important to bound $\|\nabla_t \mathbf{u} - \mathbf{X}\beta^*\|_\infty$, with the reason described as follows in Lemma C.2.

Lemma C.2. Suppose the conditions in Lemma C.1 and Corollary C.1 hold and we set $M = O(N)$, then there exist finite positive constant $\mathcal{C}_{(\sigma, \|u\|_{L^\infty(\Omega)})} > 0$ such that for any ϵ satisfying

$$\epsilon > \mathcal{C}_{(\sigma, \|u\|_{L^\infty(\Omega)})} \frac{\log(N)}{N^{3/7-r}},$$

and any $r \in (0, \frac{3}{7})$, there exist $\dot{N} > 0$, such that when $N > \dot{N}$, we have

$$P(\|\nabla_t \mathbf{u} - \mathbf{X}\beta^*\|_\infty > \epsilon) < N e^{-N^r},$$

where $\mathcal{C}_{(\sigma, \|u\|_{L^\infty(\Omega)})}$ is a constant which do not depend on the temporal resolution M and spatial resolution N .

Proof. See Appendix F.4. □

D Tables to draw the curve in Figure 2 and Figure 8

In this section, we present the table to draw the curves in Figure 2,8 in Table 2, 3, respectively.

Table 2: Computational complexity of the functional estimation by cubic spline and local polynomial regression in transport equation

		M = 20						
		N=200	N=400	N=800	N=1000	N=1200	N=1600	N=2000
cubic spline	374,389	748,589	1,496,989	1,871,189	2,245,389	2,993,789	3,742,189	
	14,136,936	45,854,336	162,089,136	246,606,536	348,723,936	605,758,736	933,193,536	
		N = 20						
		M=200	M=400	M=800	M=1000	M=1200	M=1600	M=2000
cubic spline	398,573	875,773	207,0173	2,787,373	3,584,573	5,418,973	7,573,373	
	33,046,336	125,596,136	489,255,736	760,365,536	1,090,995,336	1,930,814,936	3,008,714,536	

Table 3: Correct identification probability of transport equation, inviscid Burgers equation and viscous Burgers's equation

		σ											
		0.01	0.05	0.1	0.25	0.3	0.4	0.5	0.7	0.75	0.8	0.9	1
		transport equation											
$M = N = 100$		100%	100%	100%	100%	100%	100%	100%	100%	100%	100%	100%	100%
$M = N = 150$		100%	100%	100%	100%	100%	100%	100%	100%	100%	100%	100%	100%
$M = N = 200$		100%	100%	100%	100%	100%	100%	100%	100%	100%	100%	100%	100%
		inviscid Burgers equation											
$M = N = 100$		100%	100%	100%	100%	100%	100%	99.9%	99.8%	99.8%	99.8%	99.8%	99.1%
$M = N = 150$		100%	100%	100%	100%	100%	100%	100%	99.8%	99.7%	99.7%	99.7%	99.7%
$M = N = 200$		100%	100%	100%	100%	100%	100%	100%	100%	100%	100%	100%	100%
		viscous Burgers equation											
$M = N = 100$		100%	99.4%	89.8%	78.0%	71.4%	82.0%	91.6%	72.8%	79.0%	72.9%	57.9%	51.3%
$M = N = 150$		100%	100%	100%	97.3%	96.5%	96.2%	97.6%	95.6%	93.3%	86.6%	79.9%	73.6%
$M = N = 200$		100%	100%	100%	100%	99.6%	99.6%	98.2%	98.8%	98.2%	97.0%	94.3%	91.3%

¹ The simulation results are based on 1000 times of simulations.

E Checking Conditions of Example 1,2,3

In this section, we check Condition 3.1 - Condition 3.6 of the above three examples: (1) example 1 (the transport equation), (2) example 2 (the inviscid Burgers' equation) and (3) example 3 (the viscous Burgers' equation).

E.1 Verification of Condition 3.1, 3.2, 3.3

In this section, we check the Condition 3.1 - Condition 3.3 under example 1,2,3, though the applicability of the results is by no means restricted to these.

The verification results can be found in Figure 9 and Figure 10, where (a),(b),(c) are the box plot of $\|\mathbf{X}_{S^c}^\top \mathbf{X}_S (\mathbf{X}_S^\top \mathbf{X}_S)^{-1}\|_\infty$ and the minimal eigenvalue of matrix $\frac{1}{NM} \mathbf{X}_S^\top \mathbf{X}_S$ of these three examples under $\sigma = 0.01, 0.1, 1$, respectively. From Figure 9, we find the value of $\|\mathbf{X}_{S^c}^\top \mathbf{X}_S (\mathbf{X}_S^\top \mathbf{X}_S)^{-1}\|_\infty$ is smaller than 1, so there exist a $\mu \in (0, 1]$ such that Condition 3.2 is met. From Figure 10, we find the minimal eigenvalue of matrix $\frac{1}{MN} \mathbf{X}_S^\top \mathbf{X}$ are all strictly larger than 0, so we declare Condition 3.3 is satisfied, and thus its weak version – Condition 3.1 – is also satisfied.

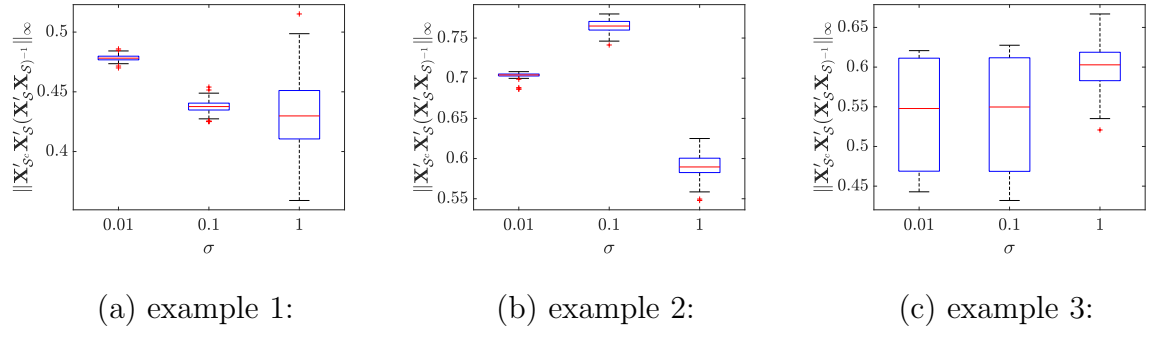


Figure 9: Box plots of $\|\mathbf{X}_{S^c}^\top \mathbf{X}_S (\mathbf{X}_S^\top \mathbf{X}_S)^{-1}\|_\infty$ under $\sigma = 0.01, 0.1, 1$ when $M = N = 100$.

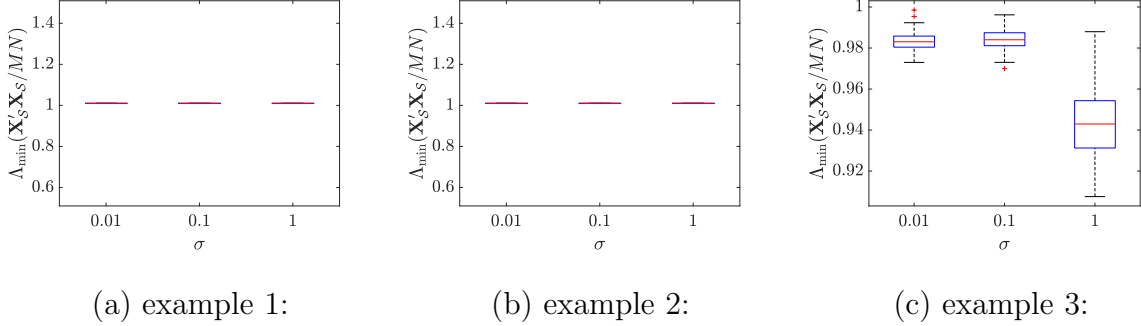


Figure 10: Box plots of the minimal eigenvalue of matrix $\frac{1}{NM} \mathbf{X}_S^\top \mathbf{X}_S$ under $\sigma = 0.01, 0.1, 1$ when $M = N = 100$.

E.2 Verification of Condition 3.4 and Condition 3.5

In example 1,2,3, the design points x_0, x_1, \dots, x_{M-1} and t_0, t_1, \dots, t_{N-1} are equally spaced, i.e., $x_0 = 1/M, x_1 = 2/M, \dots, x_{M-1} = 1$ and $t_0 = 0.1/N, t_1 = 0.2/N, \dots, t_{N-1} = 0.1$. Under this scenario, there exist an absolutely continuous distribution $F(x) = x$ for $x \in [1/M, 1]$ and $G(t) = 0.1t$ for $t \in [0.1/N, 0.1]$, where the empirical c.d.f. of the design points x_0, x_1, \dots, x_{M-1} and t_0, t_1, \dots, t_{N-1} will converge to $F(x), G(t)$, respectively, as $M, N \rightarrow +\infty$. For the $F(x), G(t)$, we know their first derivatives are bounded for $x \in [1/M, 1]$ and $t \in [0.1/N, 0.1]$, respectively. In the simulation of this paper, we take the equally spaced design points as an illustration example, and its applicability is by no means restricted to this case.

E.3 Verification of Condition 3.6.

The Condition 3.6 ensures that the smoothing parameter does not tend to zero too rapidly. Silverman (1984) shows that for the equally spaced design points, this condition meets. For other types of design points, for instance, randomly and independently dis-

tributed design points, it can also be verified that Condition 3.6 is satisfied (see Silverman, 1984, Section 2).

F Proofs

F.1 Proof of Proposition 2.1

Proof. The computational complexity in the functional estimation stage lies in calculating all elements in matrix \mathbf{X} and vector $\nabla_t \mathbf{u}$, including

$$\left\{ \widehat{u(x_i, t_n)}, \widehat{\frac{\partial u(x_i, t_n)}{\partial x}}, \widehat{\frac{\partial^2 u(x_i, t_n)}{\partial x^2}}, \widehat{\frac{\partial^2 u(x_i, t_n)}{\partial t}} \right\}_{i=0, \dots, M-1, n=0, \dots, N-1}.$$

by cubic spline in (4).

We divide our proof into two scenarios: (1) $\alpha = 1$ and (2) $\alpha \in (0, 1)$.

- First of all, we discuss a very simple case, i.e., $\alpha = 1$. When $\alpha = 1$, we call the cubic spline as *interpolating cubic spline* since there is no penalty on the smoothness.

For the zero-order derivative, i.e., $\left\{ \widehat{u(x_i, t_n)} \right\}_{i=0, \dots, M-1, n=0, \dots, N-1}$, it can be estimated as $\widehat{u(x_i, t_n)} = u_i^n$ for $i = 0, 1, \dots, M-1, n = 0, 1, \dots, N-1$. So there is no computational complexity involved.

For the second order derivatives, i.e., $\left\{ \widehat{\frac{\partial^2 u(x_i, t_n)}{\partial x^2}} \right\}_{i=0, \dots, M-1}$, with $n \in \{0, \dots, N-1\}$ fixed, it can be solved in a closed-form, i.e.,

$$\widehat{\boldsymbol{\sigma}} = \mathbf{M}^{-1} \mathbf{A} \mathbf{u}^n$$

where $\widehat{\boldsymbol{\sigma}} = \left(\widehat{\frac{\partial^2 u(x_0, t_n)}{\partial x^2}}, \widehat{\frac{\partial^2 u(x_1, t_n)}{\partial x^2}}, \dots, \widehat{\frac{\partial^2 u(x_{M-1}, t_n)}{\partial x^2}} \right)^\top$. So the main computational load lies in the calculation of \mathbf{M}^{-1} . Recall $\mathbf{M} \in \mathbb{R}^{(M-2) \times (M-2)}$ is a tri-diagonal

matrix:

$$\mathbf{M} = \begin{pmatrix} \frac{h_0+h_1}{3} & \frac{h_1}{6} & 0 & \dots & 0 & 0 \\ \frac{h_1}{6} & \frac{h_1+h_2}{3} & \frac{h_2}{6} & \dots & 0 & 0 \\ 0 & \frac{h_2}{6} & \frac{h_2+h_3}{3} & \ddots & 0 & 0 \\ \vdots & \vdots & \ddots & \ddots & \ddots & \vdots \\ 0 & 0 & 0 & \ddots & \frac{h_{M-4}+h_{M-3}}{3} & \frac{h_{M-3}}{6} \\ 0 & 0 & 0 & \dots & \frac{h_{M-3}}{6} & \frac{h_{M-3}+h_{M-2}}{3} \end{pmatrix}.$$

For this type of tri-diagonal matrix, there exist a fast algorithm to calculate its inverse. The main idea of this fast algorithm is to decompose \mathbf{M} through Cholesky decomposition as

$$\mathbf{M} = \mathbf{L}\mathbf{D}\mathbf{L}^\top,$$

where $\mathbf{L} \in \mathbb{R}^{(M-2) \times (M-2)}$, $\mathbf{D} \in \mathbb{R}^{(M-2) \times (M-2)}$ has the form of

$$\mathbf{L} = \begin{pmatrix} 1 & 0 & 0 & \dots & 0 \\ l_1 & 1 & 0 & \dots & 0 \\ 0 & l_2 & 1 & \dots & 0 \\ \vdots & \vdots & \ddots & \ddots & \vdots \\ 0 & 0 & 0 & l_{M-3} & 1 \end{pmatrix}, \mathbf{D} = \begin{pmatrix} d_1 & 0 & \dots & 0 \\ 0 & d_2 & \dots & 0 \\ \vdots & \vdots & \ddots & \vdots \\ 0 & 0 & \dots & d_{M-2} \end{pmatrix}.$$

After decomposing matrix \mathbf{M} into $\mathbf{L}\mathbf{D}\mathbf{L}^\top$, the second derivatives $\hat{\boldsymbol{\sigma}}$ can be solved as

$$\hat{\boldsymbol{\sigma}} = (\mathbf{L}^\top)^{-1} \mathbf{D}^{-1} \mathbf{L}^{-1} \underbrace{\mathbf{A}\mathbf{u}^n}_{\boldsymbol{\xi}}.$$

In the remaining of the proof in this scenario, we will verify the following two issues:

1. the computational complexity to decompose \mathbf{M} into $\mathbf{L}\mathbf{D}\mathbf{L}^\top$ is $O(M)$ with $n \in \{0, \dots, N-1\}$ fixed;

2. the computational complexity to compute $\widehat{\boldsymbol{\sigma}} = (\mathbf{L}^\top)^{-1} \mathbf{D}^{-1} \mathbf{L}^{-1} \boldsymbol{\xi}$ is $O(M)$ with $n \in \{0, \dots, N-1\}$ fixed and \mathbf{L}, \mathbf{D} available.

For the decomposition of $\mathbf{M} = \mathbf{LDL}^\top$, its essence is to derive l_1, \dots, l_{M-3} in matrix \mathbf{L} and d_1, \dots, d_{M-2} in matrix \mathbf{D} . By utilizing the method of undetermined coefficients to inequality $\mathbf{M} = \mathbf{LDL}^\top$, we have:

$$= \begin{bmatrix} d_1 & d_1 l_1 & 0 & \dots & 0 & 0 \\ d_1 l_1 & d_2 & d_2 l_2 & \dots & 0 & 0 \\ 0 & d_2 l_2 & d_3 & \dots & 0 & 0 \\ \vdots & \vdots & \vdots & \ddots & \vdots & \vdots \\ 0 & 0 & 0 & \dots & d_{M-3} l_{M-3} & d_{M-3} l_{M-3}^2 + d_{M-2} \\ M_{11} & M_{12} & \dots & & 0 & \\ M_{21} & M_{22} & \dots & & 0 & \\ 0 & M_{32} & \dots & & 0 & \\ \vdots & \vdots & \ddots & & \vdots & \\ 0 & 0 & \dots & & M_{M-2,M-2} & \end{bmatrix},$$

where $M_{i,j}$ is the (i, j) th entry in matrix \mathbf{M} . Through the above method of undetermined coefficients, we can solve the exact value of the entries in matrix \mathbf{L}, \mathbf{D} , which is summarized in Algorithm 3. It can be seen from Algorithm 3 that, the computational complexity of solve \mathbf{L}, \mathbf{D} is of order $O(M)$.

For the calculation of $\widehat{\boldsymbol{\sigma}} = (\mathbf{L}^\top)^{-1} \mathbf{D}^{-1} \mathbf{L}^{-1} \boldsymbol{\xi}$ with matrix \mathbf{L}, \mathbf{D} available, we will first verify that the computational complexity to solve $\bar{\boldsymbol{\xi}} = \mathbf{L}^{-1} \boldsymbol{\xi}$ is $O(M)$. Then, we will verify that the computational complexity to solve $\bar{\bar{\boldsymbol{\xi}}} = \mathbf{D}^{-1} \bar{\boldsymbol{\xi}}$ is $O(M)$. Finally, we will verify that the computational complexity to solve $\bar{\bar{\boldsymbol{\xi}}} = (\mathbf{L}^\top)^{-1} \bar{\bar{\boldsymbol{\xi}}}$ is $O(M)$. First,

the computational complexity of calculating $\bar{\boldsymbol{\xi}} = \mathbf{L}^{-1}\boldsymbol{\xi}$ is $O(M)$, this is because by $\mathbf{L}\bar{\boldsymbol{\xi}} = \boldsymbol{\xi}$, we have the following system of equations:

$$\begin{cases} \xi_1 = \bar{\xi}_1 \\ \xi_2 = \bar{\xi}_2 + l_1 \bar{\xi}_1 \\ \vdots \\ \xi_{M-2} = \bar{\xi}_{M-2} + l_{M-3} \bar{\xi}_{M-3} \end{cases}$$

where $\xi_i, \bar{\xi}_i$ is the i -th entry in $\boldsymbol{\xi}, \bar{\boldsymbol{\xi}}$, respectively. Through the above system of equations, we can solve the values of all entries in $\bar{\boldsymbol{\xi}}$, which is summarized in Algorithm 4. From Algorithm 4, we know that the computational complexity of solving $\mathbf{L}^{-1}\boldsymbol{\xi}$ is $O(M)$. Next, it is obvious that the computational complexity of $\bar{\boldsymbol{\xi}} = \mathbf{D}^{-1}\bar{\boldsymbol{\xi}}$ is $O(M)$, because \mathbf{D} is a diagonal matrix. Finally, with the similar logic flow, we can verify that the computational complexity of $\bar{\bar{\boldsymbol{\xi}}} = (\mathbf{L}^\top)^{-1}\bar{\boldsymbol{\xi}}$ is still $O(M)$. So, the computational complexity is to calculate $\hat{\boldsymbol{\sigma}} = (\mathbf{L}^\top)^{-1}\mathbf{D}^{-1}\mathbf{L}^{-1}\boldsymbol{\xi}$, with known \mathbf{L}, \mathbf{D} is $O(M)$.

As a summary, the computational complexity is to calculate $\left\{ \widehat{\frac{\partial^2}{\partial x^2}u(x_i, t_n)} \right\}_{i=0, \dots, M-1}$ with a fixed $n \in \{0, 1, \dots, N-1\}$ is $O(M)$. Accordingly, the computational complexity to solve $\left\{ \widehat{\frac{\partial^2}{\partial x^2}u(x_i, t_n)} \right\}_{i=0, \dots, M-1, n=0, \dots, N-1}$ is $O(MN)$.

For the first order derivatives, i.e., $\left\{ \widehat{\frac{\partial}{\partial x}u(x_i, t_n)}, \widehat{\frac{\partial}{\partial x}u(x_i, t_n)} \right\}_{i=0, \dots, M-1, n=0, \dots, N-1}$, we can verify the computational complexity to solve them is also $O(MN)$ with the similar logic as that in the second order derivatives.

Algorithm 3: Pseudo code to solve \mathbf{L}, \mathbf{D}

Input: matrix \mathbf{M}

Output: matrix \mathbf{L}, \mathbf{D}

```

1 Initialize  $d_1 = M_{1,1}$ 
2 for  $i = 1, 2, \dots, M - 3$  do
3    $l_i = M_{i,i+1}/d_i$ 
4    $d_{i+1} = M_{i+1,i+1} - d_i l_i^2$ 

```

Algorithm 4: Pseudo code to solve $\mathbf{L}^{-1} \boldsymbol{\xi}$

Input: matrix $\mathbf{L}, \boldsymbol{\xi}$

Output: matrix $\bar{\boldsymbol{\xi}}$

```

1 Initialize  $\bar{\boldsymbol{\xi}}_1 = \boldsymbol{\xi}_1$ 
2 for  $i = 2, \dots, M - 2$  do
3    $\bar{\boldsymbol{\xi}}_i = \boldsymbol{\xi}_i - l_{i-1} \bar{\boldsymbol{\xi}}_{i-1}$ 

```

- Next, we discuss the scenario when $\alpha \in (0, 1)$.

Since all the derivatives has similar closed-form formulation as shown in (5), (22), (21), we take the zero-order derivative $\{u(x_i, t_n)\}_{i=0, \dots, M-1, n=0, \dots, N-1}$ as an illustration example, and other derivatives can be derived similarly.

Recall that in Section 2.1, the zero-order derivative $\{u(x_i, t_n)\}_{i=0, \dots, M-1}$ with $n \in \{0, 1, \dots, N-1\}$ fixed can be estimated through cubic spline as in equation (5):

$$\hat{\mathbf{f}} = \underbrace{[\alpha \mathbf{W} + (1 - \alpha) \mathbf{A}^\top \mathbf{M} \mathbf{A}]}_{\mathbf{Z}}^{-1} \underbrace{\alpha \mathbf{W} \mathbf{u}^n}_{\mathbf{y}},$$

where $\alpha \in (0, 1)$ trades off the fitness of the cubic spline and the smoothness of the cubic spline, vector $\hat{\mathbf{f}} = (\widehat{u(x_0, t_n)}, \widehat{u(x_1, t_n)}, \dots, \widehat{u(x_{M-1}, t_n)})^\top$, vector $\mathbf{u}^n =$

$(u_0^n, \dots, u_{M-1}^n)^\top$, matrix $\mathbf{W} = \text{diag}(w_0, w_1, \dots, w_{M-1})$, matrix $\mathbf{A} \in \mathbb{R}^{(M-2) \times M}$, $\mathbf{M} \in \mathbb{R}^{(M-2) \times (M-2)}$ are defined as

$$\mathbf{A} = \begin{pmatrix} \frac{1}{h_0} & -\frac{1}{h_0} - \frac{1}{h_1} & \frac{1}{h_1} & 0 & \dots & 0 & 0 & 0 \\ 0 & \frac{1}{h_1} & -\frac{1}{h_1} - \frac{1}{h_2} & \frac{1}{h_2} & \dots & 0 & 0 & 0 \\ \vdots & \vdots & \vdots & \vdots & \ddots & \vdots & \vdots & \vdots \\ 0 & 0 & 0 & 0 & \dots & \frac{1}{h_{M-3}} & -\frac{1}{h_{M-3}} - \frac{1}{h_{M-2}} & \frac{1}{h_{M-2}} \end{pmatrix},$$

$$\mathbf{M} = \begin{pmatrix} \frac{h_0+h_1}{3} & \frac{h_1}{6} & 0 & \dots & 0 & 0 \\ \frac{h_1}{6} & \frac{h_1+h_2}{3} & \frac{h_2}{6} & \dots & 0 & 0 \\ 0 & \frac{h_2}{6} & \frac{h_2+h_3}{3} & \dots & 0 & 0 \\ \vdots & \vdots & \vdots & \ddots & \vdots & \vdots \\ 0 & 0 & 0 & \dots & \frac{h_{M-4}+h_{M-3}}{3} & \frac{h_{M-3}}{6} \\ 0 & 0 & 0 & \dots & \frac{h_{M-3}}{6} & \frac{h_{M-3}+h_{M-2}}{3} \end{pmatrix}$$

with $h_i = x_{i+1} - x_i$ for $i = 0, 1, \dots, M-2$.

By simple calculation, we know that matrix $\mathbf{Z} = \alpha \mathbf{W} + (1 - \alpha) \mathbf{A}^\top \mathbf{M} \mathbf{A} \in \mathbb{R}^{M \times M}$ is a symmetric seventh-diagonal matrix:

$$\mathbf{Z} = \begin{pmatrix} z_{11} & z_{12} & z_{13} & z_{14} & 0 & \dots \\ z_{21} & z_{22} & z_{23} & z_{24} & z_{25} & \dots \\ z_{31} & z_{32} & z_{33} & z_{34} & z_{35} & \ddots \\ z_{41} & z_{42} & z_{43} & z_{44} & z_{45} & \ddots \\ 0 & z_{52} & z_{53} & z_{54} & z_{55} & \ddots \\ \vdots & \vdots & \ddots & \ddots & \ddots & \ddots \end{pmatrix}$$

By applying Cholesky decomposition to matrix \mathbf{Z} as $\mathbf{Z} = \mathbf{P} \boldsymbol{\Sigma} \mathbf{P}^\top$, we can calculate $\hat{\mathbf{f}}$ as

$$\hat{\mathbf{f}} = \mathbf{Z}^{-1} \mathbf{y} = (\mathbf{P}^\top)^{-1} \boldsymbol{\Sigma}^{-1} \mathbf{P}^{-1} \mathbf{y},$$

where $\mathbf{P} \in \mathbb{R}^{M \times M}$, $\Sigma \in \mathbb{R}^{M \times M}$ has the form of

$$\mathbf{P} = \begin{pmatrix} 1 & 0 & 0 & 0 & \dots & 0 & 0 \\ \ell_1 & 1 & 0 & 0 & \dots & 0 & 0 \\ \gamma_1 & \ell_2 & 1 & 0 & \dots & 0 & 0 \\ \eta_1 & \gamma_2 & \ell_3 & 1 & \dots & 0 & 0 \\ 0 & \eta_2 & \gamma_3 & \ell_4 & \ddots & 0 & 0 \\ \vdots & \vdots & \ddots & \ddots & \ddots & 1 & 0 \\ 0 & 0 & \dots & \eta_{M-3} & \gamma_{M-2} & \ell_{M-1} & 1 \end{pmatrix}, \Sigma = \begin{pmatrix} s_1 & 0 & 0 & \dots & 0 \\ 0 & s_2 & 0 & \dots & 0 \\ 0 & 0 & s_3 & \dots & 0 \\ \vdots & \vdots & \vdots & \ddots & 0 \\ 0 & 0 & 0 & \dots & s_M \end{pmatrix}.$$

In the remaining of the proof in this scenario, we will verify the following two issues:

1. the computational complexity to decompose \mathbf{Z} into $\mathbf{P}\Sigma\mathbf{P}^\top$ is $O(M)$ with $n \in \{0, \dots, N-1\}$ fixed;
2. the computational complexity to compute $(\mathbf{P}^\top)^{-1}\Sigma^{-1}\mathbf{P}^{-1}\mathbf{y}$ is $O(M)$ with $n \in \{0, \dots, N-1\}$ fixed.

First of all, we verify that the computational complexity to decompose \mathbf{Z} into $\mathbf{P}\Sigma\mathbf{P}^\top$ is $O(M)$ when $n \in \{0, \dots, N-1\}$ fixed. By applying method of undetermined coefficients, we can verify that the matrix \mathbf{P} has the following form:

cients to equality $\mathbf{Z} = \mathbf{P}\Sigma\mathbf{P}^\top$, we have

$$\left[\begin{array}{ccccc} s_1 & s_1\ell_1 & s_1\gamma_1 & \dots & 0 \\ s_1\ell_1 & s_1\ell_1^2 + s_2 & s_1\ell_1\gamma_1 + s_2\ell_2 & \dots & 0 \\ s_1\gamma_1 & s_1\ell_1\gamma_1 + s_2\ell_2 & s_1\gamma_1^2 + s_2\ell_2^2 + s_3 & \dots & 0 \\ s_1\eta_1 & s_1\eta_1\ell_1 + s_2\gamma_2 & s_1\eta_1\gamma_1 + s_2\gamma_2\ell_2 + s_3\ell_3 & \dots & 0 \\ 0 & s_2\eta_2 & s_2\eta_2\ell_2 + s_3\gamma_3 & \dots & 0 \\ 0 & 0 & s_3\eta_3 & \dots & 0 \\ \vdots & \vdots & \vdots & \ddots & \vdots \\ 0 & 0 & 0 & \dots & s_{M-3}\eta_{M-3}^2 + s_{M-2}\gamma_{M-2}^2 \\ & & & & +s_{M-1}\gamma_{M-1}\ell_{M-1}^2 + s_M \end{array} \right] = [z_{i,j}],$$

where $[z_{ij}]$ denotes matrix \mathbf{Z} with its (i, j) th entry as $z_{i,j}$. Through the above method of undetermined coefficients, we can solve the explicit value of all entries in matrix \mathbf{P}, Σ , i.e., $\ell_1, \dots, \ell_{M-1}, \gamma_1, \dots, \gamma_{M-2}, \eta_1, \dots, \eta_{M-3}$ in matrix \mathbf{P} and s_1, \dots, s_M in matrix Σ , which is summarized in Algorithm 5. From Algorithm 5, we can see that the computational complexity to decompose \mathbf{Z} into $\mathbf{P}\Sigma\mathbf{P}^\top$ is $O(M)$ with $n \in \{0, \dots, N-1\}$ fixed.

Second, we verify the computational complexity to compute $(\mathbf{P}^\top)^{-1}\Sigma^{-1}\mathbf{P}^{-1}\mathbf{y}$ is $O(M)$ with $n \in \{0, \dots, N-1\}$ fixed and matrix \mathbf{P}, Σ available. To realize this objective, we will first verify that the computational complexity to calculate $\bar{\mathbf{y}} = \mathbf{P}^{-1}\mathbf{y}$ is $O(M)$. Then, we will first verify that the computational complexity to calculate $\bar{\mathbf{y}} = \Sigma^{-1}\bar{\mathbf{y}}$ is $O(M)$. Finally, we will first verify that the computational complexity to calculate $\bar{\bar{\mathbf{y}}} = (\mathbf{P}^\top)^{-1}\bar{\mathbf{y}}$ is $O(M)$. First of all, let us verify the computational complexity to compute $\bar{\mathbf{y}} = \mathbf{P}^{-1}\mathbf{y}$ is $O(M)$ with $n \in \{0, \dots, N-1\}$ fixed. Because we have a system

of equations derived from $\mathbf{P}\bar{\mathbf{y}} = \mathbf{y}$:

$$\left\{ \begin{array}{lcl} \bar{y}_1 & = & y_1 \\ \bar{y}_2 & = & y_2 - \ell_1 \bar{y}_1 \\ \bar{y}_3 & = & y_3 - \gamma_1 \bar{y}_1 - \ell_2 \bar{y}_2 \\ \bar{y}_4 & = & y_4 - \eta_1 \bar{y}_1 - \gamma_2 \bar{y}_2 - \ell_3 \bar{y}_3 \\ \bar{y}_5 & = & y_5 - \eta_2 \bar{y}_3 - \gamma_3 \bar{y}_3 - \ell_4 \bar{y}_4 \\ \vdots & & \\ \bar{y}_M & = & y_M - \eta_{M-3} \bar{y}_{M-3} - \gamma_{M-2} \bar{y}_{M-2} - \ell_{M-1} \bar{y}_{M-1} \end{array} \right. ,$$

we can solve vector $\bar{\mathbf{y}} = (\bar{y}_1, \bar{y}_2, \dots, \bar{y}_M)^\top$ explicitly through Algorithm 6, which only requires $O(M)$ computational complexity. After deriving $\bar{\mathbf{y}} = \mathbf{P}^{-1}\mathbf{y}$, we can easily verify that the computational complexity to derive $\bar{\bar{\mathbf{y}}} = \Sigma^{-1}\bar{\mathbf{y}}$ is still $O(M)$ because $\boldsymbol{\sigma}$ is a diagonal matrix. Finally, after deriving $\bar{\bar{\mathbf{y}}} = \Sigma^{-1}\bar{\mathbf{y}}$, we can verify that the computational complexity to derive $\bar{\bar{\mathbf{y}}} = (\mathbf{P}^\top)^{-1}\bar{\bar{\mathbf{y}}}$ is still $O(M)$ with the similar logic as that in $\bar{\mathbf{y}} = \mathbf{P}^{-1}\mathbf{y}$.

From the above discussion, we know that the computational complexity to calculate $\hat{\mathbf{f}} = (\widehat{u(x_0, t_n)}, \widehat{u(x_1, t_n)}, \dots, \widehat{u(x_{M-1}, t_n)})^\top$, is $O(M)$ with $n \in \{0, 1, \dots, N-1\}$ fixed. In other words, the computational complexity to derive $\left\{ \widehat{u(x_i, t_n)} \right\}_{i=0, \dots, M-1}$ is $O(M)$. According, the computational complexity to derive $\left\{ \widehat{u(x_i, t_n)} \right\}_{i=0, \dots, M-1, n=0, \dots, N-1}$ is $O(MN)$.

Algorithm 5: Pseudo code to solve \mathbf{P}, Σ

Input: matrix \mathbf{Z}

Output: matrix \mathbf{P}, Σ

```
1 Initialize  $s_j = \eta_j = \gamma_j = \ell_j = 0 \forall j \leq 0$ 
2 for  $i = 1, 2, \dots, M$  do
3    $s_i = z_{ii} - s_{i-3}\eta_{i-3}^2 - s_{i-2}\gamma_{i-2}^2 - s_{i-1}\ell_{i-1}^2$ 
4    $\ell_i = (z_{i,i+1} - s_{i-2}\gamma_{i-2}\eta_{i-2} - s_{i-1}\gamma_{i-1}\ell_{i-1})/s_i$ 
5    $\eta_i = a_{i,i+3}/s_i$ 
```

Algorithm 6: Pseudo code to solve $\mathbf{P}^{-1}\mathbf{y}$

Input: matrix \mathbf{P}, \mathbf{y}

Output: vector $\bar{\mathbf{y}}$

```
1 Initialize  $\eta_i = \gamma_i = \ell_i = 0 \forall i \leq 0$ 
2 for  $i = 1, \dots, M$  do
3    $\bar{y}_i = y_i - \eta_{i-3}\bar{y}_{i-3} - \gamma_{i-2}\bar{y}_{i-2} - \ell_{i-1}\bar{y}_{i-1}$ 
```

□

F.2 Proof of Proposition 2.2

Proof. In Appendix A, we discuss how to use cubic spline to derive derivatives of $u(x, t)$. In this section, we discuss how to use local polynomial regression to derive derivatives, as a benchmark method.

Recall that the derivatives can be estimated by local polynomial regression includes $u(x_i, t_n), \frac{\partial}{\partial x}u(x_i, t_n), \frac{\partial^2}{\partial x^2}u(x_i, t_n), \dots$. And here we take the derivation $\frac{\partial^l}{\partial x^l}u(x, t_n)$ as an example ($l = 0, 1, 2, \dots$), and the other derivatives can be derived with the same logic

flow. To derive the estimation of $\frac{\partial^l}{\partial x^l}u(x, t_n)$, we fix the temporal variable t_n for a general $n \in \{0, 1, \dots, N-1\}$. Then we locally fit a degree \check{p} polynomial over the data $\{(x_i, u_i^n)\}_{i=0, \dots, M-1}$, i.e.,

$$\left\{ \begin{array}{lcl} u(x_0, t_n) & = & u(x, t_n) + \frac{\partial}{\partial x}u(x, t_n)(x_0 - x) + \dots + \frac{\partial^{\check{p}}}{\partial x^{\check{p}}}u(x, t_n)(x_0 - x)^{\check{p}} \\ u(x_1, t_n) & = & u(x, t_n) + \frac{\partial}{\partial x}u(x, t_n)(x_1 - x) + \dots + \frac{\partial^{\check{p}}}{\partial x^{\check{p}}}u(x, t_n)(x_1 - x)^{\check{p}} \\ \vdots & & \vdots \\ u(x_{M-1}, t_n) & = & u(x, t_n) + \frac{\partial}{\partial x}u(x, t_n)(x_{M-1} - x) + \dots + \frac{\partial^{\check{p}}}{\partial x^{\check{p}}}u(x, t_n)(x_{M-1} - x)^{\check{p}} \end{array} \right. .$$

For the choice of \check{p} , we choose $\check{p} = l+3$ to realize minmax efficiency (see Fan et al., 1997). If we denote $\mathbf{b}(x) = \left(u(x, t_n), \frac{\partial}{\partial x}u(x, t_n), \dots, \frac{\partial^{\check{p}}}{\partial x^{\check{p}}}u(x, t_n)\right)^\top$, then $\frac{\partial^l}{\partial x^l}u(x, t_n)$ can be obtained as the $(l+1)$ -th entry of the vector $\widehat{\mathbf{b}(x)}$, and $\widehat{\mathbf{b}(x)}$ is obtained by the following optimization problem:

$$\widehat{\mathbf{b}(x)} = \arg \min_{\mathbf{b}(x)} \sum_{i=0}^{M-1} \left[u_i^n - \sum_{j=0}^{\check{p}} \frac{\partial^j}{\partial x^j}u(x, t_n)(x_i - x)^j \right]^2 \mathcal{K}\left(\frac{x_i - x}{h}\right), \quad (23)$$

where h is the bandwidth parameter, and \mathcal{K} is a kernel function, and in our paper, we use the Epanechnikov kernel $\mathcal{K}(x) = \frac{3}{4} \max\{0, 1 - x^2\}$ for $x \in \mathbb{R}$. Essentially, the optimization problem in equation (23) is a weighted least squares model, where $\mathbf{b}(x)$ can be solved in a close form:

$$\mathbf{b}(x) = (\mathbf{X}_{\text{spa}}^\top \mathbf{W}_{\text{spa}} \mathbf{X}_{\text{spa}})^{-1} \mathbf{X}_{\text{spa}}^\top \mathbf{W}_{\text{spa}} \mathbf{u}_\cdot^n, \quad (24)$$

where

$$\mathbf{X}_{\text{spa}} = \begin{bmatrix} 1 & (x_0 - x) & \dots & (x_0 - x)^{\check{p}} \\ 1 & (x_1 - x) & \dots & (x_1 - x)^{\check{p}} \\ \vdots & \vdots & \ddots & \vdots \\ 1 & (x_{M-1} - x) & \dots & (x_{M-1} - x)^{\check{p}} \end{bmatrix}, \mathbf{u}_\cdot^n = \begin{bmatrix} u_0^n \\ u_1^n \\ \vdots \\ u_{M-1}^n \end{bmatrix}$$

and $\mathbf{W}_{\text{spa}} = \text{diag}(\mathcal{K}(\frac{x_0-x}{h}), \dots, \mathcal{K}(\frac{x_{M-1}-x}{h}))$.

By implementing the local polynomial in this way, the computational complexity is much higher than our method, and we summarize its computational complexity in the following proposition.

Following please find the proof.

Similar to the proof of the computational complexity in cubic spline, the proof of the computational complexity of local polynomial regression in the functional estimation stage lies in calculating all elements in matrix \mathbf{X} and vector $\nabla_t \mathbf{u}$, including

$$\left\{ \widehat{u(x_i, t_n)}, \widehat{\frac{\partial}{\partial x} u(x_i, t_n)}, \widehat{\frac{\partial^2}{\partial x^2} u(x_i, t_n)}, \widehat{\frac{\partial}{\partial t} u(x_i, t_n)} \right\}_{i=0, \dots, M-1, n=0, \dots, N-1}.$$

We will take the estimation of $\widehat{\frac{\partial^p}{\partial x^p} u(x_i, t_n)}$ with a general $p \in \mathbb{N}$ as an example. To solve $\left\{ \widehat{\frac{\partial^p}{\partial x^p} u(x_i, t_n)} \right\}_{i=0, \dots, M-1, n=0, \dots, N-1}$, we first focus on $\left\{ \widehat{\frac{\partial^p}{\partial x^p} u(x_i, t_n)} \right\}_{i=0, \dots, M-1}$, with $n \in \{0, \dots, N-1\}$ fixed. To solve it, the main idea of local polynomial regression is to do Taylor expansion:

$$\left\{ \begin{array}{lcl} u(x_0, t_n) & = & u(x, t_n) + \frac{\partial}{\partial x} u(x, t_n)(x_0 - x) + \dots + \frac{\partial^{\check{p}}}{\partial x^{\check{p}}} u(x, t_n)(x_0 - x)^{\check{p}} \\ u(x_1, t_n) & = & u(x, t_n) + \frac{\partial}{\partial x} u(x, t_n)(x_1 - x) + \dots + \frac{\partial^{\check{p}}}{\partial x^{\check{p}}} u(x, t_n)(x_1 - x)^{\check{p}} \\ \vdots & & \vdots \\ u(x_{M-1}, t_n) & = & u(x, t_n) + \frac{\partial}{\partial x} u(x, t_n)(x_{M-1} - x) + \dots + \frac{\partial^{\check{p}}}{\partial x^{\check{p}}} u(x, t_n)(x_{M-1} - x)^{\check{p}} \end{array} \right.,$$

where \check{p} is usually set as $\check{p} = p + 3$ to obtain asymptotic minimax efficiency (see Fan et al., 1997). In the above system of equations, if we denote

$$\mathbf{b}(x) = \left(u(x, t_n), \frac{\partial}{\partial x} u(x, t_n), \dots, \frac{\partial^{\check{p}}}{\partial x^{\check{p}}} u(x, t_n) \right)^\top,$$

then we can solve $\mathbf{b}(x)$ through the optimization problem in (23) with a closed-form solution

shown in (24):

$$\mathbf{b}(x) = (\mathbf{X}_{\text{spa}}^\top \mathbf{W}_{\text{spa}} \mathbf{X}_{\text{spa}})^{-1} \mathbf{X}_{\text{spa}}^\top \mathbf{W}_{\text{spa}} \mathbf{u}_\cdot^n, \quad (25)$$

where

$$\mathbf{X}_{\text{spa}} = \begin{bmatrix} 1 & (x_0 - x) & \dots & (x_0 - x)^{\check{p}} \\ 1 & (x_1 - x) & \dots & (x_1 - x)^{\check{p}} \\ \vdots & \vdots & \ddots & \vdots \\ 1 & (x_{M-1} - x) & \dots & (x_{M-1} - x)^{\check{p}} \end{bmatrix}, \mathbf{u}_\cdot^n = \begin{bmatrix} u_0^n \\ u_1^n \\ \vdots \\ u_{M-1}^n \end{bmatrix}$$

and $\mathbf{W}_{\text{spa}} = \text{diag}(\mathcal{K}(\frac{x_0-x}{h}), \dots, \mathcal{K}(\frac{x_{M-1}-x}{h}))$.

The main computational complexity to derive $\mathbf{b}(x)$ lies in the computation of inverse of matrix $\mathbf{X}_{\text{spa}}^\top \mathbf{W}_{\text{spa}} \mathbf{X}_{\text{spa}} \in \mathbb{R}^{(\check{p}+1) \times (\check{p}+1)}$, where

$$\begin{aligned} & \mathbf{X}_{\text{spa}}^\top \mathbf{W}_{\text{spa}} \mathbf{X}_{\text{spa}} \\ &= \begin{bmatrix} \sum_{i=0}^{M-1} w_i & \sum_{i=0}^{M-1} w_i(x_i - x) & \sum_{i=0}^{M-1} w_i(x_i - x)^2 & \dots & \sum_{i=0}^{M-1} w_i(x_i - x)^{\check{p}} \\ \sum_{i=0}^{M-1} w_i(x_i - x) & \sum_{i=0}^{M-1} w_i(x_i - x)^2 & \sum_{i=0}^{M-1} w_i(x_i - x)^3 & \dots & \sum_{i=0}^{M-1} w_i(x_i - x)^{\check{p}+1} \\ \sum_{i=0}^{M-1} w_i(x_i - x)^2 & \sum_{i=0}^{M-1} w_i(x_i - x)^3 & \sum_{i=0}^{M-1} w_i(x_i - x)^4 & \dots & \sum_{i=0}^{M-1} w_i(x_i - x)^{\check{p}+2} \\ \vdots & \vdots & \vdots & \ddots & \vdots \\ \sum_{i=0}^{M-1} w_i(x_i - x)^{\check{p}} & \sum_{i=0}^{M-1} w_i(x_i - x)^{\check{p}+1} & \sum_{i=0}^{M-1} w_i(x_i - x)^{\check{p}+2} & \dots & \sum_{i=0}^{M-1} w_i(x_i - x)^{2\check{p}} \end{bmatrix} \end{aligned}$$

and

$$\mathbf{X}_{\text{spa}}^\top \mathbf{W}_{\text{spa}} \mathbf{u}_i^n = \begin{pmatrix} \sum_{i=0}^{M-1} w_i u_i^n \\ \sum_{i=0}^{M-1} w_i (x_i - x) u_i^n \\ \sum_{i=0}^{M-1} w_i (x_i - x)^2 u_i^n \\ \sum_{i=0}^{M-1} w_i (x_i - x)^3 u_i^n \\ \sum_{i=0}^{M-1} w_i (x_i - x)^4 u_i^n \end{pmatrix},$$

we know that for a fixed $n \in \{0, \dots, N-1\}$ and $x \in \{x_0, \dots, x_{M-1}\}$, the computational complexity of computing $\mathbf{X}_{\text{spa}}^\top \mathbf{W}_{\text{spa}} \mathbf{X}_{\text{spa}}$ and $\mathbf{X}_{\text{spa}}^\top \mathbf{W}_{\text{spa}} \mathbf{u}_i^n$ is $O(\check{p}^2 M)$. Besides, the computational complexity to derive $(\mathbf{X}_{\text{spa}}^\top \mathbf{W}_{\text{spa}} \mathbf{X}_{\text{spa}})^{-1}$ is $O(\check{p}^3)$. So we know that for a fixed $n \in \{0, \dots, N-1\}$ and $x \in \{x_0, \dots, x_{M-1}\}$, the computational complexity of computing $\frac{\partial^p}{\partial x^p} u(x_i, t_n)$ is $\max\{O(\check{p}^2 M), O(\check{p}^3)\}$ with \check{p} usually set as $\check{p} = p + 3$. Accordingly, the computational complexity of computing $\{\widehat{\frac{\partial^p}{\partial x^p} u(x_i, t_n)}\}_{i=0, \dots, M-1, n=0, \dots, N-1}$ is $\max\{O(\check{p}^2 M^2 N), O(\check{p}^3 M N)\}$. Because $p \leq q_{\max}$, we know that the computational complexity of computing all derivatives with respective to x with highest order as q_{\max} is $\max\{O(q_{\max}^2 M^2 N), O(q_{\max}^3 M N)\}$. Similarly, the computational complexity of computing the first order derivatives with respective to t is $\max\{O(M N^2), O(M N)\}$. In conclusion, the computational complexity to derive all elements in matrix \mathbf{X} and vector $\nabla_t \mathbf{u}$, including

$$\left\{ \widehat{u(x_i, t_n)}, \widehat{\frac{\partial}{\partial x} u(x_i, t_n)}, \widehat{\frac{\partial^2}{\partial x^2} u(x_i, t_n)}, \widehat{\frac{\partial}{\partial t} u(x_i, t_n)} \right\}_{i=0, \dots, M-1, n=0, \dots, N-1}.$$

by local polynomial regression in (4) is $\max\{O(q_{\max}^2 M^2 N), O(M N^2), O(q_{\max}^3 M N)\}$, where q_{\max} is the highest order of derivatives desired in (3). \square

F.3 Proof of Lemma C.1

Proof. In this proof, we take $k = 0$ as an illustration example, i.e., prove that when

$$\epsilon > \mathcal{C}(\sigma, \|u\|_{L^\infty(\Omega)}) \max \left\{ \frac{4K_{\max}}{M^{3/7}}, 4AM^{-3/7}, 4\sqrt{2} \frac{d^3}{dx^3} f^*(0) M^{-3/7}, \frac{16(C \log M + \gamma) \log(M)}{M^{3/7}}, \right. \\ \left. 16\sqrt{\frac{\omega}{7}} \tilde{C}(\sigma, \|u\|_{L^\infty(\Omega)}) \frac{\sqrt{\log(M)}}{M^{3/7}} \right\},$$

we have

$$P \left[\sup_{x \in [0, X_{\max}]} \left| \widehat{u(x, t_n)} - u(x, t_n) \right| > \epsilon \right] < 2M e^{-\frac{M^{2/7}}{2\sigma^2}} + Q e^{-L\gamma} + 4\sqrt{2}\eta^4 M^{-\frac{2}{7}\omega}$$

for a fixed t_n with $n \in \{0, 1, \dots, N-1\}$. For $k = 1, 2$, it can be derived with the same logic flow.

Recall in Section 2.1, the fitted value of the smoothing cubic spline $s(x)$ is the minimizer of the optimization problem in (4). From Theorem A in Silverman (1984) (also mentioned by Messer et al. (1991) in the Section 1, and equation (2.2) in Craven and Wahba (1978)) that when Condition 3.4 - Condition 3.5 hold and for large M and small $\tilde{\lambda} = \frac{1-\alpha}{\alpha}$, we have

$$\widehat{f}_i = \frac{1}{M\tilde{\lambda}^{1/4}} \sum_{j=0}^{M-1} K \left(\frac{x_i - x_j}{\tilde{\lambda}^{1/4}} \right) u_j^n,$$

where $\widehat{f}_i = \widehat{u(x_i, t_n)}$, $\tilde{\lambda}$ trades off the goodness-of-fit and smoothness of the cubic spline in (4) and $K(\cdot)$ is a fixed kernel function defined as

$$K(x) = \frac{1}{2} e^{-|x|/\sqrt{2}} \left[\sin(|x|/\sqrt{2} + \pi/4) \right].$$

For a general spatial variable x and fixed $n \in \{0, 1, \dots, N-1\}$, we denote

$$f^*(x) = u(x, t_n),$$

which is the ground truth of the underlying dynamic function $u(x, t_n)$ with t_n fixed. Besides, we denote $\widehat{f}(x) = \widehat{u(x, t_n)}$, which is an estimation of the ground truth of $f^*(x) = u(x, t_n)$ with t_n fixed. Accordingly to the above discussion, this estimation of $\widehat{f}(x)$ can be written as

$$\widehat{f}(x) = \frac{1}{M\tilde{\lambda}^{1/4}} \sum_{j=0}^{M-1} K\left(\frac{x - x_j}{\tilde{\lambda}^{1/4}}\right) u_j^n,$$

where $\widehat{f}_i = \widehat{f}(x_i)$ for $i \in \{0, 1, \dots, M-1\}$

In order to bound $P\left(\sup |\widehat{f}(x) - f^*(x)| > \epsilon\right)$ for a general x , we decompose it as follows:

$$\begin{aligned} & P\left(\sup |\widehat{f}(x) - f^*(x)| > \epsilon\right) \\ &= P\left(\sup |\widehat{f}(x) - \widehat{f}^B(x) + \widehat{f}^B(x) - f^*(x)| > \epsilon\right) \\ &= P\left(\sup |\widehat{f}(x) - \widehat{f}^B(x) - E(\widehat{f}(x) - \widehat{f}^B(x)) + E(\widehat{f}(x) - \widehat{f}^B(x)) + \widehat{f}^B(x) - f^*(x)| > \epsilon\right) \\ &= P\left(\sup \underbrace{|\widehat{f}(x) - \widehat{f}^B(x)|}_{\mathcal{A}} - \underbrace{E(|\widehat{f}(x) - \widehat{f}^B(x)|)}_{\mathcal{B}} + \underbrace{E(\widehat{f}(x) - f^*(x)) + \widehat{f}^B(x) - E(\widehat{f}^B(x))}_{\mathcal{C} + \mathcal{D}} > \epsilon\right), \\ &\leq P\left(\sup |\mathcal{A}| > \frac{\epsilon}{4}\right) + P\left(\sup |\mathcal{B}| > \frac{\epsilon}{4}\right) + P\left(\sup |\mathcal{C}| > \frac{\epsilon}{4}\right) + P\left(\sup |\mathcal{D}| > \frac{\epsilon}{4}\right) \end{aligned} \tag{26}$$

where the $\widehat{f}^B(x)$ in (26) the truncated estimator defined as

$$\widehat{f}^B(x) = \frac{1}{M\tilde{\lambda}^{1/4}} \sum_{j=0}^{M-1} K\left(\frac{x - x_j}{\tilde{\lambda}^{1/4}}\right) u_j^n \mathbb{1}\{u_j^n < B_M\}.$$

Here $\{B_M\}$ is an increasing sequence and $B_M \rightarrow +\infty$ as $M \rightarrow +\infty$, i.e., $B_M = M^b$ with constant $b > 0$, and we will discuss the value of b at the end of this proof.

In the remaining of the proof, we work on the upper bound of the four decomposed terms, i.e., $P\left(\sup |\mathcal{A}| > \frac{\epsilon}{4}\right), P\left(\sup |\mathcal{B}| > \frac{\epsilon}{4}\right), P\left(\sup |\mathcal{C}| > \frac{\epsilon}{4}\right), P\left(\sup |\mathcal{D}| > \frac{\epsilon}{4}\right)$.

First, let us discuss the upper bound of $P\left(\sup |\mathcal{A}| > \frac{\epsilon}{4}\right)$.

Because

$$\begin{aligned}
P\left(\sup |\mathcal{A}| > \frac{\epsilon}{4}\right) &= P\left(\sup \left|\widehat{f}(x) - \widehat{f}^B(x)\right| > \frac{\epsilon}{4}\right) \\
&= P\left(\sup \left|\frac{1}{M\tilde{\lambda}^{1/4}} \sum_{j=0}^{M-1} K\left(\frac{x-x_j}{\tilde{\lambda}^{1/4}}\right) u_j^n \mathbb{1}\{u_j^n \geq B_M\}\right| > \frac{\epsilon}{4}\right) \\
&\leq P\left(\sup \left|\frac{K_{\max}}{M\tilde{\lambda}^{1/4}} \sum_{j=0}^{M-1} u_j^n \mathbb{1}\{u_j^n \geq B_M\}\right| > \frac{\epsilon}{4}\right),
\end{aligned}$$

where $K_{\max} = \max_{x \in [0, X_{\max}] \cup [0, T_{\max}]} K(x)$. If we let $\frac{\epsilon}{4} > \frac{K_{\max}}{M\tilde{\lambda}^{1/4}} B_M$, then we have

$$\begin{aligned}
P\left(\sup |\mathcal{A}| > \frac{\epsilon}{4}\right) &\leq P(\exists i = 0, \dots, M-1, \text{s.t. } |u_i^n| \geq B_M) \\
&= P\left(\max_{i=0, \dots, M-1} |u_i^n| \geq B_M\right)
\end{aligned}$$

Let $C_M = B_M - \|U\|_{L^\infty(\Omega)}$, where U is the random variable generated from the unknown dynamic system, i.e., $U = u(x, t) + \epsilon$ with $\epsilon \sim N(0, \sigma^2)$. Then we have

$$\begin{aligned}
P\left(\sup |\mathcal{A}| > \frac{\epsilon}{4}\right) &= P\left(\sup \left|\widehat{f}(x) - \widehat{f}^B(x)\right| > \frac{\epsilon}{4}\right) \\
&\leq P\left(\max_{i=0, \dots, M-1} |U_i^n - u_i^n| \geq C_M\right) \\
&\leq 2M e^{-C_M^2/(2\sigma^2)}
\end{aligned}$$

Next, let us discuss the upper bound of $P(\sup |\mathcal{B}| > \frac{\epsilon}{4})$.

$$\begin{aligned}
\mathcal{B} &= E(|\widehat{f}(x) - \widehat{f}^B(x)|) \\
&= E\left(\left|\frac{1}{M\tilde{\lambda}^{1/4}} \sum_{j=0}^{M-1} K\left(\frac{x-x_j}{\tilde{\lambda}^{1/4}}\right) u_j^n \mathbb{1}\{u_j^n \geq B_M\}\right|\right) \\
&\leq E\left(\frac{1}{M\tilde{\lambda}^{1/4}} \sum_{j=0}^{M-1} \left|K\left(\frac{x-x_j}{\tilde{\lambda}^{1/4}}\right)\right| |u_j^n| \mathbb{1}\{u_j^n \geq B_M\}\right) \\
&= \frac{1}{\tilde{\lambda}^{1/4}} \int \int_{|u| \geq B_M} \left|K\left(\frac{x-a}{\tilde{\lambda}^{1/4}}\right)\right| |u| dF_M(a, u) \tag{27}
\end{aligned}$$

$$\leq \underbrace{\int |K(\xi)| d\xi}_{\mathcal{V}} \times \sup_{\alpha} \int_{|u| \geq B_M} |u| f_M(\alpha, u) du \tag{28}$$

Here in (27), $F_M(\cdot, \cdot)$ is the empirical c.d.f. of (x, u) 's, and in (28), $f_M(\cdot, \cdot)$ is the empirical p.d.f. of (x, u) 's.

Now let us take a look at the upper bound of \mathcal{V} . For any $s > 0$, we have

$$\begin{aligned}
\sup_{\alpha} \int_{|u| \geq B_M} \frac{|u|}{B_M} f_M(\alpha, u) du &\leq \sup_{\alpha} \int_{|u| \geq B_M} \left(\frac{|u|}{B_M}\right)^s f_M(\alpha, u) du \\
&\leq \sup_{\alpha} \int \left(\frac{|u|}{B_M}\right)^s f_M(\alpha, u) du,
\end{aligned}$$

which gives

$$\mathcal{V} := \sup_{\alpha} \int_{|u| \geq B_M} |u| f_M(\alpha, u) du \leq B_M^{1-s} \underbrace{\sup_{\alpha} \int |u|^s f_M(\alpha, u) du}_{\pi_s}.$$

From the lemma statement we know that when $s = 2$, we have $\pi_s := \sup_{\alpha} \int |u|^s f_M(\alpha, u) du < +\infty$. If we set $A = \pi_s \int |K(\xi)| d\xi$, then we have

$$\mathcal{B} \leq AB_M^{1-s}$$

So when $\frac{\epsilon}{4} > AB_M^{1-s}$, we have

$$P\left(\sup |\mathcal{B}| > \frac{\epsilon}{4}\right) = P\left(E\left(|\widehat{f}(x) - \widehat{f}^B(x)|\right) \geq \frac{\epsilon}{4}\right) = 0.$$

Then, let us discuss the upper bound of $P\left(\sup |\mathcal{C}| > \frac{\epsilon}{4}\right)$. According to Lemma 5 in Rice and Rosenblatt (1983), when

$f^*(x) \in C^4$, $\frac{d^2}{dx^2}f^*(x_0) = \frac{d^2}{dx^2}f^*(x_{M-1}) = 0$ and $\frac{d^3}{dx^3}f^*(x_0) \neq 0$, $\frac{d^3}{dx^3}f^*(x_{M-1}) = 0$, we have

$$\begin{aligned} & E(\widehat{f}(x)) - f^*(x) \\ = & \sqrt{2} \frac{d^3}{dx^3}f^*(0) \tilde{\lambda}^{3/4} \exp\left(\frac{-x}{\sqrt{2}}\tilde{\lambda}^{-1/4}\right) \cos\left(\frac{x}{\sqrt{2}}\tilde{\lambda}^{-1/4}\right) + \ell(x), \end{aligned}$$

where the error term $\ell(x)$ satisfies

$$\int [\ell(x)]^2 dx = o\left(\int [E(\widehat{f}(x)) - f^*(x)]^2 dx\right).$$

So when $\frac{\epsilon}{4} > \sqrt{2} \frac{d^3}{dx^3}f^*(0) \tilde{\lambda}^{3/4}$ and M is sufficiently large then we have

$$P\left(\sup |\mathcal{C}| > \frac{\epsilon}{4}\right) = 0$$

Finally, let us discuss the upper bound of $P\left(\sup |\mathcal{D}| > \frac{\epsilon}{4}\right)$.

In order to bound $P\left(\sup |D| > \frac{\epsilon}{4}\right)$, we further decompose \mathcal{D} into two components, i.e.,

$$\mathcal{D} := \widehat{f}^B(x) - E(\widehat{f}^B(x)) = e_M(x, t_n) + \frac{1}{\sqrt{M}}\rho_M(x, t_n).$$

The decomposition procedure and the definition of $e_M(x, t_n), \rho_M(x, t_n)$ are described in the

following system of equations (see Mack and Silverman, 1982, Proposition 2):

$$\begin{aligned}
\mathcal{D} &= \widehat{f}^B(x) - E(\widehat{f}^B(x)) \\
&= \frac{1}{M\widetilde{\lambda}^{1/4}} \sum_{j=0}^{M-1} K\left(\frac{x-x_j}{\widetilde{\lambda}^{1/4}}\right) u_j^n \mathbb{1}\{u_j^n < B_M\} - \\
&\quad E\left(\frac{1}{M\widetilde{\lambda}^{1/4}} \sum_{j=0}^{M-1} K\left(\frac{x-x_j}{\widetilde{\lambda}^{1/4}}\right) u_j^n \mathbb{1}\{u_j^n < B_M\}\right) \\
&= \frac{1}{\sqrt{M\widetilde{\lambda}^{1/4}}} \int_{a \in \mathbb{R}} \int_{|u| < B_M} K\left(\frac{x-a}{\widetilde{\lambda}^{1/4}}\right) u \underbrace{d\left(\sqrt{M}(F_M(a, u) - F(a, u))\right)}_{Z_M(a, u)} \quad (29) \\
&= \frac{1}{\sqrt{M\widetilde{\lambda}^{1/4}}} \int_{a \in \mathbb{R}} K\left(\frac{x-a}{\widetilde{\lambda}^{1/4}}\right) \int_{|u| < B_M} u d(Z_M(a, u)) \\
&= \frac{1}{\sqrt{M\widetilde{\lambda}^{1/4}}} \int_{a \in \mathbb{R}} K\left(\frac{x-a}{\widetilde{\lambda}^{1/4}}\right) \left[\int_{|u| < B_M} u d(Z_M(a, u) - B_0(T(a, u))) + \right. \\
&\quad \left. \int_{|u| < B_M} u dB_0(T(a, u)) \right] \quad (30) \\
&= \underbrace{\frac{1}{\sqrt{M\widetilde{\lambda}^{1/4}}} \int_{a \in \mathbb{R}} \int_{|u| < B_M} K\left(\frac{x-a}{\widetilde{\lambda}^{1/4}}\right) u d(Z_M(a, u) - B_0(T(a, u)))}_{e_M(x, t_n)} \\
&\quad + \underbrace{\frac{1}{\sqrt{M}} \frac{1}{\widetilde{\lambda}^{1/4}} \int_{a \in \mathbb{R}} \int_{|u| < B_M} K\left(\frac{x-a}{\widetilde{\lambda}^{1/4}}\right) u dB_0(T(a, u))}_{\rho_M(x, t_n)}.
\end{aligned}$$

In (29), $F_M(\cdot, \cdot) := F_M(\cdot, \cdot | t_n)$ is the empirical c.d.f of (x, u) with a fixed t_n , and $Z_M(a, u) = \sqrt{M}(F_M(a, u) - F(a, u))$ is a two-dimensional empirical process (see Tusnády, 1977; Mack and Silverman, 1982). In (30), $B_0(T(a, u))$ is a sample path of two-dimensional Brownian bridge. And $T(a, u) : \mathbb{R}^2 \rightarrow [0, 1]^2$ is the transformation defined by Rosenblatt (1952), i.e., $T(a, u) = (F_A(x), F_{U|A}(u|a))$, where F_A is the marginal c.d.f of A and $F_{U|A}$ is the conditional c.d.f of U given A (see Mack and Silverman, 1982, Proposition 2).

Through the above decomposition of \mathcal{D} , we have

$$P\left(\sup |D| > \frac{\epsilon}{4}\right) \leq P\left(\sup |e_M(x, t_n)| > \frac{\epsilon}{8}\right) + P\left(\sup \frac{1}{\sqrt{M}}|\rho_M(x, t_n)| > \frac{\epsilon}{8}\right).$$

For $e_M(x, t_n)$, we have

$$\begin{aligned} & P\left(\sup |e_M(x, t_n)| > \frac{\epsilon}{8}\right) \\ = & P\left(\sup \left| \frac{1}{\sqrt{M}\tilde{\lambda}^{1/4}} \int_{a \in \mathbb{R}} \int_{|u| < B_M} K\left(\frac{x-a}{\tilde{\lambda}^{1/4}}\right) u \, d(Z_M(a, u) - B_0(T(a, u))) \right| > \frac{\epsilon}{8}\right) \\ \leq & P\left(\frac{2B_M K_{\max}}{\sqrt{M}\tilde{\lambda}^{1/4}} \sup_{a,u} |Z_M(a, u) - B_0(T(a, u))| > \frac{\epsilon}{8}\right). \end{aligned}$$

Proved by Theorem 1 in Tusnády (1977), we know that, for any γ , we have

$$P\left(\sup_{a,u} |Z_M(a, u) - B_0(T(a, u))| > \frac{(C \log M + \gamma) \log M}{\sqrt{M}}\right) \leq Q e^{-L\gamma},$$

where C, Q, L are absolute positive constants which is independent of temporal resolution N and spatial resolution M . Thus, when $\frac{\epsilon}{8} \geq \frac{2B_M K_{\max}}{\sqrt{M}\tilde{\lambda}^{1/4}} \frac{(C \log M + \gamma) \log M}{\sqrt{M}}$, we have

$$P\left(\sup |e_M(x, t_n)| > \frac{\epsilon}{8}\right) < Q e^{-L\gamma}.$$

For $\rho_M(x, t_n)$, by equation (7) in Mack and Silverman (1982), we have

$$\begin{aligned} \frac{\tilde{\lambda}^{1/8} \sup |\rho_M(x, t_n)|}{\sqrt{\log(1/\tilde{\lambda}^{1/4})}} & \leq \underbrace{16(\log V)^{1/2} S^{1/2} \left(\log\left(\frac{1}{\tilde{\lambda}^{1/4}}\right)\right)^{-1/2} \int |\xi|^{1/2} |dK(\xi)| +}_{\mathcal{W}_{1,M}} \\ & \underbrace{16\sqrt{2}\tilde{\lambda}^{-1/8} \left(\log\left(\frac{1}{\tilde{\lambda}^{1/4}}\right)\right)^{-1/2} \int q(S\tilde{\lambda}^{1/4}|\tau|) |d(K(\tau))|,}_{\mathcal{W}_{2,M}} \end{aligned}$$

where V is a random variable satisfying $E(V) \leq 4\sqrt{2}\eta^4$ for $\eta^2 = \max_{i=0, \dots, M-1, n=0, \dots, N-1} E(U_i^n)^2$, $S = \sup_x \int u^2 f(x, u) du$ with $f(\cdot, \cdot)$ as the distribution function of (x_i, u_i^n) , and $q(z) =$

$\int_0^z \frac{1}{2} \sqrt{\frac{1}{y} \log \left(\frac{1}{y} \right)} dy$. So we have the following system of equations:

$$\begin{aligned}
& P \left(\sup \frac{1}{\sqrt{M}} |\rho_M(x, t_n)| > \frac{\epsilon}{8} \right) \\
&= P \left(\frac{\tilde{\lambda}^{1/8} \sup |\rho_M(x, t_n)|}{\sqrt{\log(1/\tilde{\lambda}^{1/4})}} > \frac{\sqrt{M} \tilde{\lambda}^{1/8} \epsilon}{8 \sqrt{\log(1/\tilde{\lambda}^{1/4})}} \right) \\
&\leq P \left(\mathcal{W}_{1,M} + \mathcal{W}_{2,M} > \frac{\sqrt{M} \tilde{\lambda}^{1/8} \epsilon}{8 \sqrt{\log(1/\tilde{\lambda}^{1/4})}} \right) \\
&\leq P \left(\mathcal{W}_{1,M} \geq \frac{\sqrt{M} \tilde{\lambda}^{1/8} \epsilon}{16 \sqrt{\log(1/\tilde{\lambda}^{1/4})}} \right) + P \left(\mathcal{W}_{2,M} \geq \frac{\sqrt{M} \tilde{\lambda}^{1/8} \epsilon}{16 \sqrt{\log(1/\tilde{\lambda}^{1/4})}} \right) \tag{31}
\end{aligned}$$

Now let us bound $P \left(\mathcal{W}_{1,M} \geq \frac{\sqrt{M} \tilde{\lambda}^{1/8} \epsilon}{16 \sqrt{\log(1/\tilde{\lambda}^{1/4})}} \right)$, $P \left(\mathcal{W}_{2,M} \geq \frac{\sqrt{M} \tilde{\lambda}^{1/8} \epsilon}{16 \sqrt{\log(1/\tilde{\lambda}^{1/4})}} \right)$ in (31) separately.

1. For the first term in (31), we have

$$\begin{aligned}
& P \left(\mathcal{W}_{1,M} \geq \frac{\sqrt{M}\tilde{\lambda}^{1/8}\epsilon}{16\sqrt{\log(1/\tilde{\lambda}^{1/4})}} \right) \\
&= P \left(16(\log V)^{1/2} S^{1/2} \left(\log \left(\frac{1}{\tilde{\lambda}^{1/4}} \right) \right)^{-1/2} \int |\xi|^{1/2} |dK(\xi)| \geq \frac{\sqrt{M}\tilde{\lambda}^{1/8}\epsilon}{16\sqrt{\log(1/\tilde{\lambda}^{1/4})}} \right) \\
&= P \left((\log V)^{1/2} \geq \frac{\sqrt{M}\tilde{\lambda}^{1/8}\epsilon}{16^2 S^{1/2} \int |\xi|^{1/2} |dK(\xi)|} \right) \\
&= P \left(\log V \geq \left(\frac{\sqrt{M}\tilde{\lambda}^{1/8}\epsilon}{16^2 S^{1/2} \int |\xi|^{1/2} |dK(\xi)|} \right)^2 \right) \\
&= P \left(V \geq \exp \left[\left(\frac{\sqrt{M}\tilde{\lambda}^{1/8}\epsilon}{16^2 S^{1/2} \int |\xi|^{1/2} |dK(\xi)|} \right)^2 \right] \right) \\
&\leq \frac{E(V)}{\exp \left[\left(\frac{\sqrt{M}\tilde{\lambda}^{1/8}\epsilon}{16^2 S^{1/2} \int |\xi|^{1/2} |dK(\xi)|} \right)^2 \right]} \tag{32}
\end{aligned}$$

$$\begin{aligned}
&\leq \frac{4\sqrt{2}\eta^4}{\exp \left[\left(\frac{\sqrt{M}\tilde{\lambda}^{1/8}\epsilon}{16^2 S^{1/2} \int |\xi|^{1/2} |dK(\xi)|} \right)^2 \right]} \tag{33}
\end{aligned}$$

$$= 4\sqrt{2}\eta^4 \tilde{\lambda}^{\omega/4} \tag{34}$$

Here inequality (32) is due to Markov's inequality, and inequality (33) is due to the fact that $E(V) \leq 4\sqrt{2}\eta^4$. Equality (34) is because we set $\frac{\sqrt{M}\tilde{\lambda}^{1/8}\epsilon}{16\sqrt{\log(1/\tilde{\lambda}^{1/4})}} = \sqrt{\omega}\tilde{C}(t_n, \sigma, \|u\|_{L^\infty}(\Omega))$, where

$$\tilde{C}(t_n, \sigma, \|u\|_{L^\infty}(\Omega)) := 16\sqrt{S} \int |\xi|^{1/2} |dK(\xi)|$$

and $\omega > 1$ is an arbitrary scalar.

2. For the second term of (31), it converges to $\tilde{C}(t_n, \sigma, \|u\|_{L^\infty(\Omega)})$ by using arguments similar to Silverman (1978) (page. 180-181) under the condition in Lemma C.1 that $\int \sqrt{|x \log(|x|)|} |dK(x)| < +\infty$. Here we add $(t_n, \sigma, \|u\|_{L^\infty(\Omega)})$ after \tilde{C} to emphasize that the constant $\tilde{C}(t_n, \sigma, \|u\|_{L^\infty(\Omega)})$ is dependent on $t_n, \sigma, \|u\|_{L^\infty(\Omega)}$.

It should be noted that

$$\tilde{C}(t_n, \sigma, \|u\|_{L^\infty(\Omega)}) < +\infty, \quad (35)$$

given the reasons listed as follows. First, it can be easily verified that the term $\int |\xi|^{1/2} |dK(\xi)|$ in $\tilde{C}(t_n, \sigma, \|u\|_{L^\infty(\Omega)})$ is bounded. Second, for $S = \sup_x \int u^2 f(x, u) du$, it is also bounded. The reasons are described as follows. For a general $\varrho > 0$, we have

$$\begin{aligned} \sup_{x \in [0, X_{\max}]} \int |u|^\varrho f(x, u) du &= \sup_{x \in [0, X_{\max}]} \int |u|^\varrho \frac{1}{\sqrt{2\pi\sigma^2}} \exp\left(-\frac{(u - u(x, t_n))^2}{2\sigma^2}\right) du \\ &= \sup_{x \in [0, X_{\max}]} \frac{1}{\sqrt{2}} \sigma^2 2^{\varrho/2} \Gamma\left(\frac{1+\varrho}{2}\right) G\left(-\frac{\varrho}{2}, \frac{1}{2}, -\frac{1}{2} \left(\frac{u(x, t_n)}{\sigma}\right)^2\right), \end{aligned}$$

where $G(a, b, z)$ is Kummer's confluent hypergeometric function of $z \in \mathbb{C}$ with parameters $a, b \in \mathbb{C}$ (see Winkelbauer, 2012). Because $G\left(-\frac{\varrho}{2}, \frac{1}{2}, \cdot\right)$ is an entire function for fixed parameters, we have

$$\begin{aligned} &\sup_{x \in [0, X_{\max}]} \int |u|^\varrho f(x, u) du \\ &\leq \sup_{x \in [0, X_{\max}]} \frac{1}{\sqrt{2}} \sigma^2 2^{\varrho/2} \Gamma\left(\frac{1+\varrho}{2}\right) \sup_{z \in \left[-\frac{\max_{t \in \Omega} u^2(x, t)}{2\sigma^2}, -\frac{\min_{t \in \Omega} u^2(x, t)}{2\sigma^2}\right]} G\left(-\frac{\varrho}{2}, \frac{1}{2}, z\right) \\ &< +\infty. \end{aligned}$$

So we can bound $\sup_{x \in [0, X_{\max}]} \int |u|^\varrho f(x, u) du$ by a constant. If we take $\varrho = 2$, we can obtain $S = \sup_x \int u^2 f(x, u) du$ bounded by a constant. So we can declare the statement in (35).

We would also like to declare that there exist a constant $\tilde{C}(\sigma, \|u\|_{L^\infty(\Omega)}) > 0$ such that for any $N \geq 1$, we have

$$\max_{n=0,\dots,N-1} \tilde{C}(t_n, \sigma, \|u\|_{L^\infty(\Omega)}) \leq \tilde{C}(\sigma, \|u\|_{L^\infty(\Omega)}),$$

where $\bar{C}(\sigma, \|u\|_{L^\infty(\Omega)})$ is independent of t_n, x_i, M, N , and only depends on the noisy data \mathcal{D} itself.

From the above discussion, we learn that $\mathcal{W}_{2,M}$ converges to $\tilde{C}(t_n, \sigma, \|u\|_{L^\infty(\Omega)})$, which can be bounded by $\tilde{C}(\sigma, \|u\|_{L^\infty(\Omega)})$. If we set $\frac{\sqrt{M\tilde{\lambda}^{1/8}\epsilon}}{16\sqrt{\log(1/\tilde{\lambda}^{1/4})}} > \sqrt{\omega}\tilde{C}(\sigma, \|u\|_{L^\infty(\Omega)})$ with $\omega > 1$, then there exists a positive integer $\dot{M}(\omega)$ such that as long as $M > \dot{M}(\omega)$, we have $P\left(\mathcal{W}_{2,M} \geq \frac{\sqrt{M\tilde{\lambda}^{1/8}\epsilon}}{16\sqrt{\log(1/\tilde{\lambda}^{1/4})}}\right) = 0$.

For the value of ω , we set it as $\omega = M^{2r}$ with $r > 0$. And we will discuss the value of r later.

By combining $P\left(\mathcal{W}_{1,M} \geq \frac{\sqrt{M\tilde{\lambda}^{1/8}\epsilon}}{16\sqrt{\log(1/\tilde{\lambda}^{1/4})}}\right), P\left(\mathcal{W}_{2,M} \geq \frac{\sqrt{M\tilde{\lambda}^{1/8}\epsilon}}{16\sqrt{\log(1/\tilde{\lambda}^{1/4})}}\right)$ together, we have when $\frac{\epsilon}{16} > \sqrt{\omega}\tilde{C}(\sigma, \|u\|_{L^\infty(\Omega)})\sqrt{\frac{\log(1/\tilde{\lambda}^{1/4})}{M\tilde{\lambda}^{1/4}}}$ and $M > \dot{M}(\omega)$, we have

$$P\left(\sup \left| \frac{1}{\sqrt{M}} \rho_M(x, t_n) \right| > \frac{\epsilon}{8}\right) < 4\sqrt{2}\eta^4\tilde{\lambda}^{\omega/4}.$$

By combining the discussion on $P\left(\sup |\mathcal{A}| > \frac{\epsilon}{4}\right), P\left(\sup |\mathcal{B}| > \frac{\epsilon}{4}\right), P\left(\sup |\mathcal{C}| > \frac{\epsilon}{4}\right)$, and $P\left(\sup |\mathcal{D}| > \frac{\epsilon}{4}\right)$, we can conclude that when

- $\frac{\epsilon}{4} > \frac{K_{\max}}{M\tilde{\lambda}^{1/4}} B_M$
- $\frac{\epsilon}{4} > AB_M^{1-s}$ ($s = 2$)
- $\frac{\epsilon}{4} > \sqrt{2}\frac{d^3}{dx^3}f^*(0)\tilde{\lambda}^{3/4}$

- $\frac{\epsilon}{8} > \frac{2B_M K_{\max}(C \log M + \gamma) \log M}{\tilde{\lambda}^{1/4} M}$
- $\frac{\epsilon}{16} > \sqrt{\omega} \tilde{C}(\sigma, \|u\|_{L^\infty(\Omega)}) \sqrt{\frac{\log(1/\tilde{\lambda}^{1/4})}{M \tilde{\lambda}^{1/4}}}$

we have

$$P(\sup |\mathcal{A} + \mathcal{B} + \mathcal{C} + \mathcal{D}| > \epsilon) < \underbrace{2M e^{-\frac{C_M^2}{2\sigma^2}}}_{\mathcal{Z}_1} + \underbrace{Q e^{-L\gamma}}_{\mathcal{Z}_2} + \underbrace{4\sqrt{2}\eta^4 \tilde{\lambda}^{\omega/4}}_{\mathcal{Z}_3}. \quad (36)$$

Let

$$\begin{cases} E_1 = \frac{4K_{\max}}{M\tilde{\lambda}^{1/4}} B_M \\ E_2 = 4AB_M^{1-s} \\ E_3 = 4\sqrt{2} \frac{d^3}{dx^3} f^*(0) \tilde{\lambda}^{3/4} \\ E_4 = \frac{16B_M K_{\max}(C \log M + \gamma) \log M}{\tilde{\lambda}^{1/4} M} \\ E_5 = 16\sqrt{\omega} \tilde{C}(\sigma, \|u\|_{L^\infty(\Omega)}) \sqrt{\frac{\log(1/\tilde{\lambda}^{1/4})}{M \tilde{\lambda}^{1/4}}} \end{cases},$$

by setting $\tilde{\lambda} = M^{-a}, B_M = M^b$ with $a, b > 0$, we have

$$\begin{cases} E_1 = \frac{4K_{\max}}{M\tilde{\lambda}^{1/4}} B_M = \frac{4K_{\max}}{M^{1-a/4-b}} \\ E_2 = 4AB_M^{1-s} = 4A \frac{1}{M^{b(s-1)}} \\ E_3 = 4\sqrt{2} \frac{d}{dx} f^*(0) \tilde{\lambda}^{3/4} = 4\sqrt{2} \frac{d}{dx} f^*(0) M^{-3a/4} \\ E_4 = \frac{16B_M K_{\max}(C \log M + \gamma) \log M}{\tilde{\lambda}^{1/4} M} = \frac{16K_{\max}(C \log M + \gamma) \log(M)}{M^{1-a/4-b}} \\ E_5 = 16\sqrt{\omega} \tilde{C}(\sigma, \|u\|_{L^\infty(\Omega)}) \sqrt{\frac{\log(1/\tilde{\lambda}^{1/4})}{M \tilde{\lambda}^{1/4}}} = 8\sqrt{a\omega} \tilde{C}(\sigma, \|u\|_{L^\infty(\Omega)}) \sqrt{\frac{\log(M)}{M^{1-a/4}}}. \end{cases}$$

To guarantee that $E_1, E_2, E_3, E_4, E_5 \rightarrow 0$ as $M \rightarrow +\infty$, we can set

$$\begin{cases} 1 - a/4 - b = 3a/4 \\ b(s-1) > 0 \\ \frac{1}{2}(1 - a/4) = 3a/4 \\ a, b > 0 \\ s = 2 \end{cases}.$$

then we have

$$\begin{cases} a = 4/7 \\ b = 3/7 \\ s = 2 \end{cases} .$$

Accordingly, we have

$$\begin{cases} E_1 = \frac{4K_{\max}}{M^{3/7}} \\ E_2 = 4AM^{-3/7} \\ E_3 = 4\sqrt{2}\frac{d^3}{dx^3}f^*(0)M^{-3/7} \\ E_4 = \frac{16K_{\max}(C \log M + \gamma) \log(M)}{M^{3/7}} \\ E_5 = 16\sqrt{\frac{\omega}{7}}\tilde{C}(\sigma, \|u\|_{L^\infty(\Omega)}) \frac{\sqrt{\log(M)}}{M^{3/7}} \end{cases} ,$$

where

$$E_1, E_2, E_3, E_5 \lesssim E_4$$

as $M \rightarrow +\infty$. Here, the operator \lesssim means that when $M \rightarrow +\infty$, the order of the left side hand of \lesssim will be much smaller than that on the right side hand. So we can declare that when M is sufficiently large and

$$\epsilon > \max \left\{ \frac{4K_{\max}}{M^{3/7}}, 4AM^{-3/7}, 4\sqrt{2}\frac{d^3}{dx^3}f^*(0)M^{-3/7}, \frac{16K_{\max}(C \log M + \gamma) \log(M)}{M^{3/7}}, 16\sqrt{\frac{\omega}{7}}\tilde{C}(\sigma, \|u\|_{L^\infty(\Omega)}) \frac{\sqrt{\log(M)}}{M^{3/7}} \right\}$$

we have

$$\begin{aligned} P(\sup |\mathcal{A} + \mathcal{B} + \mathcal{C} + \mathcal{D}| > \epsilon) &\leq 2Me^{-\frac{C_M^2}{2\sigma^2}} + Qe^{-L\gamma} + 4\sqrt{2}\eta^4\tilde{\lambda}^{\omega/4} \\ &= 2Me^{-\frac{(M^{3/7} - \|U\|_{L^\infty(\Omega)})^2}{2\sigma^2}} + Qe^{-L\gamma} + 4\sqrt{2}\eta^4M^{-\omega/7} \end{aligned}$$

□

F.4 Proof of Lemma C.2

Proof. For the estimation error $\|\nabla_t \mathbf{u} - \mathbf{X}\beta^*\|_\infty$, we have

$$\begin{aligned}
\|\nabla_t \mathbf{u} - \mathbf{X}\beta^*\|_\infty &= \|\nabla_t \mathbf{u} - \nabla_t \mathbf{u}^* + \nabla_t \mathbf{u}^* - \mathbf{X}\beta^*\|_\infty \\
&= \|\nabla_t \mathbf{u} - \nabla_t \mathbf{u}^* + \mathbf{X}^* \beta^* - \mathbf{X}\beta^*\|_\infty \\
&\leq \|\nabla_t \mathbf{u} - \nabla_t \mathbf{u}^*\|_\infty + \|(\mathbf{X}^* - \mathbf{X})\beta^*\|_\infty.
\end{aligned} \tag{37}$$

So accordingly, we have

$$P(\|\nabla_t \mathbf{u} - \mathbf{X}\beta^*\|_\infty > \epsilon) \leq P\left(\|\nabla_t \mathbf{u} - \nabla_t \mathbf{u}^*\|_\infty > \frac{\epsilon}{2}\right) + P(\|(\mathbf{X}^* - \mathbf{X})\beta^*\|_\infty).$$

In the remaining of the proof, we will discuss the bound of $P(\|\nabla_t \mathbf{u} - \nabla_t \mathbf{u}^*\|_\infty > \frac{\epsilon}{2})$ and $P(\|(\mathbf{X}^* - \mathbf{X})\beta^*\|_\infty)$ separately.

- First let us discuss the bound of $P(\|\nabla_t \mathbf{u} - \nabla_t \mathbf{u}^*\|_\infty > \frac{\epsilon}{2})$. Because

$$\begin{aligned}
P\left(\|\nabla_t \mathbf{u} - \nabla_t \mathbf{u}^*\|_\infty > \frac{\epsilon}{2}\right) &\leq P\left(\max_{i=0, \dots, M-1} \sup_{t \in [0, T_{\max}]} \left| \widehat{\frac{\partial}{\partial t} u(x_i, t)} - \frac{\partial}{\partial t} u(x_i, t) \right| > \frac{\epsilon}{2}\right) \\
&\leq \sum_{i=0}^{M-1} P\left(\sup_{t \in [0, T_{\max}]} \left| \widehat{\frac{\partial}{\partial t} u(x_i, t)} - \frac{\partial}{\partial t} u(x_i, t) \right| > \frac{\epsilon}{2}\right),
\end{aligned}$$

if we set

$$\begin{aligned}
\frac{\epsilon}{2} > \mathcal{C}_{(\sigma, \|u\|_{L^\infty(\Omega)})} \max & \left\{ 4K_{\max} N^{-3/7}, 4\bar{A}N^{-3/7}, 4\sqrt{2} \frac{d^3}{dx^3} \bar{f}^*(0) N^{-3/7}, \right. \\
& \frac{16K_{\max} [C_{(\sigma, \|u\|_{L^\infty(\Omega)})} \log(N) + \gamma(N)] \log(N)}{N^{3/7}}, \\
& \left. 16\sqrt{\frac{\omega(N)}{7}} \widetilde{C}_{(\sigma, \|u\|_{L^\infty(\Omega)})} \frac{\sqrt{\log(N)}}{N^{3/7}} \right\}, \tag{38}
\end{aligned}$$

then we have

$$\begin{aligned}
P\left(\|\nabla_t \mathbf{u} - \nabla_t \mathbf{u}^*\|_\infty > \frac{\epsilon}{2}\right) \\
\leq M \left[2N e^{-\frac{(N^{3/7} - \|U\|_{L^\infty(\Omega)})^2}{2\sigma^2}} + Q_{(\sigma, \|u\|_{L^\infty(\Omega)})} e^{-L\gamma(N)} + 4\sqrt{2}\eta^4 N^{-\omega(N)/7} \right], \tag{39}
\end{aligned}$$

where inequity (39) is derived according to Corollary C.1.

- Second, let us discuss the bound of $P(\|(\mathbf{X}^* - \mathbf{X})\beta^*\|_\infty)$. Because

$$\begin{aligned}
& P\left(\|(\mathbf{X}^* - \mathbf{X})\beta^*\|_\infty > \frac{\epsilon}{2}\right) \\
& \leq P\left(\|\beta^*\|_\infty \max_{n=0, \dots, N-1} \sup_{x \in [0, X_{\max}]} \sum_{k=1}^K \|(\mathbf{X}_k^*(x, t_n) - \mathbf{X}_k(x, t_n))\|_\infty > \frac{\epsilon}{2}\right) \\
& = P\left(\max_{n=0, \dots, N-1} \sup_{x \in [0, X_{\max}]} \sum_{k=1}^K \|(\mathbf{X}_k^*(x, t_n) - \mathbf{X}_k(x, t_n))\|_\infty > \frac{\epsilon}{2\|\beta^*\|_\infty}\right) \\
& \leq \sum_{n=0}^{N-1} \sum_{k=1}^K P\left(\sup_{x \in [0, X_{\max}]} \|(\mathbf{X}_k^*(x, t_n) - \mathbf{X}_k(x, t_n))\|_\infty > \frac{\epsilon}{2K\|\beta^*\|_\infty}\right),
\end{aligned}$$

if we set

$$\begin{aligned}
\frac{\epsilon}{2K\|\beta^*\|_\infty} & > \mathcal{C}_{(\sigma, \|u\|_{L^\infty(\Omega)})} \max \left\{ 4K_{\max} M^{-3/7}, 4AM^{-3/7}, 4\sqrt{2} \frac{d^3}{dx^3} f^*(0) M^{-3/7}, \right. \\
& \quad \frac{16 \left[C_{(\sigma, \|u\|_{L^\infty(\Omega)})} \log M + \gamma(M) \right] \log(M)}{M^{3/7}}, \\
& \quad \left. 16\sqrt{\frac{\omega(M)}{7}} \tilde{C}(\sigma, \|u\|_{L^\infty(\Omega_{(M)})}) \frac{\sqrt{\log(M)}}{M^{3/7}} \right\}, \\
& \tag{40}
\end{aligned}$$

then we have

$$\begin{aligned}
& P\left(\|(\mathbf{X}^* - \mathbf{X})\beta^*\|_\infty > \frac{\epsilon}{2}\right) \\
& \leq NK \left[2Me^{-\frac{(M^{3/7} - \|U\|_{L^\infty(\Omega)})^2}{2\sigma^2}} + Q_{(\sigma, \|u\|_{L^\infty(\Omega)})} e^{-L\gamma(M)} + 4\sqrt{2}\eta^4 M^{-\omega(M)/7} \right]. \tag{41}
\end{aligned}$$

Inequality (41) is derived by Lemma C.1.

By combining the results in (38), (39), (40), (41), we have that when

$$\begin{aligned}
\frac{\epsilon}{2} > \mathcal{C}_{(\sigma, \|u\|_{L^\infty(\Omega)})} \max & \left\{ 4K_{\max} M^{-3/7}, 4KK_{\max} \|\beta^*\|_\infty N^{-3/7}, \right. \\
& 4AM^{-3/7}, 4K \|\beta^*\|_\infty \bar{A}N^{-3/7}, \\
& 4\sqrt{2} \frac{d^3}{dx^3} f^*(0) M^{-3/7}, 4\sqrt{2}K \|\beta^*\|_\infty \frac{d^3}{dx^3} \bar{f}^*(0) N^{-3/7}, \\
& \frac{16KK_{\max} \|\beta^*\|_\infty \left[C_{(\sigma, \|u\|_{L^\infty(\Omega)})} \log(M) + \gamma_{(M)} \right] \log(M)}{M^{3/7}}, \\
& \frac{16K_{\max} \left[C_{(\sigma, \|u\|_{L^\infty(\Omega)})} \log(N) + \gamma_{(N)} \right] \log(N)}{N^{3/7}}, \\
& 16\sqrt{\frac{\omega_{(M)}}{7}} \tilde{C}_{(\sigma, \|u\|_{L^\infty(\Omega)})} \frac{\sqrt{\log(M)}}{M^{3/7}}, \\
& \left. 16K \|\beta^*\|_\infty \sqrt{\frac{\omega_{(N)}}{7}} \tilde{C}_{(\sigma, \|u\|_{L^\infty(\Omega)})} \frac{\sqrt{\log(N)}}{N^{3/7}} \right\},
\end{aligned}$$

we have

$$\begin{aligned}
& P(\|\nabla_t \mathbf{u} - \mathbf{X}\beta^*\|_\infty > \epsilon) \\
\leq & M \left[2Ne^{-\frac{(N^{3/7} - \|U\|_{L^\infty(\Omega)})^2}{2\sigma^2}} + Q_{(\sigma, \|u\|_{L^\infty(\Omega)})} e^{-L\gamma_{(N)}} + 4\sqrt{2}\eta^4 N^{-\omega_{(N)}/7} \right] + \\
& NK \left[2Me^{-\frac{(M^{3/7} - \|U\|_{L^\infty(\Omega)})^2}{2\sigma^2}} + Q_{(\sigma, \|u\|_{L^\infty(\Omega)})} e^{-L\gamma_{(M)}} + 4\sqrt{2}\eta^4 M^{-\omega_{(M)}/7} \right]
\end{aligned}$$

Now, let us do some simplification of the above results. Let $M = N^\kappa$, $\gamma_{(M)} = \gamma_{(N)} =$

$\frac{1}{L}N^r, \omega_{(M)} = \omega_{(N)} = N^{2r}$, and

$$\left\{ \begin{array}{lcl} \mathcal{J}_1 & = & 4KK_{\max}\|\beta^*\|_{\infty}N^{-3\kappa/7} \\ \mathcal{J}'_1 & = & 4K_{\max}N^{-3/7} \\ \mathcal{J}_2 & = & 4AK\|\beta^*\|_{\infty}N^{-3\kappa/7} \\ \mathcal{J}'_2 & = & 4\bar{A}N^{-3/7} \\ \mathcal{J}_3 & = & 4\sqrt{2}K\|\beta^*\|_{\infty}\frac{d^3}{dx^3}f^*(0)N^{-3\kappa/7} \\ \mathcal{J}'_3 & = & 4\sqrt{2}\frac{d^3}{dx^3}\bar{f}^*(0)N^{-3/7} \\ \mathcal{J}_4 & = & \frac{16KK_{\max}\|\beta^*\|_{\infty}\left[C_{(\sigma, \|u\|_{L^{\infty}(\Omega)})}(\log(\kappa)+\log(N))+N^r/L\right](\log(\kappa)+\log(N))}{N^{3\kappa/7}} \\ \mathcal{J}'_4 & = & \frac{16K_{\max}\left[C_{(\sigma, \|u\|_{L^{\infty}(\Omega)})}\log(N)+N^r\right]\log(N)}{N^{3/7}} \\ \mathcal{J}_5 & = & 16K\|\beta^*\|_{\infty}\sqrt{\frac{N^{2r}}{7}}\tilde{C}_{(\sigma, \|u\|_{L^{\infty}(\Omega)})}\frac{\sqrt{\log(\kappa)+\log(N)}}{N^{3\kappa/7}} \\ \mathcal{J}'_5 & = & 16\sqrt{\frac{N^{2r}}{7}}\tilde{C}_{(\sigma, \|u\|_{L^{\infty}(\Omega)})}\frac{\sqrt{\log(N)}}{N^{3/7}} \end{array} \right. .$$

To guarantee that $\mathcal{J}_1, \mathcal{J}'_1, \mathcal{J}_2, \mathcal{J}'_2, \mathcal{J}_3, \mathcal{J}'_3, \mathcal{J}_4, \mathcal{J}'_4, \mathcal{J}_5, \mathcal{J}'_5 \rightarrow 0$, as $N \rightarrow +\infty$, we need

$$\left\{ \begin{array}{l} 3\kappa/7 - r > 0 \\ 3/7 - r > 0 \end{array} \right. ,$$

where the optimal κ is $\kappa = 1$. Accordingly, we have

$$\mathcal{J}_1, \mathcal{J}'_1, \mathcal{J}_2, \mathcal{J}'_2, \mathcal{J}_3, \mathcal{J}'_3, \mathcal{J}_4, \mathcal{J}'_4, \mathcal{J}_5, \mathcal{J}'_5 \lesssim \mathcal{J}_4, \mathcal{J}'_4.$$

Based on the above discussion, we can declare that when N is sufficiently large, with

$$\epsilon > \mathcal{C}_{(\sigma, \|u\|_{L^{\infty}(\Omega)})} \frac{\log(N)}{N^{3/7-r}}$$

for any $r \in (0, \frac{3}{7})$ and $M = O(N)$, we have

$$\begin{aligned}
& P \|\nabla_t \mathbf{u} - \mathbf{X}\beta^*\|_\infty > \epsilon \\
\leq & M \left[2Ne^{-\frac{(N^{3/7} - \|U\|_{L^\infty(\Omega)})^2}{2\sigma^2}} + Q_{(\sigma, \|u\|_{L^\infty(\Omega)})} e^{-L\gamma_{(N)}} + 4\sqrt{2}\eta^4 N^{-\omega_{(N)}/7} \right] + \\
& NK \left[2Me^{-\frac{(M^{3/7} - \|U\|_{L^\infty(\Omega)})^2}{2\sigma^2}} + Q_{(\sigma, \|u\|_{L^\infty(\Omega)})} e^{-L\gamma_{(M)}} + 4\sqrt{2}\eta^4 M^{-\omega_{(M)}/7} \right] \\
= & M \left[2Ne^{-\frac{(N^{3/7} - \|U\|_{L^\infty(\Omega)})^2}{2\sigma^2}} + Q_{(\sigma, \|u\|_{L^\infty(\Omega)})} e^{-Nr} + 4\sqrt{2}\eta^4 N^{-N^{2r}/7} \right] + \\
& NK \left[2Me^{-\frac{(M^{3/7} - \|U\|_{L^\infty(\Omega)})^2}{2\sigma^2}} + Q_{(\sigma, \|u\|_{L^\infty(\Omega)})} e^{-Nr} + 4\sqrt{2}\eta^4 M^{-N^{2r}/7} \right] \\
= & O(Ne^{-Nr})
\end{aligned}$$

Thus, we finish the proof of the theorem. \square

F.5 Proof of Theorem 3.1

Proof. By KKT-condition, any minimizer β of (10) must satisfies:

$$-\frac{1}{MN} \mathbf{X}^\top (\nabla_t \mathbf{u} - \mathbf{X}\beta) + \lambda \mathbf{z} = 0 \quad \text{for } \mathbf{z} \in \partial\|\beta\|_1,$$

where $\partial\|\beta\|_1$ is the sub-differential of $\|\beta\|_1$. The above equation can be equivalently transformed into

$$\mathbf{X}^\top \mathbf{X}(\beta - \beta^*) + \mathbf{X}^\top [(\mathbf{X} - \mathbf{X}^*)\beta^* - (\nabla_t \mathbf{u} - \nabla_t \mathbf{u}^*)] + \lambda MN \mathbf{z} = 0. \quad (42)$$

Here matrix $\mathbf{X} \in \mathbb{R}^{MN \times K}$ is defined in (9), and matrix $\mathbf{X}^* \in \mathbb{R}^{MN \times K}$ is defined as

$$\mathbf{X}^* = (\mathbf{x}_0^0 \ \mathbf{x}_1^0 \ \dots \ \mathbf{x}_{M-1}^0 \ \mathbf{x}_1^0 \ \dots \ \mathbf{x}_{M-1}^{N-1})^\top,$$

with

$$\mathbf{x}_i^n = \left(1, \ u(x_i, t_n), \ \frac{\partial u(x_i, t_n)}{\partial x}, \ \frac{\partial^2 u(x_i, t_n)}{\partial x^2}, \ \left(\widehat{u(x_i, t_n)} \right)^2, \ \dots, \left(\frac{\partial^2 u(x_i, t_n)}{\partial x^2} \right)^{p_{\max}} \right)^\top \in \mathbb{R}^K.$$

And vector $\beta^* = (\beta_1, \dots, \beta_K) \in \mathbb{R}^K$ is the ground truth coefficients. Besides, vector $\nabla_t \mathbf{u} \in \mathbb{R}^{MN}$ is defined in (8), and vector $\nabla_t \mathbf{u}^* \in \mathbb{R}^K$ is the ground truth, i.e.,

$$\nabla_t \mathbf{u}^* = \left(\frac{\partial u(x_0, t_0)}{\partial t}, \frac{\partial u(x_1, t_0)}{\partial t}, \dots, \frac{\partial u(x_{M-1}, t_0)}{\partial t}, \frac{\partial u(x_0, t_1)}{\partial t}, \dots, \frac{\partial u(x_{M-1}, t_{N-1})}{\partial t} \right)^\top.$$

Let us denote $\mathcal{S} = \{i : \beta_i^* \neq 0 \forall i = 0, 1, \dots, K\}$, then we can decompose \mathbf{X} into $\mathbf{X}_{\mathcal{S}}$ and $\mathbf{X}_{\mathcal{S}^c}$, where $\mathbf{X}_{\mathcal{S}}$ is the columns of \mathbf{X} whose indices are in \mathcal{S} and $\mathbf{X}_{\mathcal{S}^c}$ is the complement of $\mathbf{X}_{\mathcal{S}}$. And we can also decompose β into $\beta_{\mathcal{S}}$ and $\beta_{\mathcal{S}^c}$, where $\beta_{\mathcal{S}}$ is the subvector of β only contains elements whose indices are in \mathcal{S} and $\beta_{\mathcal{S}^c}$ is the complement of $\beta_{\mathcal{S}}$.

By using the decomposition, we can rewrite (42) as

$$\begin{pmatrix} \mathbf{0} \\ \mathbf{0} \end{pmatrix} = \begin{pmatrix} \mathbf{X}_{\mathcal{S}}^\top \mathbf{X}_{\mathcal{S}} & \mathbf{X}_{\mathcal{S}}^\top \mathbf{X}_{\mathcal{S}^c} \\ \mathbf{X}_{\mathcal{S}^c}^\top \mathbf{X}_{\mathcal{S}} & \mathbf{X}_{\mathcal{S}^c}^\top \mathbf{X}_{\mathcal{S}^c} \end{pmatrix} \begin{pmatrix} \beta_{\mathcal{S}} - \beta_{\mathcal{S}}^* \\ \beta_{\mathcal{S}^c} \end{pmatrix} + \begin{pmatrix} \mathbf{X}_{\mathcal{S}}^\top \\ \mathbf{X}_{\mathcal{S}^c}^\top \end{pmatrix} [(\mathbf{X} - \mathbf{X}^*)_{\mathcal{S}} \beta_{\mathcal{S}}^* - (\nabla_t \mathbf{u} - \nabla_t \mathbf{u}^*)] + \lambda MN \begin{pmatrix} \mathbf{z}_{\mathcal{S}} \\ \mathbf{z}_{\mathcal{S}^c} \end{pmatrix} \quad (43)$$

Suppose the primal-dual witness (PDW) construction gives us an solution $(\check{\beta}, \check{\mathbf{z}}) \in \mathbb{R}^K \times \mathbb{R}^K$, where $\check{\beta}_{\mathcal{S}^c} = 0$ and $\check{\mathbf{z}} \in \partial \|\check{\beta}\|_1$. By plugging $(\check{\beta}, \check{\mathbf{z}})$ into the above equation, we have

$$\begin{aligned} \check{\mathbf{z}}_{\mathcal{S}^c} &= \mathbf{X}_{\mathcal{S}^c}^\top \mathbf{X}_{\mathcal{S}} (\mathbf{X}_{\mathcal{S}}^\top \mathbf{X}_{\mathcal{S}})^{-1} \mathbf{z}_{\mathcal{S}} - \mathbf{X}_{\mathcal{S}^c}^\top \underbrace{(\mathbf{I} - \mathbf{X}_{\mathcal{S}} (\mathbf{X}_{\mathcal{S}}^\top \mathbf{X}_{\mathcal{S}})^{-1} \mathbf{X}_{\mathcal{S}}^\top)}_{\mathbf{H}_{X_{\mathcal{S}}}} \frac{[(\mathbf{X} - \mathbf{X}^*)_{\mathcal{S}} \beta_{\mathcal{S}}^* - (\nabla_t \mathbf{u} - \nabla_t \mathbf{u}^*)]}{\lambda MN} \\ &= \mathbf{X}_{\mathcal{S}^c}^\top \mathbf{X}_{\mathcal{S}} (\mathbf{X}_{\mathcal{S}}^\top \mathbf{X}_{\mathcal{S}})^{-1} \mathbf{z}_{\mathcal{S}} - \frac{1}{\lambda MN} \mathbf{X}_{\mathcal{S}^c}^\top \mathbf{H}_{X_{\mathcal{S}}} \underbrace{(\mathbf{X}_{\mathcal{S}} \beta_{\mathcal{S}}^* - \nabla_t \mathbf{u})}_{\boldsymbol{\tau}} \end{aligned} \quad (44)$$

From (44), we have

$$\begin{aligned} P(\|\check{\mathbf{z}}_{\mathcal{S}^c}\|_\infty \geq 1) &= P\left(\left\|\mathbf{X}_{\mathcal{S}^c}^\top \mathbf{X}_{\mathcal{S}} (\mathbf{X}_{\mathcal{S}}^\top \mathbf{X}_{\mathcal{S}})^{-1} \mathbf{z}_{\mathcal{S}} - \frac{1}{\lambda MN} \mathbf{X}_{\mathcal{S}^c}^\top \mathbf{H}_{X_{\mathcal{S}}} \boldsymbol{\tau}\right\|_\infty > 1\right) \\ &\leq P\left(\left\|\mathbf{X}_{\mathcal{S}^c}^\top \mathbf{X}_{\mathcal{S}} (\mathbf{X}_{\mathcal{S}}^\top \mathbf{X}_{\mathcal{S}})^{-1} \mathbf{z}_{\mathcal{S}}\right\|_\infty > 1 - \mu\right) + \\ &\quad P\left(\left\|\frac{1}{\lambda MN} \mathbf{X}_{\mathcal{S}^c}^\top \mathbf{H}_{X_{\mathcal{S}}} \boldsymbol{\tau}\right\|_\infty > \mu\right). \end{aligned}$$

If we denote $\widetilde{Z}_j = \frac{1}{\lambda MN} (\mathbf{X}_{\mathcal{S}^c})_j^\top \mathbf{H}_{X_s} \boldsymbol{\tau}$, where $(\mathbf{X}_{\mathcal{S}^c})_j$ is the j -th column of $\mathbf{X}_{\mathcal{S}^c}$, then we have

$$P(\|\check{\mathbf{z}}_{\mathcal{S}^c}\|_\infty \geq 1) \leq P\left(\left\|\mathbf{X}_{\mathcal{S}^c}^\top \mathbf{X}_{\mathcal{S}} (\mathbf{X}_{\mathcal{S}}^\top \mathbf{X}_{\mathcal{S}})^{-1}\right\|_\infty > 1 - \mu\right) + P\left(\max_{j \in \mathcal{S}^c} |\widetilde{Z}_j| > \mu\right). \quad (45)$$

Now let us discuss the upper bound of the second term, i.e., $P\left(\max_{j \in \mathcal{S}^c} |\widetilde{Z}_j| > \mu\right)$. Because

$$\begin{aligned} P\left(\max_{j \in \mathcal{S}^c} |\widetilde{Z}_j| > \mu\right) &= P\left(\left\|\frac{1}{\lambda MN} \mathbf{X}_{\mathcal{S}^c}^\top \mathbf{H}_{X_s} \boldsymbol{\tau}\right\|_\infty > \mu\right) \\ &\leq P\left(\left\|\frac{1}{\lambda MN} \mathbf{X}_{\mathcal{S}^c}^\top \mathbf{H}_{X_s} \boldsymbol{\tau}\right\|_2 > \mu\right) \\ &\leq P\left(\left\|\frac{1}{\lambda MN} \mathbf{X}^\top \mathbf{H}_{X_s} \boldsymbol{\tau}\right\|_2 > \mu\right) \\ &\leq P\left(\frac{1}{\lambda MN} \|\mathbf{X}\|_2 \|\boldsymbol{\tau}\|_2 > \mu\right) \\ &\leq P\left(\|\boldsymbol{\tau}\|_2 > \lambda \mu \sqrt{\frac{MN}{K}}\right) \\ &\leq P\left(\|\boldsymbol{\tau}\|_\infty > \lambda \mu \frac{1}{\sqrt{K}}\right) \end{aligned} \quad (46)$$

By Lemma C.2, we know when

$$\lambda \mu \frac{1}{\sqrt{K}} > \mathcal{C}(\sigma, \|u\|_{L^\infty(\Omega)}) \frac{\log(N)}{N^{3/7-r}},$$

we have

$$P(\|\nabla_t \mathbf{u} - \mathbf{X} \boldsymbol{\beta}^*\|_\infty > \epsilon) < N e^{-N^r}.$$

So we know that

$$\begin{aligned} P\left(\|\boldsymbol{\tau}\|_\infty > \lambda \mu \frac{1}{\sqrt{K}}\right) &= P\left(\|\nabla_t \mathbf{u} - \mathbf{X}_{\mathcal{S}} \boldsymbol{\beta}_{\mathcal{S}}^*\|_\infty > \lambda \mu \frac{1}{\sqrt{K}}\right) \\ &\leq P\left(\|\nabla_t \mathbf{u} - \mathbf{X} \boldsymbol{\beta}^*\|_\infty > \lambda \mu \frac{1}{\sqrt{K}}\right) \\ &< N e^{-N^r} \end{aligned} \quad (47)$$

By plugging the results in (46) and (47) into (45), we have

$$\begin{aligned}
P(\|\check{\mathbf{z}}_{\mathcal{S}^c}\|_\infty \geq 1) &\leq P\left(\left\|\mathbf{X}_{\mathcal{S}^c}^\top \mathbf{X}_{\mathcal{S}} (\mathbf{X}_{\mathcal{S}}^\top \mathbf{X}_{\mathcal{S}})^{-1}\right\|_\infty > 1 - \mu\right) + P\left(\max_{j \in \mathcal{S}^c} |\widetilde{Z}_j| > \mu\right) \\
&\leq P\left(\left\|\mathbf{X}_{\mathcal{S}^c}^\top \mathbf{X}_{\mathcal{S}} (\mathbf{X}_{\mathcal{S}}^\top \mathbf{X}_{\mathcal{S}})^{-1}\right\|_\infty > 1 - \mu\right) + P\left(\|\boldsymbol{\tau}\|_\infty > \lambda\mu \frac{1}{\sqrt{K}}\right) \\
&\leq P\left(\left\|\mathbf{X}_{\mathcal{S}^c}^\top \mathbf{X}_{\mathcal{S}} (\mathbf{X}_{\mathcal{S}}^\top \mathbf{X}_{\mathcal{S}})^{-1}\right\|_\infty > 1 - \mu\right) + Ne^{-N^r}
\end{aligned}$$

The probability for proper support set recovery is

$$\begin{aligned}
P(\|\check{\mathbf{z}}_{\mathcal{S}^c}\|_\infty < 1) &= 1 - P(\|\check{\mathbf{z}}_{\mathcal{S}^c}\|_\infty \geq 1) \\
&\geq 1 - [P\left(\left\|\mathbf{X}_{\mathcal{S}^c}^\top \mathbf{X}_{\mathcal{S}} (\mathbf{X}_{\mathcal{S}}^\top \mathbf{X}_{\mathcal{S}})^{-1}\right\|_\infty > 1 - \mu\right) + Ne^{-N^r}] \\
&= P\left(\left\|\mathbf{X}_{\mathcal{S}^c}^\top \mathbf{X}_{\mathcal{S}} (\mathbf{X}_{\mathcal{S}}^\top \mathbf{X}_{\mathcal{S}})^{-1}\right\|_\infty \leq 1 - \mu\right) - Ne^{-N^r} \\
&\leq P_\mu - Ne^{-N^r}.
\end{aligned}$$

Thus, we finish the proof. \square

F.6 Proof of Theorem 3.2

Proof. By equation (43), we can solve $\boldsymbol{\beta}_{\mathcal{S}} - \boldsymbol{\beta}_{\mathcal{S}}^*$ as

$$\boldsymbol{\beta}_{\mathcal{S}} - \boldsymbol{\beta}_{\mathcal{S}}^* = (\mathbf{X}_{\mathcal{S}}^\top \mathbf{X}_{\mathcal{S}})^{-1} \left[-\mathbf{X}_{\mathcal{S}}^\top (\mathbf{X}_{\mathcal{S}} - \mathbf{X}_{\mathcal{S}}^*) \boldsymbol{\beta}_{\mathcal{S}}^* + \mathbf{X}_{\mathcal{S}}^\top (\nabla_t \mathbf{u} - \nabla_t \mathbf{u}^*) - \lambda MN \mathbf{z}_{\mathcal{S}} \right].$$

Thus, we have the following series of equations:

$$\begin{aligned}
& \max_{k \in \mathcal{S}} |\beta_k - \beta_k^*| \\
& \leq \|(\mathbf{X}_S^\top \mathbf{X}_S)^{-1}\|_\infty \|\mathbf{X}_S^\top [\nabla_t \mathbf{u} - \nabla_t \mathbf{u}^* - (\mathbf{X}_S - \mathbf{X}_S^*)\beta_S^*] - \lambda MN \mathbf{z}_S\|_\infty \\
& \leq \|(\mathbf{X}_S^\top \mathbf{X}_S)^{-1}\|_\infty [\|\mathbf{X}_S^\top [\nabla_t \mathbf{u} - \nabla_t \mathbf{u}^* - (\mathbf{X}_S - \mathbf{X}_S^*)\beta_S^*]\|_\infty + \lambda MN \|\mathbf{z}_S\|_\infty] \\
& = \|(\mathbf{X}_S^\top \mathbf{X}_S)^{-1}\|_\infty [\|\mathbf{X}_S^\top (\nabla_t \mathbf{u} - \mathbf{X}_S \beta_S^*)\|_\infty + \lambda MN \|\mathbf{z}_S\|_\infty] \tag{48}
\end{aligned}$$

$$\leq \left\| \left(\frac{\mathbf{X}_S^\top \mathbf{X}_S}{MN} \right)^{-1} \right\|_\infty \left(\frac{\|\mathbf{X}_S^\top (\nabla_t \mathbf{u} - \mathbf{X}_S \beta_S^*)\|_\infty}{MN} + \lambda \right) \tag{49}$$

$$\leq \sqrt{K} C_{\min} \left(\frac{\|\mathbf{X}_S^\top (\nabla_t \mathbf{u} - \mathbf{X}_S \beta_S^*)\|_\infty}{MN} + \lambda \right) \tag{50}$$

$$\leq \sqrt{K} C_{\min} \left(\frac{\|\mathbf{X}_S\|_{\infty, \infty} \|\nabla_t \mathbf{u} - \mathbf{X}_S \beta_S^*\|_\infty}{MN} + \lambda \right) \tag{51}$$

$$\begin{aligned}
& \leq \sqrt{K} C_{\min} \left(\frac{\|\mathbf{X}_S\|_F \|\nabla_t \mathbf{u} - \mathbf{X}_S \beta_S^*\|_\infty}{\sqrt{MN}} + \lambda \right) \\
& \leq \sqrt{K} C_{\min} \left(\frac{\sqrt{MNK} \|\nabla_t \mathbf{u} - \mathbf{X}_S \beta_S^*\|_\infty}{\sqrt{MN}} + \lambda \right) \tag{52}
\end{aligned}$$

$$\begin{aligned}
& = \sqrt{K} C_{\min} \left(\sqrt{K} \|\nabla_t \mathbf{u} - \mathbf{X}_S \beta_S^*\|_\infty + \lambda \right) \\
& \leq \sqrt{K} C_{\min} \left(\sqrt{K} \mathcal{C}_{(\sigma, \|u\|_{L^\infty(\Omega)})} \frac{\log(N)}{N^{3/7-r}} + \lambda \right) \tag{53}
\end{aligned}$$

Equation (48) is because $\nabla_t \mathbf{u}^* = \mathbf{X}_S \beta_S$. Inequality (49) is because $\|\mathbf{z}_S\|_\infty = 1$. Inequality (50) is because of Condition 3.3. Inequality (51) is because for a matrix \mathbf{A} and a vector \mathbf{x} , we have $\|\mathbf{A}\mathbf{x}\|_q \leq \|\mathbf{A}\|_{p,q} \|\mathbf{x}\|_p$. Here the matrix norm for matrix $\mathbf{A} \in \mathbb{R}^{m \times n}$ in $\|\mathbf{A}\|_{\infty, \infty} = \|\text{vector}(\mathbf{A})\|_\infty$. In inequality (52), the norm of matrix $\mathbf{A} \in \mathbb{R}^{m \times n}$ is that $\|\mathbf{A}\|_F = \sqrt{\sum_{i=1}^m \sum_{j=1}^n |A_{ij}|^2}$, and the norm of vector $\mathbf{a} \in \mathbb{R}^d$ is $\|\mathbf{a}\|_\infty = \max_{1 \leq i \leq d} |a_i|$. Inequality (52) is because we normalized columns of \mathbf{X} . Inequality (53) is due to Lemma Lemma C.2 under probability $1 - O(Ne^{-Nr}) \rightarrow 1$. \square